AD-A171 681 ARGO DEVELOPMENT PROGRAM(U) WOODS HOLE OCEANOGRAPHIC INSTITUTION MA DEEP SUBMERGENCE LAB JUN 86 N00014-82-C-0743 1/2

UNCLASSIFIED F/G 13/10 NL

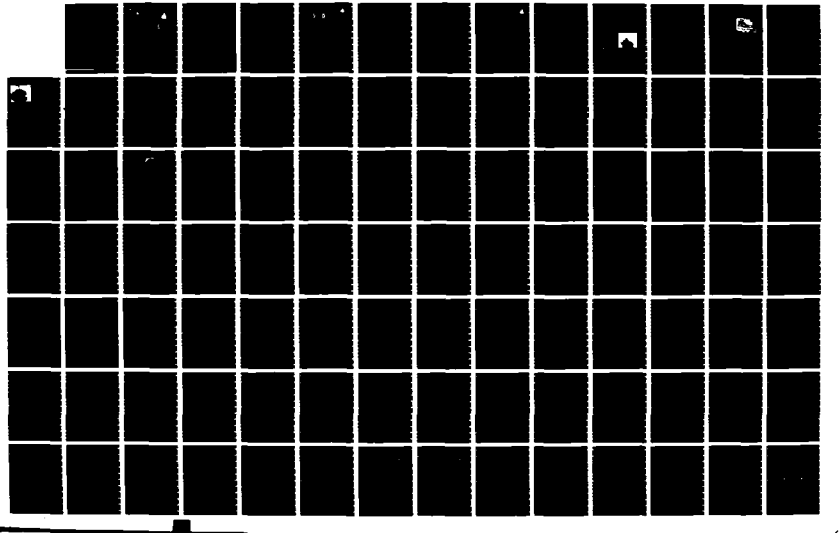

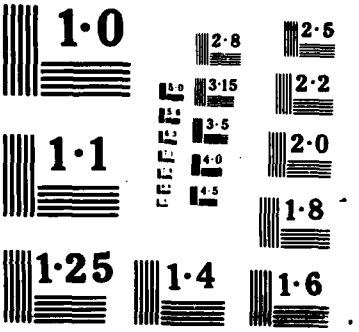
1·0
1·1
1·25
1·4
1·6
1·8
2·0
2·2
2·5
2·8
3·15
3·5
4·0
4·5

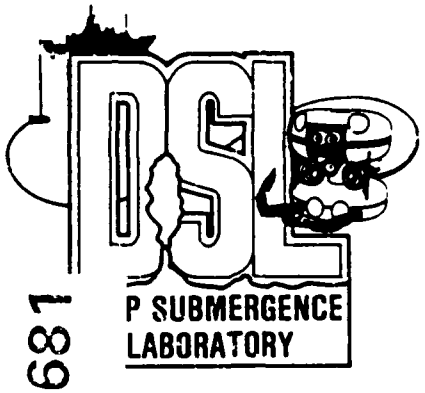

Final Report
June 1986

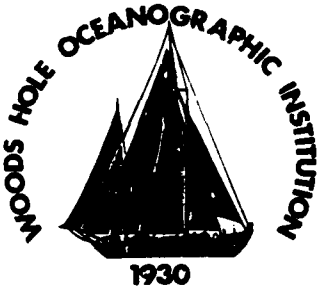

Argo Development Program

Sponsored by:
The Office of Naval Research
Contract No.
N00014-82-C-0743

DISCLAIMER NOTICE

THIS DOCUMENT IS BEST QUALITY PRACTICABLE. THE COPY FURNISHED TO DTIC CONTAINED A SIGNIFICANT NUMBER OF PAGES WHICH DO NOT REPRODUCE LEGIBLY.

FINAL REPORT
Contract No. N00014-82-C-0743

1. ARGO/JASON Development:

The purpose of the contract was to develop and place into operational status a new, combined research/inspection unmanned vehicle system called ARGO/JASON. ARGO is a high altitude search and survey vehicle for use in deep ocean exploration. A companion vehicle, JASON, which will be tethered to ARGO, will be a free swimming, highly maneuverable vehicle with manipulative capability and high quality vision for close-up inspection. This work is more fully described in the following articles (References 1-7).

2. AMUVS Refurbishment Program (Modification P00002):

This program provided for the refurbishment of the Advanced Maneuverable Underwater Viewing System (AMUVS) vehicle which included upgrading the motor, replacing the controllers, and rehabilitating the vehicle subassemblies and components.

A shallow water test was conducted at the end of the summer in 1983 with AMUVS being operated from ALVIN off the dock at Woods Hole. The results of these tests indicated that major refurbishment was necessary and a follow-on program (modification P00008) was initiated. The plan for this new program was described in detail in the enclosed article (Reference 8).

3. NR-1 Operations on the Reykjanes Ridge (Modification P00005):

In August 1984 an investigation of the axial processes of the Reykjanes Ridge was conducted using the NR-1. The NR-1 was outfitted with a special low light level TV system with funding from Naval Sea Systems Command, PMS-395. This system concept grew out of the ARGO imaging research funded by this contract. Results of the scientific exploration of the Reykjanes Ridge were published in National Geographic Magazine, April 1985.

4. Deep Ocean Search System Evaluation (Modification P00004):

The ANGUS photo reconnaissance system was used to demonstrate large area, high resolution photo search in an attempt to locate an Air Force helicopter lost on the north face of a British West Indies underwater mountain. An expedition was mounted and executed but failed to find any debris.

5. Enhancement of the ARGO/JASON Sonar System (Modification P00005):

With the funds provided for this program, the Sea MARC Ib (an advanced wide-swath sonar system) was procured from the Lamont-Doherty Geological Observatory for the purpose of upgrading the sonar capability of the ARGO vehicle. A stand-alone system (described in reference 9), Sea MARC has been developed and is presently used for deep ocean acoustic mapping in areas such as the Kane Fracture Zone (reference 10). The Sea MARC is operated in conjunction with ARGO to provide wide swath acoustic images of an area which complement the visual and acoustic imaging systems on ARGO.

Woods Hole Oceanographic Institution
Woods Hole, MA 02543
Phone: (617) 548-1400
Telex: 951679

July 28, 1986

Dr. E.A. Silva
Head, Ocean Engineering (Code 1121)
Office of Naval Research
800 N. Quincy Street
Arlington, VA 22217

Ref: Contract N00014-82-C-0743

Dear Dr. Silva:

In compliance with the requirements set forth in Section F (Deliveries or Performance) of Contract N00014-82-C-0743, the Deep Submergence Laboratory of the Woods Hole Oceanographic Institution herewith submits the Final Report of all work funded and performed under the auspices of this contract during the period 1 September 1982 through 30 April 1986.

The Deep Submergence Laboratory is indebted to you, Gene, and the Office of Naval Research for the support you've given us. Without your help and confidence in our abilities we could not have gotten this dream, ARGO/JASON, started. Fortunately, these ideas and programs have paid off and become a reality due on no small part to your own efforts and determination.

Sincerely,

Dr. Robert D. Ballard
Senior Scientist
Deep Submergence Laboratory

RDB/tln
Enclosures

6. Advanced Maneuverable Underwater Viewing System (Modification P00008):

As a result of the evaluations conducted in the AMUVS Refurbishment Program provided for in this contract under Modification P00002, the primary objectives of this program were to concentrate in solving the vehicle's reliability problems and making major improvements in its imaging and control systems. A major effort was made in the area of tether design for vehicles such as AMUVS and JASON. The results of this work are reported in Reference 11.

A series of engineering dives were undertaken as part of this work using the ALVIN manned submersible as a platform to test AMUVS. This cruise, aboard the ATLANTIS II, took place during June-July 1985 in the Guaymas (Mexico) Basin. A report of those test dives is enclosed as Reference 12.

7. ARGO Research (Modification P00008):

The terms of this modification were to continue support of the ARGO research program which included development of imaging computer simulation models and ARGO ship control system testing. An imaging model has been developed which predicts the performance of underwater camera/light systems. It has been used extensively in the support of Navy programs evaluating imaging systems for a variety of platforms. This model and its use is described in Reference 13.

8. Dynamic Positioning Preliminary Study

In addition to the above, this contract supported a preliminary investigation into the specification of a dynamic positioning (DP) system for the R/V KNORR. As one of the primary vessels for ARGO/JASON, the KNORR DP system is specially designed for positioning vehicles in the deep ocean. Reference 14 provides more detail.

References

1. Harris, Stewart E., Marquet, William M., and Ballard, Robert D., Development Status: ARGO Deep Ocean Instrument Platform, ROV '84, San Diego, CA, April 1984.

2. Harris, Stewart E. and Ballard, Robert D., ARGO: Capabilities for Deep Ocean Exploration, Oceans '86 Conference, Proceedings, MTS/IEEE, Washington, DC, 1986.

3. Harris, Stewart E. and Yoerger, Dana R., ARGO/JASON: Integrated Capabilities for Exploration of the Seafloor, Proceedings AUVS Conference, Boston, MA, 1986.

4. Yoerger, Dana R. and Newman, James B., Demonstration of Supervisory Control for ROV's and Manipulators, ROV '86 Conference, Proceedings, MTS/IEEE, Aberdeen, Scotland, June 1986.

5. Yoerger, Dana R. and Newman, James B., Demonstration of Closed-Loop Trajectory Control of an Underwater Vehicle, Oceans '85, MTS/IEEE, San Diego, CA, November 1985.

6. Yoerger, Dana R. and Newman, James B., JASON: An Integrated Approach to ROV and Control System Design, ROV '86 Conference, Proceedings, MTS/IEEE, Aberdeen, Scotland, June 1986.

7. Yoerger, Dana R., Newman, James B., Slotine, J.-J.E., Supervisory Control System for the JASON ROV, IEEE J. Oceanic Eng., 1986.

8. Stewart, William K., An Advanced Observation and Inspection ROV for 6,000 Meter Operations, ROV '84 Conference, Proceedings, MTS/IEEE, San Diego, CA, April 1984.

9. Chayes, Dale N., Evolution of Sea MARC I, IEEE Proceedings of the Third Working Symposium on Oceanographic Data Systems, 1983.

10. Benjamin, Kim C., Trip Report for CSS HUDSON Cruise 85-010 to the Kane Fracture Zone, April 27-May 27, 1985.

11. Wilkins, George, Naval Ocean Systems Center-Hawaii Laboratory, memorandum entitled Design Recommendations for AMUVS E-O Tether Cable, January 10, 1985.

12. Stewart, William K., Evaluation of AMUVS Engineering Dives and Development Priorities for Operational Use, Internal Report, September 8, 1985.

13. Jaffe, Jules S., Harris, Stewart E., and Squires, Robert, A Computer Model for Prediction of Underwater Images, ROV '85 Conference, Proceedings, MTS/IEEE, San Diego, CA, April 1985.

14. Denaro, Robert P. and Yoerger, Dana R., The Application of Differential GPS to Marine Vessel Dynamic Positioning, Institute of Navigation Annual Meetings, 1986.

WOODS HOLE OCEANOGRAPHIC INSTITUTION
WOODS HOLE, MASSACHUSETTS 02543

Pre-print

Development status: ARGO Deep Ocean Instrument Platform

by

Stuart E. Harris
William M. Marquet
Robert D. Ballard

DATE: April 1984

Reference 1

DEVELOPMENT STATUS: ARGO DEEP OCEAN INSTRUMENT PLATFORM

by

Stewart E. Harris
William M. Marquet
Robert D. Ballard

ABSTRACT

The Deep Submergence Laboratory is developing a deep ocean survey and instrument platform called ARGO. With a design depth of 6,000 meters, ARGO will be towed on a steel-armored coaxial cable which will support several channels of frequency-multiplexed signals. A bank of TV cameras in the imaging pod will provide forward-, side-, and down-looking views of the ocean floor. Strobe lighting and LIBEC geometry will extend the useful range of these cameras to 100 meters. High fidelity acoustic images will be provided by an integrated side-looking sonar. Our goal is to create a cohesive and overlapping data set of wide swath acoustic images and high resolution optical images. Presented here are early results of ARGO-like vehicle towing characteristics and "snap-shot" video systems. Additionally, we will describe ARGO's modular design approach which affords us the flexibility to incorporate, in the future, additional sensing systems and a smaller, tethered ROV, JASON.

INTRODUCTION

To satisfy the needs of oceanographic and military communities, the Deep Submergence Laboratory (D.S.L.) has undertaken the development of an unmanned search and survey vehicle called ARGO. Equipped with a complement of superior sensors for deep ocean survey and inspection, ARGO will be able to remain submerged for long periods of time measured in terms of days or weeks and dramatically increase our "bottom-staying power" compared to present manned and unmanned vehicle operations.

ARGO is a towed sled capable of operating to 6000 meters depth. Its tether is a steel-armored, coaxial cable 0.68 inches in diameter. Designed to tow in a manner similar to D.S.L.'s ANGUS vehicle (Ballard, 1980), ARGO is quite heavy (greater than 4000 lbs) and will operate close to the bottom, at an altitude less than 70 meters. Our experience with ANGUS suggests that ARGO, when towed at speeds around 1 knot, will fly about 100 meters astern of the ship, achieving a nearly vertical wire angle.

While providing mechanical support for the vehicle, ARGO's tether also carries downlink power and a variety of frequency multiplexed signals from the onboard sensors. ARGO is designed to incorporate sensors which are modular subsystems. This modularity provides flexibility for growth and ease of maintenance and development. With this technique, we will integrate a wide-area TV imaging system with a side-looking sonar to provide simultaneous broad swath acoustic and optical images which will overlap in coverage and resolution. In addition, other sensing systems and a small tethered ROV, JASON, can be integrated into ARGO, making it a versatile survey and inspection instrument platform.

The purpose of this paper is to describe the design and current status of ARGO's development.

CABLE DESIGN

Recent studies on the design of deep sea, armored coaxial cables (Wilkins, 1983a) indicate the need for an improved version of this all important link between operator and remote vehicle. ARGO's tether is a design currently under consideration as the "standard" for the oceanographic community. It's armor package and internal structure represents a compromise between requirements for ruggedness, low rotation, maximum strength, and long flexure lifetime. This cable should have a tensile strength in excess of 36,000 lbs. and provide a usable data bandwidth over 6000 meters of 5 mHz.

Although adequate for now, such a cable has a severe bandwidth limitation which we hope to eliminate using current advances in deep ocean fiber-optic cables. One design now being procured by the Naval Ocean Systems Center-Hawaii (Wilkins, 1983b) incorporates three power conductors and three optical fibers in an armor package 0.68 inches in diameter, thus offering an evolution for the ARGO tether which could increase the available bandwidth one hundred fold. This advantage is important for the integration of JASON, which has a telemetry requirement of two real-time color video channels.

IMAGING SYSTEMS

A primary thrust of the research at D.S.L. is in deep sea optical imaging, and one goal of ARGO's first sea trials, scheduled for the summer of 1984, is to study wide area optical imaging. Figure 1 shows an artist's impression of ARGO. "Flying" at an altitude of 50 to 70 meters, ARGO

will illuminate the ocean floor with high-intensity strobe lights mounted on the main vehicle. Suspended 20 to 50 meters below ARGO is an imaging pod carrying up to five video cameras. Four will be wide angle cameras. Looking forward, to each side, and straight down, they will provide us with a composite picture of an area 100 to 500 meters square. A fifth, focused telephoto camera will look down and slightly forward to obtain detailed information about the seafloor terrain. The imaged area is illustrated (not to scale) by the dark trapezoids in the figure. This geometry of a light behind the camera, (or LIBEC), was pioneered earlier for film camera systems (Patterson, 1971) and used successfully for search and survey in the FAMOUS area (Patterson, 1975). By using low light level S.I.T. cameras, with an equivalent sensitivity of 200,000 ASA (Hayward, 1981), we hope to extend our visual range capability out to 100 meters (i.e. four to five optical attenuation lengths).

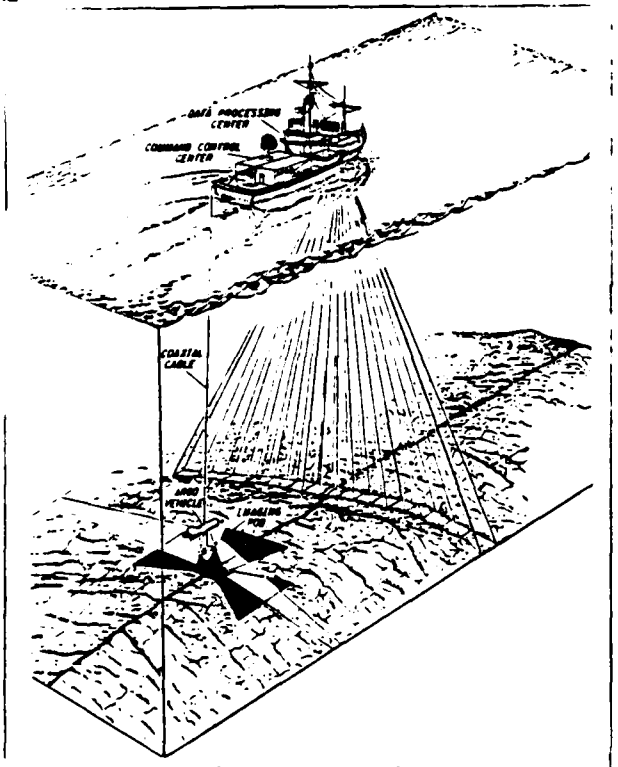

FIGURE 1: Artist's conception of ARGO towing configuration

As mentioned, lighting is provided by strobe lights which will flash every few seconds. Instantaneous video pictures, or "snapshots" will result. These images are "grabbed" by electronic frame stores for viewing and digital processing. Because the cameras will cover such a large area, pseudo-continuous coverage of the seafloor is possible by firing the strobe lights often enough for the images to overlap. Based on a 1 knot towing speed and 10 second repetition rate, down-looking images would overlap at least 70%.

In 1981, a similar wide area imaging system was tested on the manned submersible ALVIN in a series of dives off St. Croix. From an altitude over-the-bottom of 15 to 30 meters with strobes suspended 50 to 100 meters above the sub, we obtained pictures of the seafloor averaging 2,000 square meters in area. Figure 2 is a sample from this series. Here, a forward-looking camera is imaging a submerged hydrophone tower illuminated by a strobe light mounted on the tail of the sub. Taken from an altitude of 21 meters, the resulting image captures most of the 15 meter tall structure which is illustrated in Figure 3.

In addition to optical imaging, plans also call for side-looking and perhaps forward-looking sonars on ARGO. Simultaneous acoustic images, up to 1 kilometer wide, could be generated from ARGO's 70 meter altitude. Figure 1 illustrates this side-scan beam as well as the ship-based SEABEAM sonar coverage. Both of these systems provide us with the large geographical picture which is complemented by the TV coverage, thereby increasing our understanding and ability to follow the terrain.

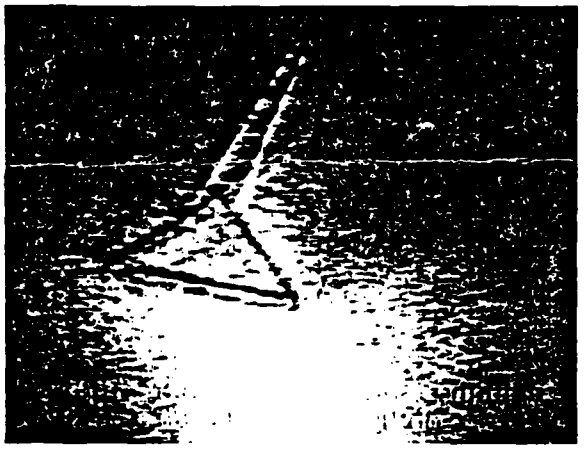

FIGURE 2: "Snapshot" video image of RCA hydrophone tower

SYSTEM ARCHITECTURE

Operators on the surface will interact with the imaging and sensor subsystems via a full duplex digital command and control loop. Employing low power microprocessors and high level software, ARGO subsystems represent a distributed network of dedicated processors. Figure 4 illustrates the system architecture. The imaging pod is one subsystem with which the operator can "talk" to via the network node, which is a part of the sequencer. While controlling the node operation, the sequencer also cycles the strobe lights and can activate the pod cameras directly. Since our current coaxial cable limits the data telemetry to one video channel, multiple cameras in the imaging pod are sequenced through a video switcher so only one camera is active when the lights flash. As subsystems are added,

they will tie into the node, power distribution, and clock network and send their data to the telemetry system for uplinking to the control center on the ship.

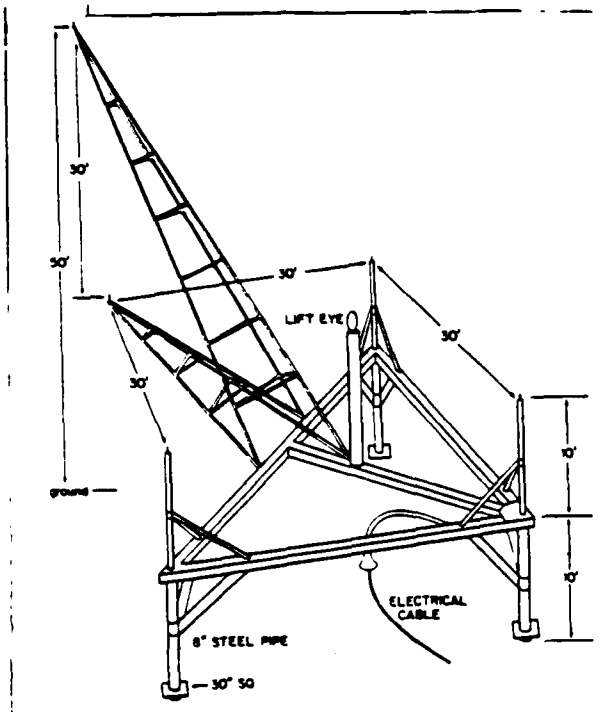

FIGURE 3: RCA hydrophone tower

SURFACE SUPPORT EQUIPMENT

All subsurface data is acquired in a control center which is containerized for easy transportation and installation on oceanographic vessels. Equipment for real-time processing and viewing as well as recording for post-mission processing and archival is located in the control center. Three operators will be responsible for the operation of ARGO, the winch system and con of the ship. Video, sonar, and navigation data are available for guidance of the ship. As each image is transmitted up the wire and displayed, the user will describe the terrain he sees using a 10,000 frame imaging library to assist him in standardizing his observations. This library is stored as still frames on video discs which provide random access and the potential for mosaic production. Onboard video editing capabilities allow production of hourly, daily, and mission summary tapes in an effort to reduce the amount of TV data to manageable proportions.

Eventually we hope to integrate dynamic positioning of the ship and finally global positioning navigation into the ARGO control center. Users will have access to a wide variety of other information, including three-dimensional imaging of SEABEAM data, real-time displays of vehicle orientation in x, y, and z and a summary of his observations along track (x, y, and depth versus distance). As the operation becomes routine, ARGO will work 24 hours a day, making it an effective tool for deep ocean exploration.

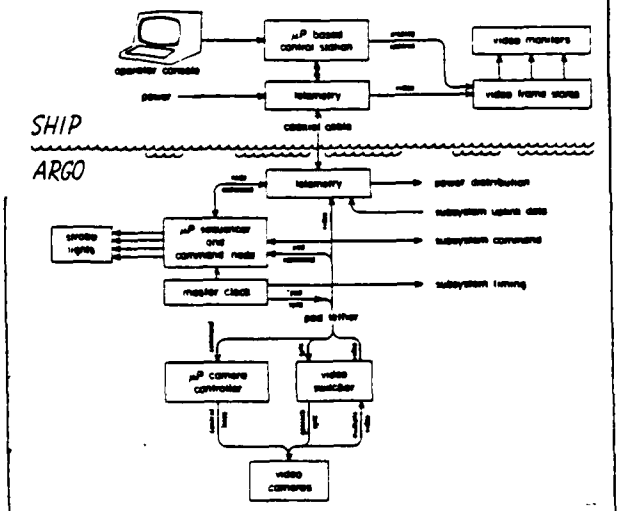

FIGURE 4: ARGO command and control architecture

ACKNOWLEDGEMENTS

This work is funded under ONR Contract No. N00014-82-C-0743.

REFERENCES

1. Ballard, R.D., Mapping the Mid-Ocean Ridge, 12th Annual Offshore Technology Conference in Houston, TX, May 5-8, 1980.

2. Wilkins, G., Specification for the Fabrication of an Armored Deep Sea Coaxial Cable, personal communication, 1983a.

3. Wilkins, G., Specification for the Fabrication of a Prototype, Deep Sea, Electro-Optical, Tether Cable, personal communication, 1983b.

4. Patterson, R.B., Increased Ranges for Conventional Underwater Cameras, Proceedings of the Society of Photo-Optical Instrumentation Engineers, 24: 253, 1971.

5. Patterson, R.B., LIBEC System Engineering, Marine Technology Society Journal, 9, (10): 3, 1975.

6. Hayward, G.G., Enhanced Inspection by New Photo and TV Techniques, International Underwater Systems Design, 3, (6): 15, 1981.

ARGO: CAPABILITIES FOR DEEP OCEAN EXPLORATION

Stewart E. Harris
Robert D. Ballard

Deep Submergence Laboratory
Woods Hole Oceanographic Institution
Woods Hole, MA 02543

ABSTRACT

Developed by the Deep Submergence Laboratory of the Woods Hole Oceanographic Institution, ARGO is an unmanned instrument platform designed for deep ocean search and survey. Integrating both visual and acoustic imaging techniques for real-time viewing, ARGO is a system which provides continuous, around-the-clock operation for seafloor exploration. With a design depth of 6,000 meters, it is towed on a steel-armored coaxial cable which supports several channels of frequency-multiplexed signals. In addition, surface support is highly integrated, bringing together ship control, navigation, and vehicle operation into a transportable control center.

In our expedition that found the TITANIC, this system was tested for the first time and proved itself by delivering the exciting pictures of the famous shipwreck lying on the bottom of the ocean. This paper will briefly describe ARGO and the reasons for its development. Examples of ARGO imaging from our first year of operation will demonstrate how modern oceanographers remotely sense the ocean floor.

INTRODUCTION

ARGO was developed to satisfy the needs of the oceanographic and military communities. It is an unmanned search and survey vehicle (Figure 1) capable of operating to 6,000 meters depth. Its tether is a steel armored, coaxial cable .68 inches in diameter. Designed to tow in a manner similar to DSL's Acoustically Navigated Geophysical Underwater Survey (ANGUS) vehicle, ARGO weighs more than 4,000 pounds and operates at altitudes of 20 to 40 meters. When ARGO is towed at speeds of approximately 1 knot, it flies about 100 meters astern of the ship, achieving a nearly vertical wire angle. When the vehicle is operated from a versatile ship, such as the R/V KNORR, we are able to position it very precisely using only the ship's propulsion system to maneuver the vehicle on the bottom. ARGO has no independent propulsion capabilities.

While providing mechanical support for the vehicle, ARGO's tether also carries power to the vehicle and a variety of signals from the sensors on board the vehicle which are modular subsystems. This modularity provides flexibility for growth and ease of maintenance and development. A wide area TV

Figure 1. Photo of ARGO during tests at the WHOI dock. The vehicle weighs 2 tons and is 15 feet long, 3.5 feet tall and 3.5 feet wide.

imaging system is integrated with side-looking sonar using this technique. This provides simultaneous broad swath acoustic and optical images that overlap in coverage and resolution.

CABLE DESIGN

ARGO's tether is the standard for the oceanographic community. Its armor package and internal structure represent a compromise among the requirements for ruggedness, low rotation, maximum strength, and long flexure lifetime. This cable has a tensile strength in excess of 36,000 pounds and provides a usable bandwidth of 5 megahertz over a 6,000-meter length. In this case, "usable" means that signal attenuation is less than a factor of 10,000. A sophisticated telemetry system allows us to multiplex the video, sonar, and power into this severely limited bandwidth.

IMAGING SYSTEMS

ARGO presently carries one forward-looking TV camera, one down-looking, and a down-looking telephoto. These are all carried on the forward end of the vehicle, as shown in Figure 2. The strobes and incandescent lights which ARGO uses to illuminate the ocean floor are carried in the after end of the vehicle. This arrangement is intended to maximize the horizontal separation between the cameras and the light sources. Computer simulations have shown that by increasing this separa-

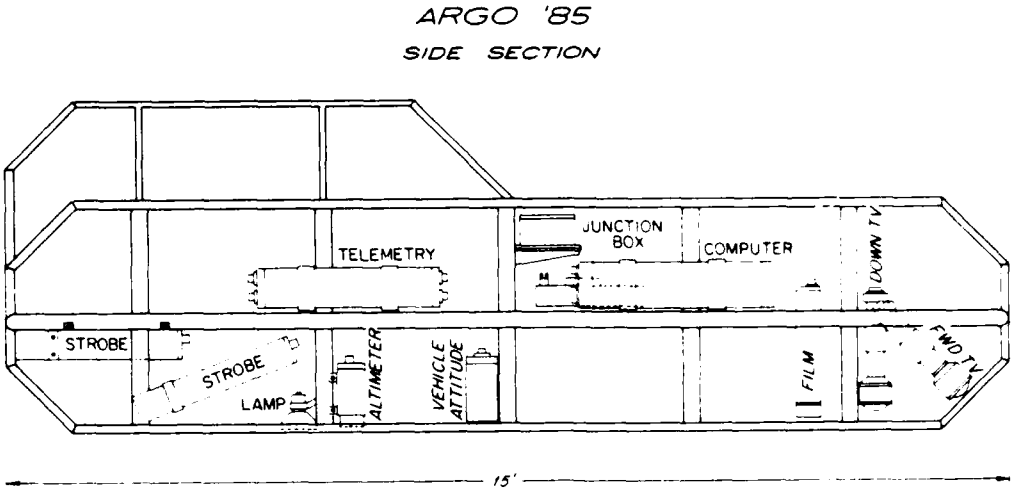

Figure 2. Schematic of ARGO showing the placement of the various components.

tion, the amount of backscatter can be significantly decreased. This in turn increases the altitude from which high-quality pictures can be obtained. Tests have shown that this geometry makes it possible to get high-quality images from an altitude of 35 meters in clear water using the strobe lights for illumination. At lower altitudes (around 10 meters) simultaneous film snapshots can be taken.

The shape of the imaged area achieved by ARGO's cameras is shown in Figure 3. By using low-light-level Silicon Intensified Target (SIT) cameras, our swath capability extends to 56 meters at 35-meter altitudes.

The high quality of video images obtained using the horizontal separation of cameras and light sources was verified during tests of of the ARGO conducted in the North Atlantic during September of 1985. During these tests good quality images were obtained in very murky water from altitudes of 15 meters. Figure 4 is an example of one of those images. This figure is a photographic still of a video image, so the resolution is lower than that available with film, and there is some blurring due to noise. The latter is emphasized when the video is frozen into a still image. This particular image is from the sequence which gave us our first verifiable evidence that we had actually discovered the TITANIC.

In addition, a simultaneous 100 KHz, side-looking sonar provides a lower resolution image of the surrounding terrain for a distance of 350 meters on each side. The optical and acoustic images complement one another: the sonar provides the large geographical picture while the video provides detail which facilitates the interpretation of the sonar images.

ADDITIONAL SENSORS

Since ARGO is intended to be a multifunctional sensor platform, additional telemetry channels are integrated to support a variety of needs. At present, vehicle attitude parameters such as altitude, depth, heading, pitch, and heave are digitized and transmitted to the surface where the data is annotated on the video image to assist operation. Other digital channels are available for this type of low bandwidth sensor. In addition, audio quality analog channels are available for sensor data. These have been used for a

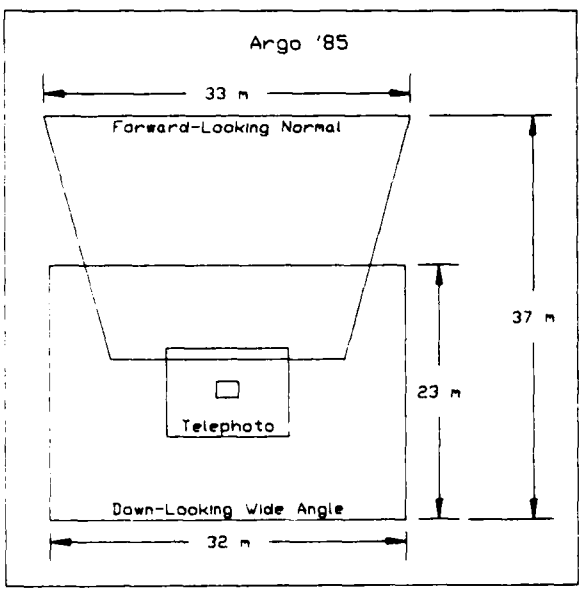

Figure 3. Footprint of ARGO's three TV cameras showing the area seen on the bottom from a 20 meter altitude.

Figure 4. A video still of an ARGO TV image taken during the TITANIC survey. Object is one of TITANIC's boilers as seen laying upright on the bottom through a telephoto lens. The boiler is about 4.8 meters in diameter.

variety of devices such as hydrophones, transmissiometer and temperature probe. The goal is for ARGO to support an arbitrary science package by providing power and digital or analog channels for downlink control and data uplink.

SURFACE SUPPORT

The real-time image processing system developed by DSL for use in the ARGO system takes advantage of state-of-the-art digital techniques for image enhancement to provide improved images, increasing user and operator understanding.

As each image is transmitted up the wire and diplayed, the user describes the terrain he sees using a 10,000-frame imaging library to assist him in standardizing his observations. This library is stored as still frames on video discs which provide random access and the potential for mosaic production. On board video editing capabilities allow production of hourly, daily, and mission summary tapes in an effort to reduce the amount of TV data to manageable proportions.

Equipment for real-time processing and viewing, as well as for recording for post-mission processing and archiving, is located in the control center, which is containerized for easy transportation and installation on oceanographic vessels.

Three operators are responsible for the operation of ARGO, the winch system, and navigation. Video, sonar and navigation data are available for use in the guidance of the ship. Eventually, we will integrate dynamic positioning of the ship, and finally global positioning navigation into the ARGO control system. Operators also will have access to a wide variety of other information, including three-dimensional imaging of Seabeam data (a commercial, highly sophisticated topographical mapping system), real-time displays of vehicle orientation, and a summary of observations along the track of the vehicle. In the future, other sensing systems and a small, tethered, remotely-operated vehicle, JASON, will be integrated into ARGO, which will increase its ability to project man's senses to the bottom of the sea.

ACKNOWLEDGEMENTS

This work was funded and supported by the Office of Naval Research, Contract No. N00014-82-C-0743.

We would like to thank the officers and crew of the R/V KNORR for their help during the expedition. Lastly, we thank the engineering and technical staff of the Deep Submergence Laboratory for their magnificent job in building and operating ARGO.

Accepted for Publication, AUVS Conference Proceedings, Boston, 1986.

ARGO/JASON: Integrated Capabilities for Exploration of the Seafloor

Stewart E. Harris
Dana R. Yoerger

Deep Submergence Laboratory
Department of Ocean Engineering
Woods Hole Oceanographic Institution
Woods Hole, MA 02543

ABSTRACT

ARGO/JASON is a remotely operated deep ocean exploration system under development at the Woods Hole Oceanographic Institution. Towed from a surface ship using a steel-armored electro-mechanical or electro-optical cable at depths up to 6000 meters, ARGO/JASON is a pair of unmanned vehicles with complementary capabilities.

ARGO is an unmanned instrument platform designed for large area search and survey. The first vehicle of its kind to fully integrate both visual and acoustic imaging for real-time viewing, ARGO is a system that provides continuous, around-the-clock operation for seafloor exploration. In our recent expedition that found the TITANIC, this system was tested for the first time and proved itself by delivering the exciting pictures of the famous shipwreck lying on the bottom of the ocean at nearly 4000 meters.

JASON is a free swimming, remotely operated vehicle that will be tethered to ARGO. JASON will complement ARGO's wide area survey capabilities with the ability to inspect objects closely and to perform manipulative tasks. JASON will feature dual manipulators, still and video cameras, and a variety of scientific payloads. A supervisory control system will permit precise movements of both cameras and manipulators from high level commands by the human operators on the surface.

This presentation will cover the history of ARGO/JASON, the reason for its development and will describe the future of this technology. Bottom

footage of the TITANIC and scenes from the expedition will be presented to describe the operation of the system and to document its performance.

ARGO

ARGO was developed to satisfy the needs of the oceanographic and military communities. It is an unmanned search and survey vehicle capable of operating to 6,000 meters depth. Its tether is a steel armored, coaxial cable .68 inches in diameter. Designed to tow in a manner similar to DSL's Acoustically Navigated Geophysical Underwater Survey (ANGUS) vehicle, ARGO weighs more than 4,000 pounds and operates at altitudes of 20 to 40 meters. When ARGO is towed at speeds of approximately 1 knot, it flies about 100 meters astern of the ship, achieving a nearly vertical wire angle. When the vehicle is operated from a versatile ship, such as the R/V KNORR, we are able to position it very precisely using only the ship's propulsion system to maneuver the vehicle on the bottom. ARGO has no independent propulsion capabilities.

While providing mechanical support for the vehicle, ARGO's tether also carries power to the vehicle and a variety of signals from the sensors on board the vehicle which are modular subsystems. This modularity provides flexibility for growth and ease of maintenance and development. A wide area TV imaging system is integrated with side-looking sonar using this technique. This provides simultaneous broad swath acoustic and optical images that overlap in coverage and resolution.

CABLE DESIGN

ARGO's tether is the standard for the oceanographic community. Its armor package and internal structure represent a compromise among the requirements for ruggedness, low rotation, maximum strength, and long flexure lifetime. This cable has a tensile strength in excess of 36,000

pounds and the coax core provides a usable bandwidth of 5 megahertz over a 6,000-meter length. In this case, "usable" means that signal attenuation is less than a factor of 10,000. A sophisticated telemetry system allows us to multiplex the video, sonar, and power into this severely limited bandwidth.

IMAGING SYSTEMS

ARGO presently carries one forward-looking TV camera, one down-looking, and a down-looking telephoto. These are all carried on the forward end of the vehicle, as shown in Figure 1. The strobes and incandescent lights which ARGO uses to illuminate the ocean floor are carried in the after end of the vehicle. This arrangement is intended to maximize the horizontal separation between the cameras and the light sources. Computer simulations have shown that by increasing this separation, the amount of backscatter can be significantly decreased. This in turn increases the altitude from which high-quality pictures can be obtained. Tests have shown that this geometry makes it possible to get high-quality images from an altitude of 35 meters in clear water using the strobe lights for illumination. At lower altitudes (around 10 meters) simultaneous film snapshots can be taken.
The shape of the imaged area achieved by ARGO's cameras is shown in Figure 4. By using low-light-level Silicon Intensified Target (SIT) cameras, our swath capability extends to 56 meters at 35-meter altitudes.

The high quality of video images obtained using the horizontal separation of cameras and light sources was verified during tests of of the ARGO conducted in the North Atlantic during September of 1985. During these tests good quality images were obtained in very murky water from altitudes of 15 meters. This expedition ultimately led to the discovery of the TITANIC which had been lost for 73 years.

In addition, a simultaneous 100 KHz, side-looking sonar provides a lower resolution image of the surrounding terrain for a distance of 350 meters on each side. The optical and acoustic images complement one another: the sonar provides the large geographical picture while the video provides detail which facilitates the interpretation of the sonar images.

ADDITIONAL SENSORS

Since ARGO is intended to be a multifunctional sensor platform, additional telemetry channels are integrated to support a variety of needs. At present, vehicle attitude parameters such as altitude, depth, heading, pitch, and heave are digitized and transmitted to the surface where the data is annotated on the video image to assist operation. Other digital channels are available for this type of low bandwidth sensor. In addition, audio quality analog channels are available for sensor data. These have been used for a variety of devices such as hydrophones, transmissiometer and temperature probe. The goal is for ARGO to support an arbitrary science package by providing user power and either digital or analog channels for downlink control and data uplink.

SURFACE SUPPORT

The real-time image processing system developed by DSL for use in the ARGO system takes advantage of state-of-the-art digital techniques for image enhancement to provide improved images, increasing user and operator understanding.

As each image is transmitted up the wire and displayed, the user describes the terrain he sees using a 10,000-frame imaging library to assist him in standardizing his observations. This library is stored as still frames on video discs which provide random access and the potential for mosaic production. On board video editing capabilities allow production of

In addition, a simultaneous 100 KHz, side-looking sonar provides a lower resolution image of the surrounding terrain for a distance of 350 meters on each side. The optical and acoustic images complement one another: the sonar provides the large geographical picture while the video provides detail which facilitates the interpretation of the sonar images.

ADDITIONAL SENSORS

Since ARGO is intended to be a multifunctional sensor platform, additional telemetry channels are integrated to support a variety of needs. At present, vehicle attitude parameters such as altitude, depth, heading, pitch, and heave are digitized and transmitted to the surface where the data is annotated on the video image to assist operation. Other digital channels are available for this type of low bandwidth sensor. In addition, audio quality analog channels are available for sensor data. These have been used for a variety of devices such as hydrophones, transmissiometer and temperature probe. The goal is for ARGO to support an arbitrary science package by providing user power and either digital or analog channels for downlink control and data uplink.

SURFACE SUPPORT

The real-time image processing system developed by DSL for use in the ARGO system takes advantage of state-of-the-art digital techniques for image enhancement to provide improved images, increasing user and operator understanding.

As each image is transmitted up the wire and displayed, the user describes the terrain he sees using a 10,000-frame imaging library to assist him in standardizing his observations. This library is stored as still frames on video discs which provide random access and the potential for mosaic production. On board video editing capabilities allow production of

hourly, daily, and mission summary tapes in an effort to reduce the amount of TV data to manageable proportions.

Equipment for real-time processing and viewing, as well as for recording for post-mission processing and archiving, is located in the control center, which is containerized for easy transportation and installation on oceanographic vessels.

Three operators are responsible for the operation of ARGO, the winch system, and navigation. Eventually, we will integrate dynamic positioning of the ship, and finally global positioning navigation into the ARGO control system. In the future, other sensing systems and a small, tethered, remotely-operated vehicle (ROV), JASON, will be integrated into ARGO.

JASON

Small, tethered ROV's are currently limited in their ability to perform manipulative tasks. A research program is currently underway to improve the capabilities of a small vehicle equipped with manipulators through the design of a supervisory control system. The goal is to approach the versatility of a human diver, rather than to develop capabilities for specific tasks. The supervisory control system will allow the operator to control the vehicle and manipulator motions in a coordinated fashion. Control system and man-machine interface issues will be investigated using computer simulation and an experimental vehicle system consisting of a modified Benthos RPV-430 and a Deep Ocean Engineering manipulator. A direct result of this work will be the supervisory control system for the JASON vehicle.

The JASON system will operate from the towed ARGO vehicle, complementing the acoustic and optical search and survey systems of ARGO. The resulting vehicle system will integrate a large area survey capability

with a small maneuverable inspection vehicle capable of dexterous manipulation. This integrated approach will allow the exploration of the ocean floor to be accomplished in a more productive manner than the current mix of towed unmanned vehicles and manned submersibles. Specifically, JASON will be applied to the detailed exploration of the Mid-Ocean Ridge system, the largest but one of the least understood geologic features on Earth.

THE JASON OPERATIONAL SCENARIO

After ARGO has located an area of interest, such as a hydrothermal vent system, ARGO will be dynamically positioned using a control system currently under development at the Deep Submergence Laboratory. Then, JASON will be deployed and maneuvered to the worksite. Typical tasks include close-up video and still photography, collection of samples, as well as the deployment and recovery of instruments and sensors. This concept is shown in Figure 3.

While outside of ARGO, JASON will be tracked using both acoustic and optical methods. Short baseline acoustic navigation carried aboard ARGO will be used to locate both vehicles relative to a single bottom transponder. Also, the optical imaging capability of ARGO will be used to track both JASON and its tether. These complementary navigation methods should allow JASON to work in a variety of difficult environments such as those encountered in mountainous underwater terrain.

JASON will communicate to the surface through the ARGO telemetry system. Both ARGO and JASON will eventually employ fiber-optic telemetry to provide high bandwidth. For JASON, the use of fiber-optics will also allow the tether to be very small and flexible.

Currently, underwater manipulative tasks are usually performed by fixing the vehicle to the worksite, either by resting on the bottom or

through the use of grabber arms. Then the task is completed using a manipulator arm with a large number of functions, typically six or more. This approach is commonly used for tasks such as salvage and recovery or cleaning and inspection of structures.

Simpler manipulative tasks can often be accomplished with some small vehicles by fixing the manipulator arm in an appropriate configuration and exploiting the vehicle's maneuverability. Observation type ROV's are often used with two or three function manipulators in this fashion to cut lines, untangle the vehicle's tether, etc.

JASON will use neither of these approaches, but will allow the operator to simultaneously control both the motions of the vehicle and manipulators in a coordinated fashion. This will allow general, six degrees-of-freedom motion of the manipulator and end effector with an arm having only a few functions. A simpler manipulator will result in the overall system being smaller, cheaper, more reliable, and decrease the required power.

This approach seems especially appropriate in deep ocean work, where currents seldom exceed a small fraction of a knot and the need to reduce size, complexity, and power is great. However, many unanswered questions remain concerning the design of such a control system, sensors, and man-machine interface.

JASON CONTROL SYSTEM

In supervisory control, a computer interacts directly with a process while a human operator manages the system. The foundations of the supervisory control system for an ROV will be closed-loop trajectory controllers.Closed-loop control of manipulator functions is common in the offshore industry today, and servo-controlled arms are available from several manufacturers. However, closed-loop control of vehicle translation

is not available, although automatic depth and altitude controls are found on many vehicles. In addition to a good control system, the vehicle and its sensors must be well designed to give good performance.

HOW DO WE DESIGN AN ROV WITH A PREDICTABLE LEVEL OF CONTROL PERFORMANCE?

Path following performance for an ROV is difficult to quantify through analysis. Generally, the speed of response and the tracking precision will be limited by a variety of factors, including sensor performance, disturbances, and the dynamic characteristics of the vehicle. Due to the nonlinear nature of underwater vehicle dynamics, existing linear control system design techniques are poorly suited to providing an understanding of an automated ROV.

Performance may also be measured in ways that have no direct relationship to tracking accuracy or response items. For instance, in the deep ocean application of JASON, quality continuous color video is a high priority. Therefore, a steady camera platform is essential. The characteristic attitude oscillations common to most ROVs constitute poor performance.

Tracking performance limitations for an ROV control system can come from a variety of sources. The available navigation sensors have limited precision and update rates and many have intrinsic time delays. The dynamics of an ROV are highly nonlinear and difficult to model precisely. Finally, the ROV is subjected to many disturbances such as forces induced by currents and a tether. In some cases, computational power may be limited.

We are currently developing control system design tools that project the closed-loop performance of an ROV given simple descriptions of the limiting factors. These techniques reveal how the different limiting factors interact, permitting the designer to concentrate on those elements

that affect performance most. The techniques can save both effort and cost by allowing simplified dynamic models to be used for the control system design while guaranteeing stability and achieving a defined level of performance.

The basis for this work is a robust control technique for nonlinear systems called sliding control. Sliding control theory [2,3] and details of its application to underwater vehicles [1,4,5] can be found in the references.

An outline of the sliding control design procedure is shown in Figure 4. There are three inputs to the design process: specification of the desired closed-loop dynamics; approximate dynamic model of the vehicle; and estimates of the uncertainties in the model. The design method not only produces simple controllers that perform well, but also directly provides information about system performance given a description of the limiting factors.

The desired closed-loop dynamics are typically specified to be those of a low-order, linear system (e.g., first order linear, critically damped linear second-order system, etc.). In each case, the desired "target" dynamics will have a low-pass characteristic with a specified bandwidth. The closed-loop system will not be expected to respond infinitely fast. The bandwidth limit reflects basic limitations of the system and may originate from several sources including navigation system specifications, actuator and power limits, unmodelled vehicle dynamics, and disturbances.

In addition to the desired or target dynamics, the open loop dynamics of the vehicle must also be specified. This model can contain nonlinear terms for the drag effects, and may also include time-varying added mass

terms. This control system design technique is completely compatible with the types of models produced by hydrodynamic analysis.

Another input consists of estimates of the uncertainty in the dynamic model. These estimates may also be in nonlinear form and account for uncertainties in model parameters, structural simplifications of the model, and disturbances.

This technique summarizes performance in a powerful way in a nonlinear context. Any control system design technique will allow evaluation of closed-loop bandwidth and disturbance responses, but sliding control provides a single unified metric for each degree of freedom that combines the effect of bandwidth limitations and dynamic uncertainty.

Sliding techniques permit a nonlinear dynamic model to be used directly to design a closed-loop system with no need for linearization. This suits the ROV control problem well, since the vehicle dynamics are highly nonlinear and there are no obvious operating points about which to linearize the model [6].

ROVs typically move in all directions, so linearizing about values of forward speed is not the best approach. Designing a stable controller using the nonlinear model directly simplifies the design and implementation of the controller and gives more uniform behavior over the entire range of operation.

An error metric and a time-varying envelope of its expected bounds, both integral to the control computation, provide simple confirmation that the controller is operating as expected, and give a direct, continuous measure of controller performance.

EXPERIMENTAL RESULTS: POOL TEST

Trials using the Benthos RPV-430 ROV in a pool demonstrated closed-loop vehicle control in a trajectory tracking task [1]. Those tests used a sliding controller running at 10 Hz to fly predetermined paths. A prototype Applied Sonics SHARPS navigation system with repeatability of a few millimeters was used for position feedback [7]. The SHARPS (Sonic High Accuracy Ranging and Positioning System) consists of a set of hard-wired receivers placed in a net with a transmitter on the vehicle.

These tests showed that following a trajectory with high accuracy is possible using sliding control. Figure 5 shows desired and measured positions while following a rectangular trajectory in the pool. Errors in position were generally less than two inches. Speeds during this trial were 1.1 feet per second.

Figure 6 shows the error metric, s, for the controller, staying within the "boundary layer", indicating that uncertainties have been adequately bounded. The model used had 50% uncertainty in both drag coefficient and effective mass. A more refined model would be directly reflected in both the metric s and the boundary layer thickness ϕ.

The uncontrolled pitch and roll modes of the RPV, at about 0.4 Hz, were found to limit bandwidth as these modes were coupled to translation. Therefore, the bandwidth of the controller had to be limited to well below 0.4 Hz.

APPLICATION TO JASON

Via sliding control, we have developed some concepts regarding what constitutes "good" vehicle design from a control perspective. Generally these concepts would also improve vehicle performance using other closed-loop design methods of manual control.

These concepts are being employed to make JASON a productive scientific instrument. Components and techniques are being refined in shallow water tests using the RPV-430 vehicle. This summer we expect to test the RPV in high currents to investigate high-bandwidth and adaptive control techniques for both the vehicle and manipulator.

ACKNOWLEDGEMENTS

This work was sponsored by the Office of Naval Research, Contract No. N00014-84-K-0070, N00014-82-C-0743, N00014-85-C-0410. Material support was also received from IBM and Applied Sonics, Inc., Gloucester, Virginia, USA.

REFERENCES

1. D.R. Yoerger, J.B. Newman, J.-J.E. Slotine, Supervisory Control System for the JASON ROV, to appear, IEEE J. Oceanic Eng., 1986.

2. J.-J.E. Slotine, Tracking Control of Nonlinear Systems Using Sliding Surfaces, Ph.D. Thesis, MIT Dept. of Aero. and Astro., May 1983.

3. J.-J.E. Slotine, The Robust Control of Robot Manipulators, Int. J. Robotics Res., Vol. 4, No. 2.

4. D.R. Yoerger, J.-J.E. Slotine, Robust Trajectory Control of Underwater Vehicles, IEEE J. Oceanic Eng., Vol. OE10, #4, October 1985.

5. D.R. Yoerger, J.B. Newman, Demonstration of Closed-Loop Trajectory Control of an Underwater Vehicle, Proc. Oceans 85, IEEE/MTS, San Diego, 1985.

6. D.H. Lewis, J.M. Lipscombe, P.G. Thomasson, The Simulation of Remotely Operated Vehicles, Proc. ROV 84, MTS, 1984.

7. D.A. Hahn, G.N. Williams, M. Wilcox, P. Wilcox, A Computerized High Resolution Underwater Triangulation Mapping System, Proc. Oceans 85, MTS, 1985.

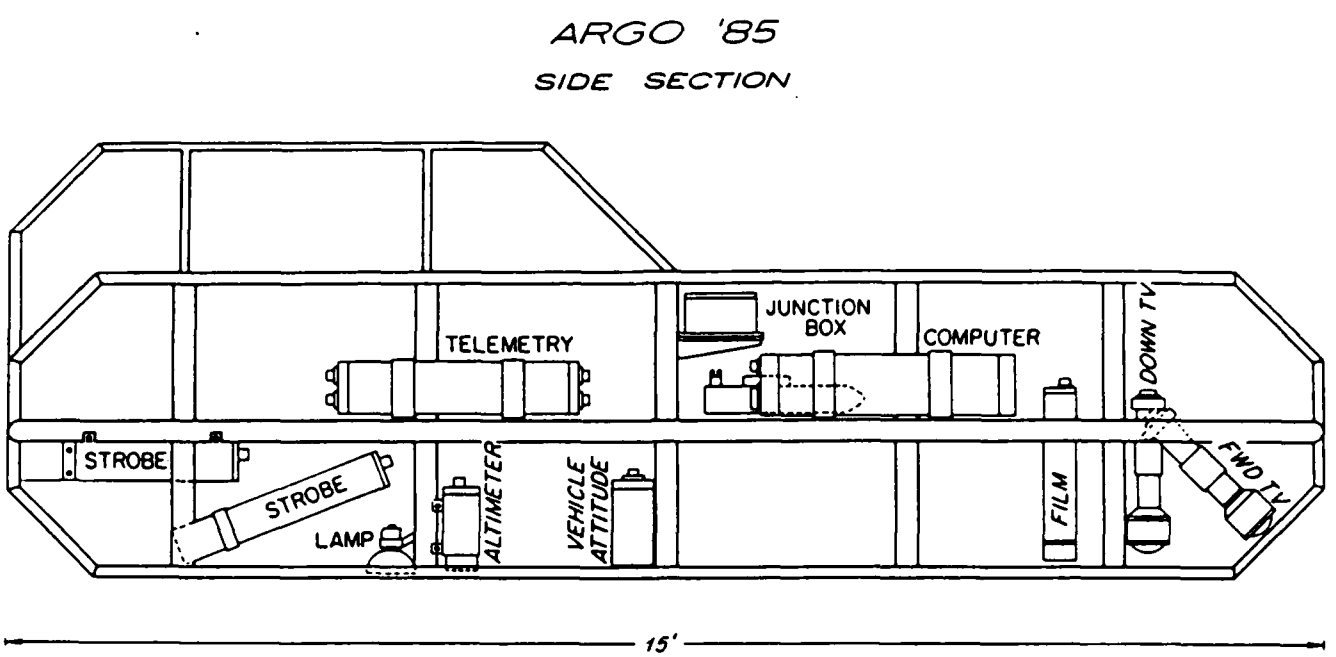

FIGURE 1: Schematic of ARGO showing the placement of the various components.

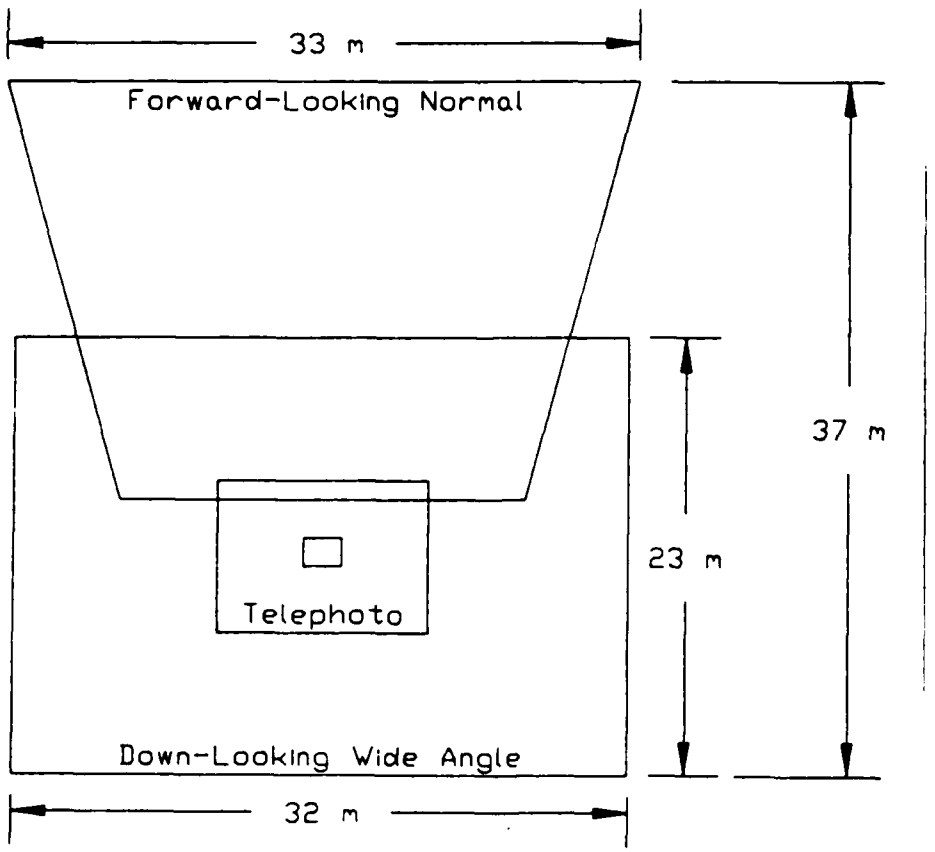

Figure 2: Footprint of ARGO's three TV cameras showing the area seen on the bottom from a 20 meter altitude.

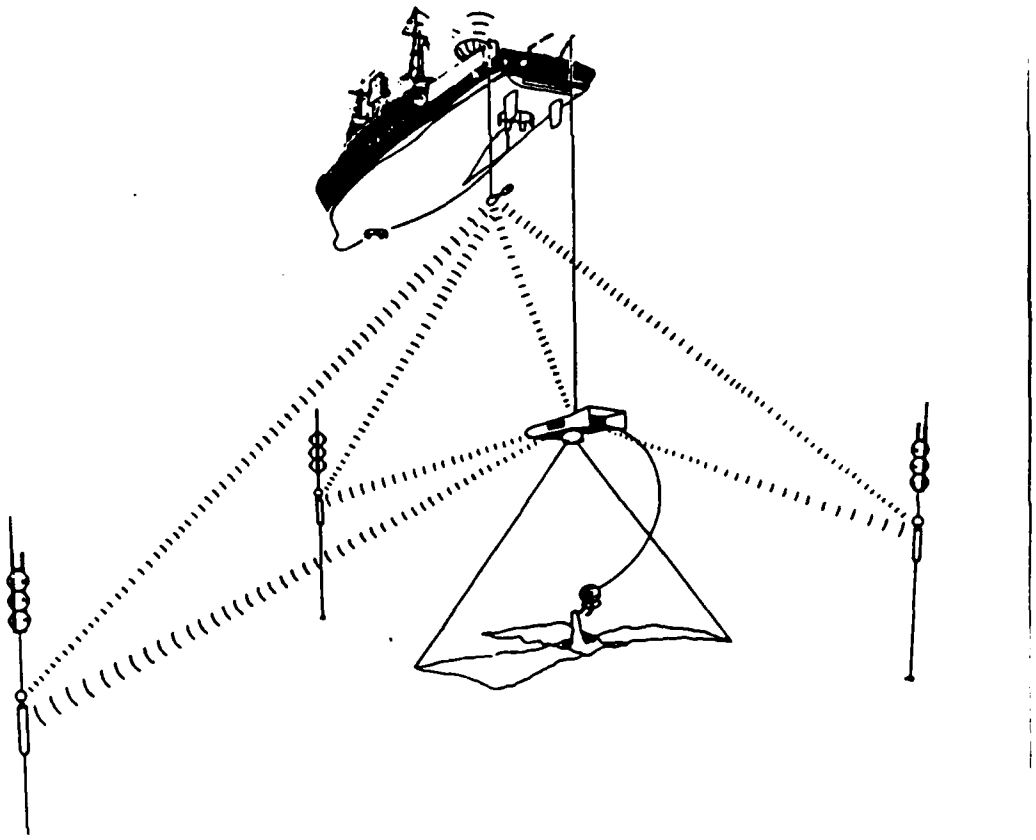

FIGURE 3: JASON will be deployed while ARGO and the surface vessel are dynamically positioned. JASON will be tracked both acoustically and optically from ARGO.

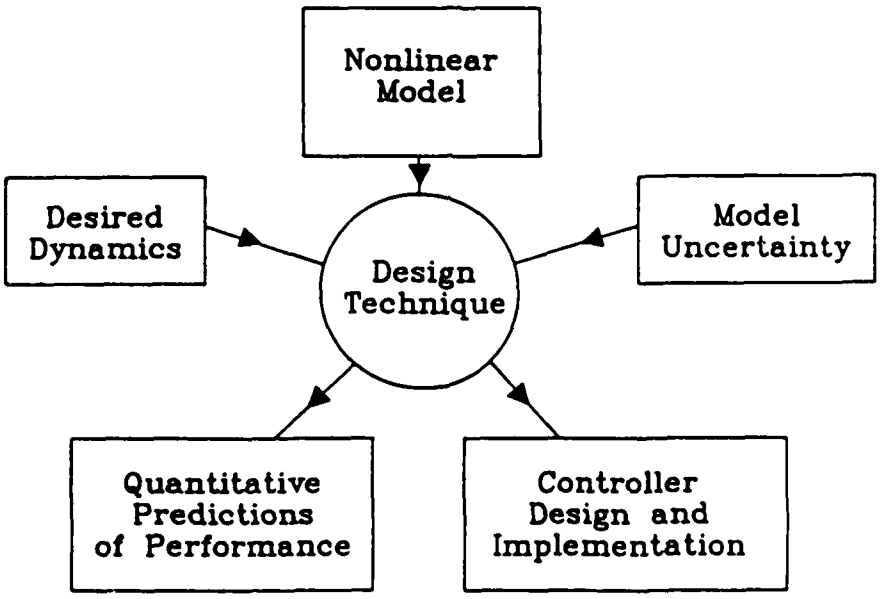

FIGURE 4: A summary of the sliding control design method. Given an approximate dynamic model of the vehicle, a desired dynamic characteristic, and estimates of model uncertainty, the performance of the closed-loop system can be easily projected.

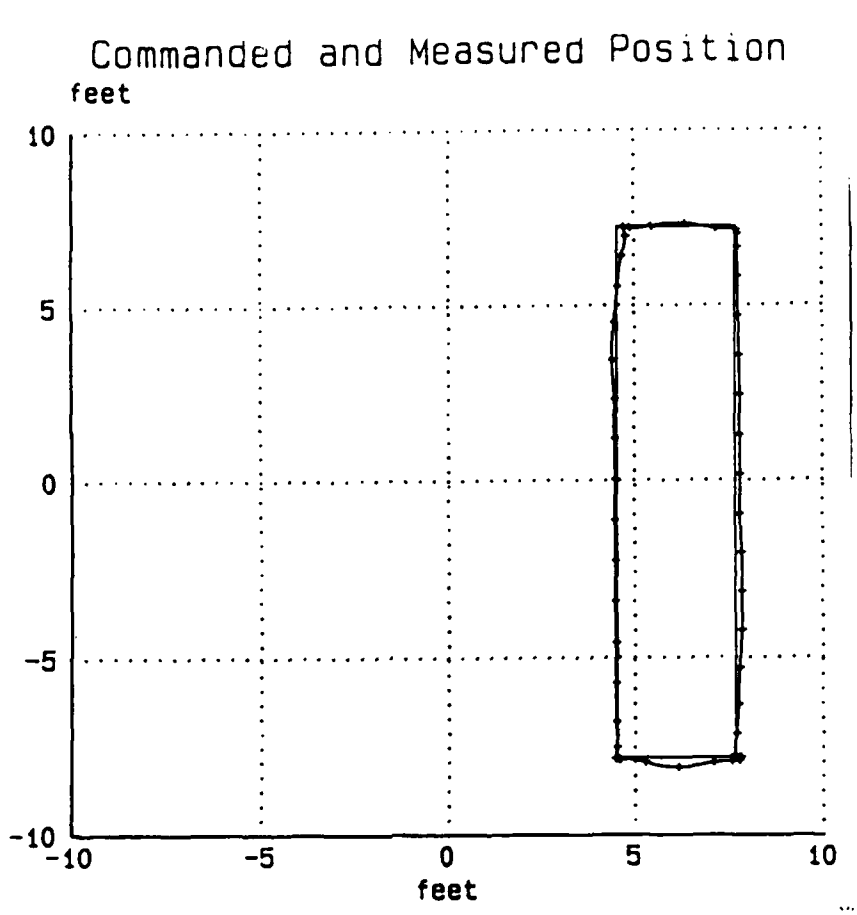

FIGURE 5: Commanded position (plain line) and measured position (with ticks) from an automatic control test in a pool. X direction is to the right. Position errors do not exceed a few inches.

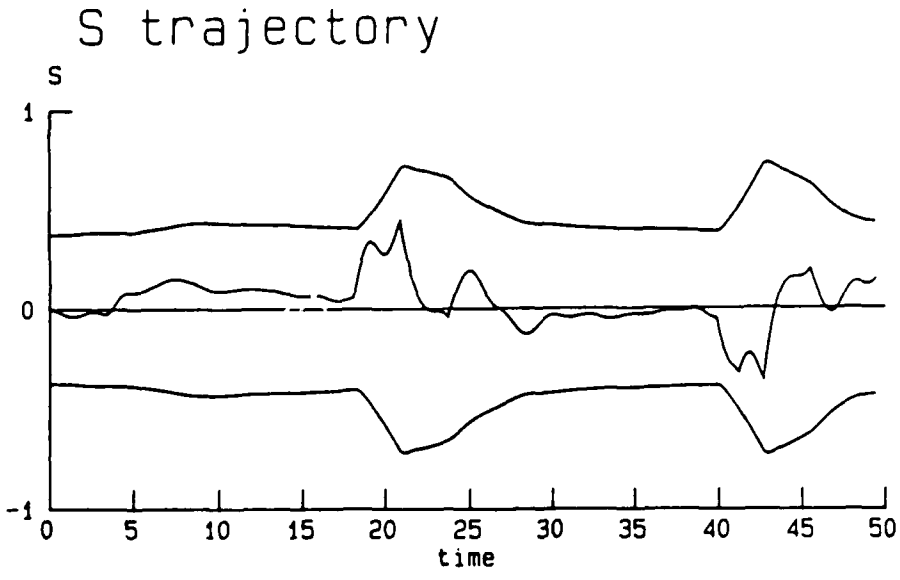

FIGURE 6: The error metric for the X direction during the automatic control test. A time-varying envelope (called the "boundary layer") is also shown. The error metric (called "s") is guaranteed to remain inside the boundary layer if uncertainty is bounded correctly.

ROV '86 IEEE/MTS

DEMONSTRATION OF SUPERVISORY CONTROL FOR ROV'S AND MANIPULATORS

Dana R. Yoerger James B. Newman

Deep Submergence Laboratory
Department of Ocean Engineering
Woods Hole Oceanographic Institution
Woods Hole, Massachusetts 02543

ABSTRACT

JASON is an ROV for deep ocean scientific tasks currently under development at the Deep Submergence Laboratory of the Woods Hole Oceanographic Institution. A key element of the vehicle will be a supervisory control system that coordinates the movements of the vehicle and manipulators, allowing more complex and precise tasks to be performed.

In this paper, the low level control system that provides precise positioning of the vehicle is described. These closed loop controllers underlie the higher level supervisory functions such as planning, teaching and monitoring.

The control system is designed to deal with the specific problems of underwater vehicles and manipulators, including nonlinear and imprecise models, coupling between movements, noisy measurements, and limited computational power. The control system is very general, and is readily adaptable to different vehicles and manipulator systems. Simulation results for a Benthos RPV-430 vehicle are presented.

INTRODUCTION

The Deep Submergence Laboratory of the Woods Hole Oceanographic Institution is currently designing JASON, an ROV for deep ocean scientific applications. Deployed from the ARGO wide area survey vehicle [1], JASON will act as the eyes and hands of the scientists aboard the research vessel. One emphasis in the JASON program is the refinement of supervisory control techniques.

JASON will be one member of a family of vehicles developed and operated by DSL for the exploration of the Mid-Ocean Ridge. Other DSL assets include several sidescan sonars, video survey systems, and photographic systems. All systems operate to depths of 2000 ft. (6000m).

The Deep Submergence Laboratory has an ongoing program of research in the control system techniques that will make vehicles like JASON more capable and easier to operate. JASON will include a control system that allows the motions of the vehicle and the manipulators to be controlled and coordinated. Vehicle attitude and position as well as manipulator position will be controlled by very precise automatic control loops.

A supervisory control system that includes control of vehicle translation can improve a vehicle's capability substantially, particularly for manipulation tasks. For a small ROV, closed loop control of vehicle translation will allow the vehicle motions to compliment the manipulator movements, reducing the need for heavy grabber arms to hold the vehicle on station. Taking advantage of vehicle movement can also reduce the number of manipulator degrees of freedom required to execute a specific task. The resulting decrease in vehicle size, weight, power, and mechanical complexity are especially attractive for a full ocean depth vehicle such as JASON. Although automatic depth and attitude controls are commonly found on many vehicles, full closed loop control of translational position and velocity requires that many difficult problems be solved.

An automatic control system relies on measurements or estimates of the vehicle state. To control the position of a vehicle, good estimates of both position and velocity are required. The most practical means to sense the position of the vehicle is by acoustic travel times or direction measurements. The resulting measurement noise and low sampling rate inherent in typical acoustic navigation systems makes the extraction of velocity information difficult, generally requiring a very low system bandwidth. An existing high frequency acoustic positioning system combined with state estimation techniques have been shown in simulation to permit precise, high bandwidth control.

The dynamics of vehicles moving through a fluid are fundamentally nonlinear due to inertial, buoyancy, and hydrodynamic effects [2]. These nonlinear effects are difficult to model and identify, and can change significantly when manipulators or other work packages are added. The dynamics of the tether are also difficult to model and contribute very large forces. Forces induced by currents can be large and are difficult to estimate. For these reasons, traditional linear design methodologies are poorly suited to this type of problem, and at best produce results that are difficult to extend from one type of vehicle to the other. A recently developed robust nonlinear design methodology can deal directly with these types of difficulties and has been demonstrated in simulation.

Reference 4

An overall view of the low level control system currently being tested is shown in figure 1. Beginning at the lower right, vehicle position information is obtained from the acoustic navigation system. Vehicle attitude and manipulator position and velocity are obtained through the telemetry link from the vehicle. The estimator removes noise from the measured positions and computes the velocities. The nonlinear control law computes the appropriate forces and moments given the desired and estimated states. Since there are generally more thrusters than vehicle degrees of freedom, a thruster allocation module chooses the appropriate combination of thrusters to produce the desired forces and moments.

This control system is currently being tested using a vehicle and manipulator similar to those planned for the operational JASON vehicle. A Deep Ocean Engineering Manipulator has been added to a Benthos RPV 430 vehicle. Additional telemetry has been added to the RPV system using an 8 bit microprocessor system. Navigation processing, control system, and display functions have been implemented using an IBM PC AT computer.

MEASUREMENT AND STATE ESTIMATION

Obtaining good estimates of the entire vehicle state is one of the most difficult problems in designing an automatic position control system for an ROV. Most acoustic navigation systems have relatively low update rates (1 sample per second or slower), and have high noise or "jitter" specifications (typically a large fraction of a meter). High noise and a low sampling rate require that the state estimator have a slow response time, resulting in a low overall system bandwidth.

Fortunately, precise, high bandwidth control is often required only in a small area. This is especially true of manipulation tasks. This implies that much higher frequency, shorter range navigation can be used. Higher frequencies yield higher precision (less jitter), and allow much higher update rates because echoes die quickly.

On an experimental basis, an 800 khz. positioning system is being tested at DSL for application to vehicle control. The system is called SHARPS (Sonic High Accuracy Ranging/Positioning System) and is produced by Applied Sonics Corporation of

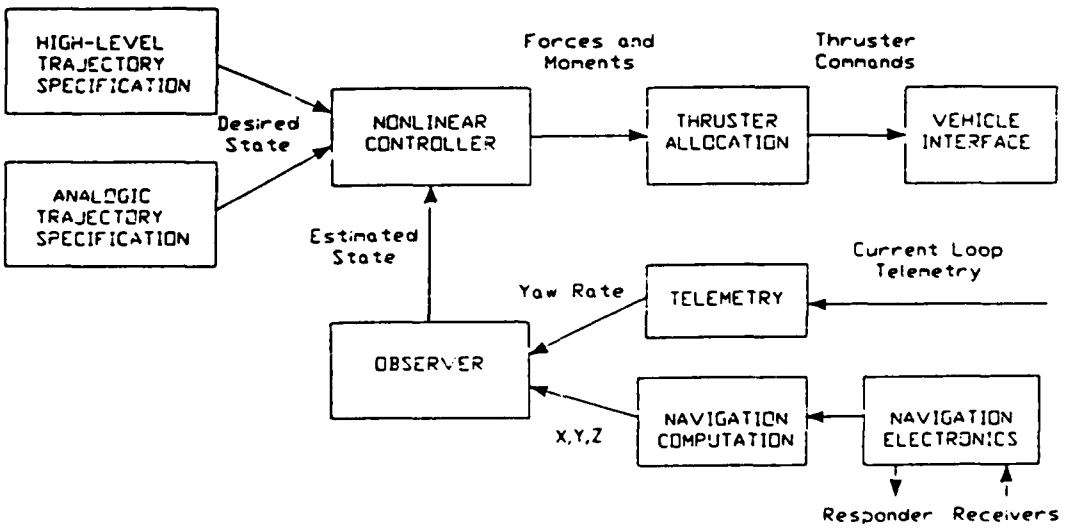

Figure 1. Control System Block Diagram. The prototype control system now being tested at DSL is implemented on a microcomputer on the surface. After a series of experiments using a Benthos RPV 430 vehicle and a Deep Ocean Engineering manipulator, portions of the control system will be moved to microcomputers on the JASON vehicle.

Gloucester, Virginia. The system uses a set of hardwired transceivers to determine range between any two transceivers, one of which is placed on the ROV. Range resolution of the system is better than 2 mm. and the maximum range is 30 meters. Position updates can be obtained over 20 times per second. Although the hardwired nature of the system limits its application to relatively shallow applications, the transducer technology employed is not fundamentally depth limited, and a transponding version will likely be produced for the JASON program. The current system is ideal as a control system development tool and can also be used to measure the average current through the navigation net.

A state estimator has been used to construct both position and velocity estimates from the noisy position data. Currently, good results have been obtained using a suboptimal (fixed gain) Kalman filter. To show the insensitivity of the estimator to modelling errors, a simulation was performed using an estimator based on an ROV model where the effective mass was 20% in error, and the drag coefficients were 50% in error.

Figure 2 shows measured and estimated position during a complex vehicle movement. The simulated measurements contain several times more noise than the level demonstrated in the SHARPS system. The two curves are nearly identical, except that the high frequency component has been removed from the estimate.

Figure 3 shows a close up view of several seconds from figure 2. The simulated measurements are noisy, but the estimate is smooth. Although the estimate is well filtered, no lag is apparent when the system starts to move at the end of the plot. This is possible because the estimator includes a dynamic model of the vehicle that is driven with the same commanded forces as the actual vehicle. Simply filtering the navigation fixes would always introduce phase lag.

Figure 4 shows estimated and actual velocity from the simulation. Note that actual velocity is not available in practice, but is available in the simulation to check operation of the estimator. Agreement is close, little noise appears in the estimate, and little phase lag is introduced.

In addition to filtering position and estimating the velocity, the estimator is also used to reject spurious navigation fixes. Each fix can be compared to the previous estimate (not the previous fix) and ignored if it exceeds a limit. The appropriate limit can also be derived from the estimator. When fixes are rejected, the estimator continues to extrapolate the state based upon the last good fix and from the requested control forces and moments.

Manipulator state information is easier to obtain. The DOE manipulator has been modified to include optical encoders on the shoulder and elbow, allowing position and velocity to be computed directly.

NONLINEAR CONTROL TECHNIQUES FOR ROV'S AND MANIPULATORS

ROV's are nonlinear, high order dynamic systems which are difficult to model and control. ROV's are more difficult to control in many respects than other types of vehicles such as submarines, ships, and aircraft. Drag and added mass coefficients are difficult to obtain, and at best models only approximate the real behavior of real vehicles. The dynamics of bodies that are not streamlined such as ROV's can be influenced by highly nonlinear phenomena such as vortex shedding. There is generally a large amount of coupling between axes. The omnidirectional motion characteristics of most ROV's make coupling effects very important. As a result, decomposing the control system into a number of low order loops is difficult. These problems become even more severe if simultaneous motion of manipulators is also present.

The important qualities for a control system design methodology for combined control of ROV's and manipulators result from these complex dynamic properties. The method should be able to deal directly with nonlinear dynamics, and must produce consistent and predictable results from approximate or even poor models. The method must take into account the coupling between axes without becoming unwieldy. The low bandwidth of the vehicle thrusters must also be dealt with.

A recently developed variation on sliding mode control [3] meets these requirements and also has other attractive features. The method is called "suction control", although this name refers to a geometric description of the resulting state space behavior, not any hydrodynamic effect. Simulation results show great promise, and tests in the water are currently in progress. The theory and application of the method are covered in the references [3,4,5] and will not be repeated here. Instead, a description of the method will be given and some simulation results presented.

The first important quality of the method is its ability to directly deal with nonlinear systems. Traditional linear design methods require that the plant equations be linearized. For a submarine, torpedo, or airplane, the system equations are linearized about different values of forward speed and a different controller designed about each operating point. Since an ROV can generally move in any direction, the equations must be linearized about many combinations of operating points or important aspects of the dynamic behavior will be ignored. Using this new technique, no linearization is required and one control configuration can give stable, consistent performance over the entire operating range of the vehicle.

Suction control can guarantee stability and performance despite errors in the model used to design the controller [3]. In other words, it is a robust technique. If limits can be placed on the modelling errors, then stability is assured. Additionally, tracking error bounds can also be

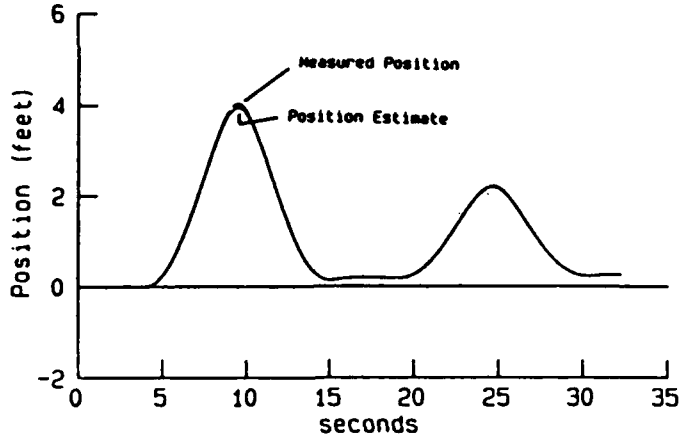

Figure 2. Estimator Performance for Position. The position estimate follows the navigation fixes, but with noise removed. Estimation errors occur only during the periods of high acceleration. To show insensitivity to model errors, the estimator was based on a model substantially different from the vehicle simulation.

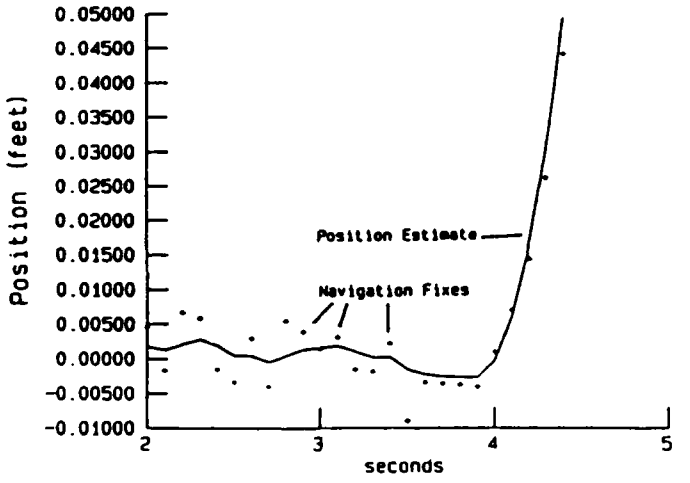

Figure 3. Details of Position Estimation Performance. Although the estimator smooths the noisy position data, little phase lag is introduced because the estimator includes a model of the vehicle that is driven by the same thrust commands as the vehicle.

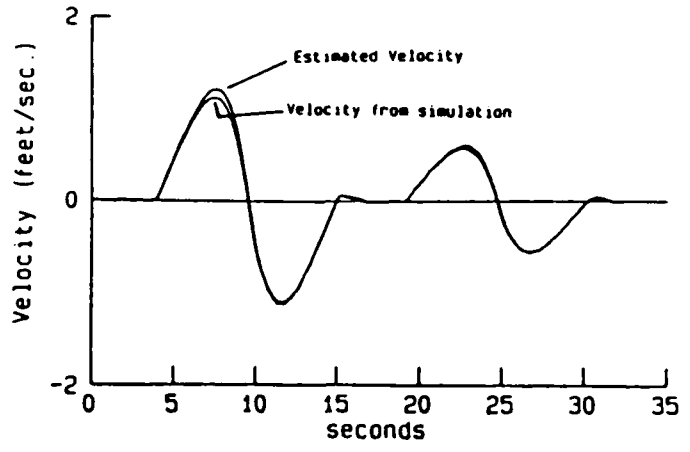

Figure 4. Velocity Estimation Performance. An estimate of velocity must be obtained since there is no way of measuring it directly. Despite modelling errors, the velocity estimate follows the velocity of the simulation with little phase lag.

guaranteed given limits on model uncertainty and the parameters of the desired trajectory. This powerful view of robustness is extremely useful for control system design. The designer can determine the required model precision depending on the performance desired. Often analysis will show that exhaustive tank testing of the vehicle or extensive computer modelling is not needed. The designer can also drop high order terms in the model, and in each case the effect on system tracking performance can be seen directly. These capabilities will generally allow the system model to be simplified dramatically without changing performance significantly. Similarly, the system parameters that should be known with good precision can also be identified. The relationship between model precision and tracking error for a simulated ROV is demonstrated in one of the references [5].

The methodology also allows a system with many degrees of freedom to be controlled using a set of low order controllers, one for each axis [4]. A feedforward or "inverse plant" type of control action is computed based on the system model, which can reflect any amount of interaction between axes. All available information about coupling is utilized. To this inverse plant control action, the nonlinear feedback loops are added. These loops, which are completely local, guarantee stability and performance despite the errors in the inverse plant control action resulting from an imprecise model. This property of the technique makes designing control systems for multi-axis systems such as vehicles with manipulators much easier. Often no single loop must be more than second order.

The Benthos RPV 430 vehicle was simulated. A control system was designed using a model that differed from the simulation by 20% for the effective mass, and 50% for the drag coefficients. Simulation runs showed that the system performs as anticipated when combined with the state estimator and noisy measurements described earlier. Tracking error remained below the projected limits, and commanded thruster forces contained no high frequency components.

Figure 5 shows a simulation run for a multi-axis motion. The plot shows the horizontal plane, and both the desired and estimated tracks are shown. During the first segment the vehicle moved sideways through a half circle while keeping the camera pointed towards the center of the circle, a typical inspection maneuver. During this segment, the vehicle accelerated to the maximum sideways velocity, then deccelerates to zero velocity. During the second segment, the vehicle moves closer to the center of the circle, again using a constant acceleration-constant deceleration trajectory. The third segment is similar to the first, but at slower speed and in the reverse direction. A disturbance force of 10 lbs. acting in the negative X direction was included. Maximum position errors during the entire trajectory are less than two inches.

Figures 6 and 7 show close-up views of interesting regions of figure 5. Desired and estimated position are plotted, and the measured positions are also included. The errors that can be seen arise from several sources. The disturbance force gives rise to small errors in both the state estimates and the control. The limited bandwidth imposed on the system to protect the vehicle thrusters is responsible for some of the error. The outstanding performance of the control system implies that there is little to be gained by improving the model.

CONCLUSION

Combined closed-loop control of ROV and manipulator motions appears quite feasible from a control system design perspective. A new nonlinear design technique matches the dynamic problem well. Controllers capable of outstanding performance can be designed using approximate nonlinear models of vehicle dynamics. These controllers have been shown in simulation to work will in combination with short range, high precision acoustic navigation systems now appearing on the market and traditional state estimation techniques.

These techniques can greatly improve the usefulness of small ROV's for manipulation tasks. By eliminating grabber arms and eliminating degrees of freedom that are redundant with the motions of the vehicle, simpler systems can be used to perform complex, precise work tasks.

These control techniques can underlie sophisticated supervisory control systems, which have been shown to improve performance and decrease reliance on visual feedback in a variety of tasks. Experiments are now being conducted in the water to refine these techniques and demonstrate their usefulness for a variety of tasks.

ACKNOWLEDGEMENTS

This work was sponsored by the Office of Naval Research, Contract No. N00014-84-K-0070 and Contract No. N00014-82-C-0743. Support was also received from IBM and Benthos, Inc.

REFERENCES

1. Ballard, R.D., ROV Development at Woods Hole's Deep Submergence Laboratory, Proc. ROV '84, MTS, 1984.
2. Lewis, D.J., Lipscombe, J.M., Thomasson, P.G., The Simulation of Remotely Operated Vehicles, Proc. ROV '84, MTS, 1984.
3. Slotine, J.-J. E., Tracking Control of Nonlinear Systems Using Sliding Surfaces, Ph.D. Thesis, MIT Dept. of Aero. and Astro., May 1983.
4. Slotine, J.-J. E., The Robust Control of Robot Manipulators, Int. J. Robotics Res., Vol 4, No. 2.
5. Yoerger, D.R., Slotine, J.-J. E., Robust Trajectory Control of Underwater Vehicles Using Nonlinear Design Techniques, in press.

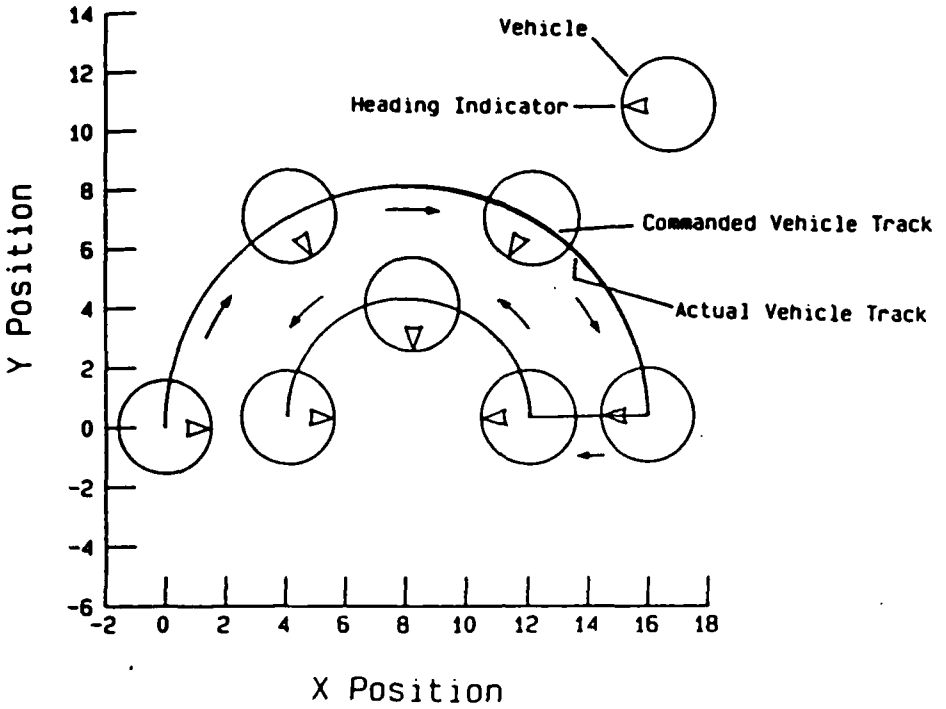

Figure 5. Closed Loop Simulation Performance. A complex trajectory is commanded that includes simultaneous movement about sideways translation and heading. Although the peak velocity reaches the maximum for the vehicle, tracking errors are extremely low despite modelling errors and a simulated current force.

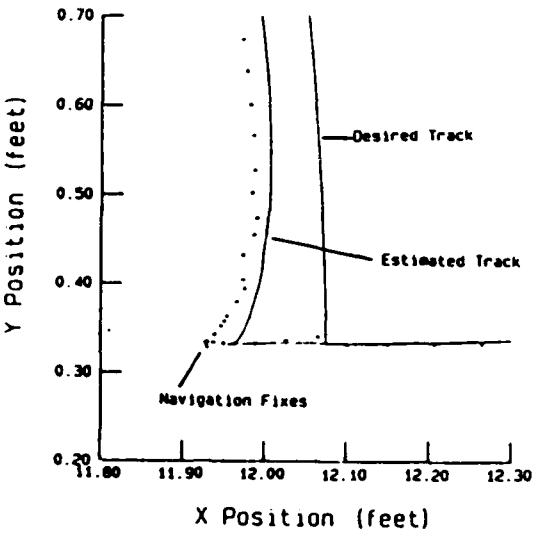

Figure 6. Details of the Simulation. The simulated noise in the position fixes can be seen. The simulated current causes both estimation errors and control errors and accounts for the observed offsets. The overshoot results from the bandwidth limit imposed on the controller as well as modelling errors.

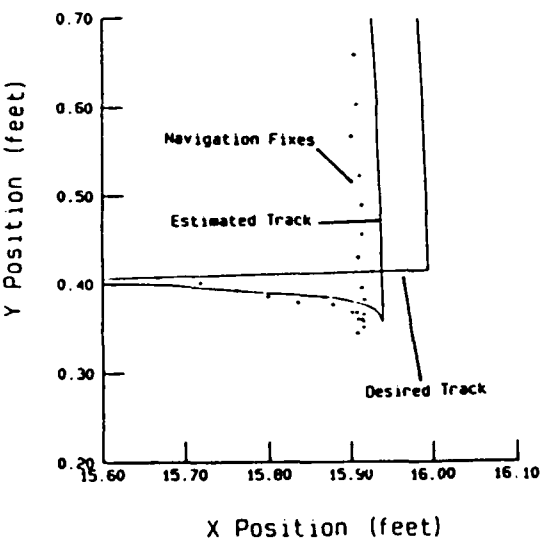

Figure 7. Additional simulation details. Again, errors are very low and are mainly caused by bandwidth limitations and the simulated current.

DEMONSTRATION OF CLOSED-LOOP TRAJECTORY CONTROL OF AN UNDERWATER VEHICLE

Dana R. Yoerger
James B. Newman

Deep Submergence Laboratory
Department of Ocean Engineering
Woods Hole Oceanographic Institution
Woods Hole, MA 02543

ABSTRACT

The design of the closed-loop control system is a primary issue for any underwater vehicle that is not controlled manually. Precise control of all vehicle movements is particularly difficult due to the high-order, nonlinear, uncertain nature of the dynamics of underwater systems. A new control system design methodology called sliding control has been shown to deal with these difficult problems effectively. In this paper, the methodology is reviewed and results from in-water tests are described.

INTRODUCTION

Any underwater vehicle that is not controlled manually must include some type of closed-loop control system. A present goal of the Deep Submergence Laboratory is to develop design techniques that enable this problem to be solved generally rather than on a case by case basis. A new nonlinear control system design technique called sliding control matches this problem well. Control systems designed using this technique have been demonstrated in simulation and on a test bed vehicle in the water.

Using sliding control, the closed-loop system can be designed more easily and effectively than by using traditional linear techniques. No linearization of the plant equations is required, and the resulting design is explicitly robust to model uncertainty and disturbances. Unlike other robust nonlinear techniques, the control action can be bandwidth limited to prevent excitation of unmodelled high frequency modes. Also, sliding control features a quantitative trade-off between model uncertainty and tracking performance. This feature usually allows the model of the vehicle to be greatly simplified without jeopardizing stability while the effects of the simplification on performance are explicit.

The closed-loop system must be monitored for either an autonomous or a teleoperated vehicle. Sensor failures, thruster degradation, collisions, or other changes in the vehicle dynamics should be detected quickly. However, separating the tracking errors caused by acknowledged uncertainty from errors caused by failures is a difficult task.

Sliding control also addresses this issue directly. The quantitative relationship between model uncertainty and performance can be directly used to monitor the system for unexpected change.

UNDERWATER VEHICLE DYNAMICS AND CONTROL SYSTEM DESIGN

Underwater vehicles represent a difficult control system design problem not well suited to traditional approaches. The dynamics of vehicles are described by high order models that are nonlinear and uncertain. A typical model of an ROV can have over two hundred coefficients representing various nonlinear effects [1,2].

While techniques for producing good models of vehicles are well advanced, the corresponding control methods are not. Linear control techniques are generally used for control system design. These techniques often cannot easily take advantage of the detailed, nonlinear models that modern hydrodynamic analysis can provide. Much detailed information about the dynamics of the system is usually discarded when the model is linearized unless the system state remains close to the state about which the dynamics were linearized.

While linear techniques can produce stable designs for high-order nonlinear systems such as vehicles, a set of many linearized controllers is often required for good performance. A single linear controller may not perform consistantly as the velocity of the vehicle changes. For example, a linear controller for a submarine may use several controllers, each designed using a model of the submarine linearized about one value of forward speed [3]. As the submarine changes speed, the gains will be changed accordingly.

This approach is not practical for a vehicle that can move omnidirectionally like many underwater inspection and work vehicles, since there are no obvious operating points about which

to linearize. Such a situation could only be handled by a large number of linear controllers designed for different combinations of speed along all axes. Even if a complex design utilizing many linear controllers was implemented, the stability of such "gain scheduled" systems may be questionable.

A good control system design methodology for underwater vehicles would allow a designer to use a single nonlinear model of vehicle behavior directly without linearization. This would permit one controller to be used regardless of how the vehicle is moving, rather than changing the controllers as the speed changes.

A good control system design technique for underwater vehicles should also allow the model upon which the controller is based to be systematically simplified while explicitly preserving stability. Clearly, two hundred nonlinear terms do not need to be considered to obtain good control system performance. The problem is to put the simplification on a rational basis. The performance implications of all simplifications should also be explicit, allowing the designer to preserve the terms that contribute most to performance.

ROBUST CONTROL OF NONLINEAR SYSTEMS USING SLIDING CONTROL

This section will describe the basic features of sliding control, with emphasis on the design implications. More complete discussions of the underlying theory and details of implementation can be found in the references [4,5,6].

Specification of the Desired Closed-Loop Dynamics

All closed-loop control system design involves transforming the natural dynamics of a system to dynamics that are more desirable. While vehicle dynamics are nonlinear, it is reasonable that the desired or target dynamics should be linear.

Traditional regulators are not sufficient for control of the trajectory of a vehicle or a manipulator, instead tracking controllers are required. Given a desired trajectory specified in terms of velocity, displacement, and perhaps acceleration, the controller should make reasonable compromises between position and velocity errors. This requires that the target dynamics include both position and velocity error terms.

For a second order mechanical system, reasonable linear target dynamics would specify a stable first order relationship between position and velocity errors, for example:

$$0 = \dot{\tilde{x}} + \lambda \tilde{x},$$

where $\tilde{x}$ is the displacement error and λ is a constant used to set the break frequency of the desired first order error response.

Linear error dynamics such as this can be represented as a surface in state space that passes through the desired state. For a second order example, this corresponds to a line that passes through the point $(x_d, \dot{x}_d)$. As shown in Figure 1, this line will move with the desired state. If the system state can be forced to remain on the line, then the target dynamics are exactly achieved and the state will proceed toward the desired state in a manner consistent with the target dynamics. As a result the state "slides" along the line, which is called the sliding surface. As detailed in [4,5], this concept can be directly extended to higher order systems.

In the case where the desired dynamics are not perfectly obtained, the sliding surface also provides a convenient metric of the error. The vertical distance between the sliding surface and the state is used:

$$s = \dot{\tilde{x}} + \lambda \tilde{x}.$$

The error metric "s" will also be used as the feedback term in the controller, and is also useful in system monitoring.

The Sliding Control Law

For a single degree of freedom system, the sliding control law consists of two parts. The first part is a model-based or "computed" element, and the second part is a nonlinear feedback component.

$$u = \hat{u} - k(\underline{X};t)\,\mathrm{sat}(s/\Phi)$$

where
$$\mathrm{sat}(x) = x \quad \text{for} \quad |x| \le 1$$
$$\mathrm{sat}(x) = 1 \quad \text{for} \quad x > 1$$
$$\mathrm{sat}(x) = -1 \quad \text{for} \quad x < -1$$

The computed control $\hat{u}$ uses the available model of the system dynamics and the sliding surface definition to determine a control action that would keep the state on the sliding surface.

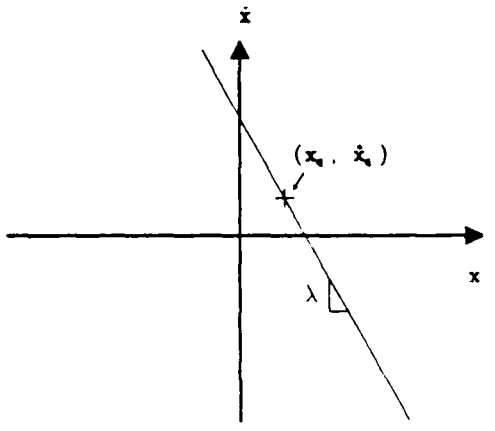

Figure 1. For a second order system, a sliding surface may be defined as a line that passes through the desired state.

The maximum magnitude of the feedback component is determined by a state-dependent gain $k(\underline{X};t)$. The error term s is used to drive the feedback component. The term Φ represents a time-varying upper bound on the magnitude of s. Both $k(\underline{X};t)$ and Φ are obtained directly from the system model, the sliding surface definition, and the uncertainty of the model. Both $k(\underline{X};t)$ and Φ increase as dynamic uncertainty increases.

The parameter Φ may be interpreted as the thickness of a time-varying "boundary layer" that lies on each side of the sliding surface (Figure 2). The state is guaranteed to remain inside the boundary layer if the actual dynamics of the controlled plant do not differ from the model by more than the uncertainty estimates.

This structure can assure stability, guarantee a prescribed level of performance, and also insure that high frequency unmodelled modes in the system are not excited. The procedure for composing $\hat{u}$, $k(\underline{X};t)$, and Φ are detailed in the references [4,5,6].

Extension to Systems with Many Degrees of Freedom

The nonlinear equations describing the dynamics of a vehicle or a manipulator are often highly cross-coupled, making the control problem difficult. If such a nonlinear model is linearized, the resulting linear system is also highly coupled. A high order linear controller must be designed, or important coupling terms will be ignored. Sliding control allows the control system to be decoupled into a set of low-order controllers, one for each axis, without ignoring the coupling terms.

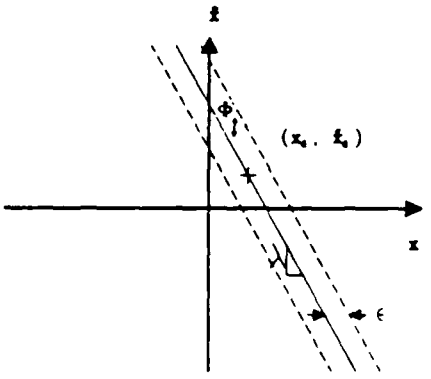

Figure 2. The bandwidth of the control action can be limited by interpolating the control action across a "boundary layer"

For each axis of the vehicle or manipulator, a separate low-order sliding surface is specified. For most vehicles, each sliding surface need be only first order.

For a multi-axis system, each axis will have a control law of the form:

$$u_i = \hat{u}_i - k_i(\underline{X};t)\,\mathrm{sat}(s_i/\Phi_i).$$

The model used to compute $\hat{u}_i$ can contain as many cross-coupling terms are desired. All modelled aspects of cross-coupling are used to compute $\hat{u}$, while uncertainty in the cross-coupling effects contributes to the magnitude of $k_i(\underline{X};t)$. This allows a series of low order controllers to be used rather than a single high order controller, producing more tractable design.

Implications for Modelling and Parameter Estimation

Models of vehicles can be uncertain due to errors in the model structure, errors in the model parameters, or because certain parameters have been dropped completely. The sliding control methodology allows the designer to judge the importance of a given element of the model directly in terms of tracking performance. For a nonlinear vehicle model with several hundred terms, many terms can be discarded in the model used to design the controller. The controller can be made explicitly robust to their elimination with only a small performance penalty. Likewise, if bounds on the disturbance forces can be estimated, their contribution to tracking error can be computed directly.

The quantitative relationship between model uncertainty, disturbances, and performance has important implications for the entire design process. Rather than starting the control system design with a model with very low uncertainty (probably obtained at great expense and probably more uncertain than one expects), a much simpler model can be used with confidence. Large simplifications in the model can be made without jeopardizing stability and often without significantly degrading performance. Simplifications can be chosen according to their influence on tracking performance. Generally, only a few parameters are required for each axis, greatly reducing the amount of model testing or analysis required. Simplifying the model also leads to a design that is much easier to implement.

Sliding Control and Monitoring

Sliding control includes important elements for sophisticated monitoring of the status of the closed-loop system. The key is the quantified uncertainty-performance tradeoff. If the state remains inside the time-varying boundary layer ($|s| \leq \Phi$), then the total uncertainty is below that acknowledged in the design of the system. However, if the state goes outside the boundary layer, a problem has arisen. This could either alert the human operator, or signal an autonomous subsystem.

DEMONSTRATION OF SLIDING CONTROL FOR UNDERWATER VEHICLES

The control technique was demonstrated in a pool using the Benthos RPV-430 vehicle. These tests provided confirmation of the usefulness of the method following simulation studies [6,7].

A prototype navigation system was used to provide high quality position information. The SHARPS (Sonic High Accuracy Ranging and Positioning System) developed by Applied Sonics Corp. provides high resolution (several millimeters) at update rates exceeding 10 samples/second even in high multipath environments. The system consists of a responder placed on the vehicle and a set of hard-wired receivers placed in a triangular net.

Using traditional state estimation techniques, velocity estimates were constructed from the position measurements and the yaw rate measurements from the vehicle. The state estimator was also able to throw out bad position fixes caused by vehicle electrical noise.

All functions, including navigation, state estimation, control, data logging and graphic displays, were implemented on an IBM PC-AT, an 80286 based microcomputer equipped with an 80287 math coprocessor. All computations ran at 10 hz.

A very simple model of the vehicle was used for this test. For each axis controlled by the computer, a single inertia and drag coefficient was determined from simple step response tests using the vehicle. Uncertainty estimates were 50% for each term. Due to an unmodelled coupling between translation and attitude of the vehicle, the closed loop bandwidth of the system was limited to 0.2 hz.

Figure 3 shows the desired and measured track of the vehicle. Each straight line segment consisted of constant acceleration, constant velocity, and constant deceleration sections. Heading was held constant throughout the test. Position errors are typically less than a few inches at full speed, and very small as the system slows down.

Figure 4 shows the desired and estimated x displacement of the vehicle. Errors are very small and transient behavior good despite the extremely low closed-loop bandwidth.

Figure 5 shows s plotted versus time for the forward motion of the vehicle. The boundary layer is plotted as well. Uncertainty increases as the vehicle speeds up due to the uncertainty in the drag coefficient, so the boundary layer expands. Errors (as shown by the value of s) also increase, however, they remain below the anticipated magnitude, indicated by Φ.

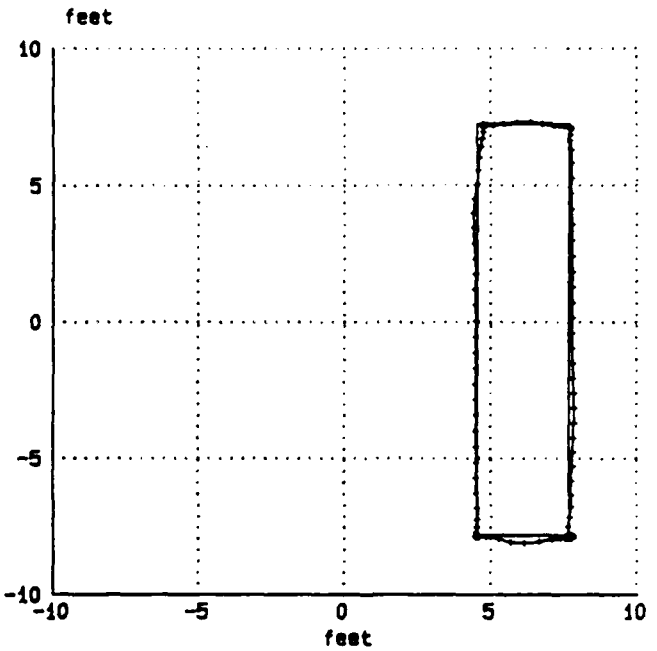

Figure 3. This plot shows the commanded and actual track of the vehicle in the test pool. The heading and depth of the vehicle remained constant.

Sliding control provides analytical guidance about how performance can be improved. The boundary layer thickness Φ corresponds to a time-varying bound on the magnitude of the error metric s. The contribution of the uncertainty of each model element, the disturbances, and the desired closed-loop bandwidth λ to the magnitude of Φ can each be examined. For a second order system, the maximum position error can be related to the boundary layer thickness Φ by:

$$x_{max} = \Phi/\lambda$$

Figure 6 shows the maximum magnitude of the displacement error at zero and maximum speed as projected by the boundary layer of figure 5. This projection can be broken down into components that depend on the following:

the specified closed-loop bandwith λ,
the multiplicative uncertainty in the effective mass β,
the additive uncertainty of the drag force $F(\underline{X})$,
the maximum disturbance magnitude γ,
a portion of the computed control U_0.

This plot shows the relative importance of these terms, and also indicates how their importance varies with speed. All components are inversely proportional to λ^2, and at least proportional to the multiplicative uncertainty in the effective mass β. The additive uncertainty of the drag $F(\underline{X})$ and the disturbance magnitude each contribute in an additive fashion. The ability to compare the influence of these factors in a nonlinear setting is extremely useful to a designer and unique to this approach.

Increasing the closed-loop bandwidth is clearly the best way to improve performance, as translation errors will be reduced by λ^2. In this implementation could not be increased beyond 0.2 hz. or the attitude modes of the vehicle would be excited by translational motion.

The closed loop bandwidth could be increased if the coupling between translation and attitude could be reduced, the frequency of the oscillations increased, or if the oscillations could be measured. The coupling between translation and attitude could be reduced by moving the center of mass closer to the line of action of the horizontal thrusters. The frequency of the attitude oscillations could be increased by enlarging the metacentric height of the vehicle. Finally, the attitude of the vehicle could be instrumented, probably using a vertical gyro. Any of these changes would allow the closed-loop bandwidth to be increased. As shown in figure 6, any increase in the closed loop bandwidth contributes strongly to performance.

Reducing the uncertainty of the effective mass will reduce the maximum error. However, improving the the effective mass estimate from the coarse value used here ($\beta = 1.5$) to a very certain value (such as $\beta = 1.1$) would reduce the maximum displacement error by less than 30%. This would probably not justify the effort required to produce the refined estimate.

Reducing the uncertainty in the drag and disturbance forces will have direct benefit. With little effort, the uncertainty in the drag force could be reduced by more refined testing. However, unless some method is available for measuring or estimating the drag force, the overall effect might not be very significant.

CONCLUSION

Sliding control has been demonstrated to be extremely useful for the control of underwater vehicles. Uncertain, nonlinear models can be used to directly produce controllers. A quantified relationship between model uncertainty and performance allows the designer great freedom in developing a model appropriate for a specific application. The model elements that contribute most strongly to performance can be identified, while the control system is made robust to the remaining terms that can be eliminated from the model. Sliding control provides an analytical framework for evaluating the impact of the design of the vehicle, its instrumentation, and the available model on performance.

Current work at the Deep Submergence Laboratory is extending and building on these results. The behavior of the system in high currents has been examined in simulation and these results will be confirmed in tests off the Woods Hole dock this year.

The sliding controllers will serve as the foundation of an advanced supervisory control system. A variety of interactive path specification techniques are currently being implemented. These include methods that allow the operator to indicate both transformations of his inputs, as well as constraints that reduce the number of degrees of freedom controlled by the operator. An interactive monitoring system based on sliding control is also in development.

These developments will make a strong contribution to the development of JASON, a teleoperated vehicle currently under development at the Deep Submergence Laboratory. However these techniques are generic to many types of vehicles. Robust trajectory control, monitoring, and interactive path planning are elements that are required by both autonomous and advanced teleoperated systems.

ACKNOWLEDGEMENTS

This work was supported by the Office of Naval Research, Contract No. N00014-84-K-0070 and Contract No. N00014-82-C-0743. Support was also received from IBM, Benthos Inc., and Applied Sonics Corporation.

REFERENCES

1. D.E. Humphries, K.W. Watkinson, Hydrodynamic Stability and Control Analyses of the UNH-EAVE Autonomous Underwater Vehicle, University of New Hampshire, Durham, 1982.
2. D.J. Lewis, J.M. Liscombe, P.G. Thomasson, The Simulation of Remotely Operated Underwater Vehicles, Proc. ROV '84, MTS, 1984.
3. L.G. Milliken, Multivariable Control of an Underwater Submersible, SM Thesis, MIT Departments of Mechanical and Ocean Engineering, May 1984.
4. J.-J. E. Slotine, Tracking Control of Nonlinear Systems Using Sliding Surfaces, Ph.D. Thesis, MIT Department of Aero. and Astro., May 1983.
5. J.-J. E. Slotine, The Robust Control of Robot Manipulators, Int. J. Robotics Research, Vol. 4, No. 2.
6. D.R. Yoerger, J.-J. E. Slotine, Robust Trajectory Control of Underwater Vehicles, IEEE J. Oceanic Eng., Vol. 10, No. 4.
7. D.R. Yoerger, J.B. Newman, Supervisory Control of Underwater Vehicles and Manipulators, Proc. ROV '85, MTS, 1985.

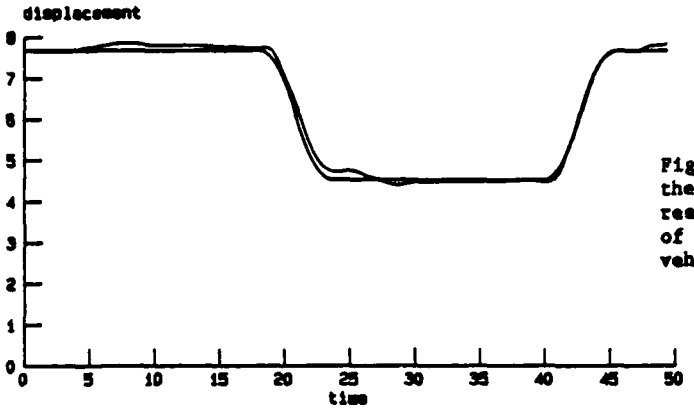

Figure 4. Commanded and actual displacement in the x direction. Errors are low and transient response good despite the low bandwidth. Evidence of the attitude oscillation can be seen when the vehicle decelerates.

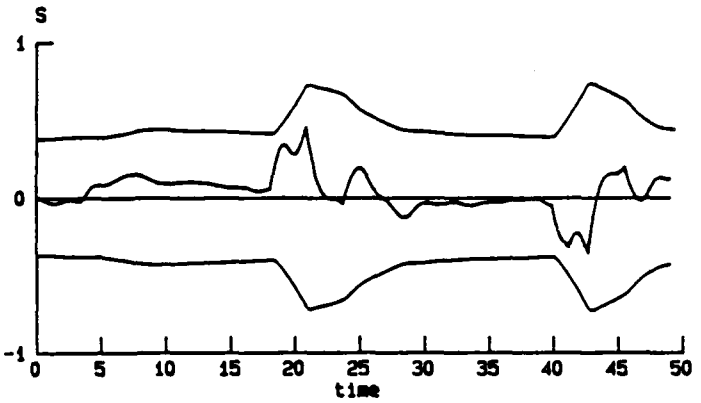

Figure 5. The error metric s is plotted along with the time-varying boundary layer. The boundary layer expands when the system speeds up, since the drag is uncertain. The state always remains inside the boundary layer.

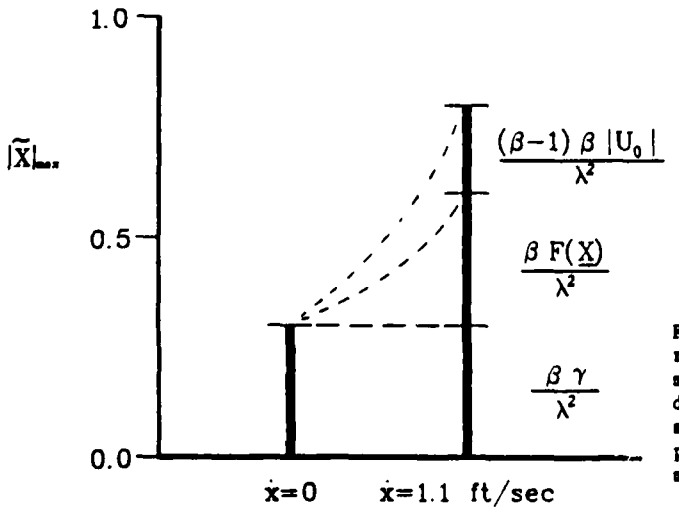

Figure 6. The maximum displacement error can be related to the closed loop bandwidth λ and the model uncertainty. These computations allow the designer to easily determine the effect of various model uncertainties and disturbances on performance. Using this technique, the vehicle modelling task can often be greatly simplified.

JASON: An Integrated Approach to ROV and Control System Design

Dana R. Yoerger
James B. Newman

Deep Submergence Laboratory
Department of Ocean Engineering
Woods Hole Oceanographic Institution
Woods Hole, Massachusetts 02543
USA

ABSTRACT

ROVs can be made more capable and easier to operate through the use of supervisory control techniques. Supervisory control systems combine precision navigation, closed-loop control, and a well-designed man-machine interface. They can improve ROV performance and decrease operator workload. Survey and inspection tasks can be performed and repeated more precisely and efficiently. Performance can be maintained in poor visibility and high currents. Vehicle motions can complement manipulator movements, so that more difficult manipulative tasks can be completed with simple arms.

While closed-loop control can be added to existing platforms, performance may be limited by several factors. First, high quality navigation data is required. Also, the vehicle dynamics must be well behaved. Finally, performance is limited by disturbances and by uncertainty in the vehicle dynamic model. In this paper, the interaction of these factors is discussed focussing on JASON, a new ROV under development that will perform scientific tasks on the sea floor to depths of 6000 meters.

INTRODUCTION

With few exceptions, underwater vehicles do not yet take advantage of recent advances in automation and robotics technology that can make vehicles more productive and easier to operate. In this paper, work in automated positioning and track-following will be described. Recent advances in control theory produce controllers that can deal with the nonlinear, poorly known dynamics of ROVs. Additionally, the methods presented provide understanding of how ROVs can be made more suitable for automatic control.

This work is being applied to JASON, an ROV for deep ocean scientific applications which is under development at Woods Hole. JASON will be deployed from the ARGO optical and acoustic imaging vehicle [1]. The JASON program emphasizes the refinement of supervisory control techniques that will control and coordinate the movements of the vehicle and manipulators from high level commands given by the human operator. Supervisory control will permit precise, repeatable surveys and will boost productivity in sampling.

In supervisory control a computer interacts directly with a process while a human operator manages the system. The foundations of the supervisory control system for an ROV will be closed-loop trajectory controllers. Closed-loop control of manipulator functions is common in the offshore industry today, and servo-controlled arms are available from several manufacturers. However, closed-loop control of vehicle translation is not available, although automatic depth and attitude controls are found on many vehicles. In addition to a good control system, the vehicle and its sensors must be well designed to give good performance.

Simultaneous control of both vehicle and manipulator motions has many important benefits. The need for heavy grabber arms or variable ballast systems that allow the vehicle to park on the sea floor may be avoided by controlling the vehicle movements in closed-loop. The amount of time required to perform manipulation tasks can be shortened by eliminating the need to anchor the vehicle. Also, fine control of vehicle movements allows tasks to be executed using fewer manipulation degrees of freedom. The resulting reductions in vehicle size, weight, power, and mechanical complexity are especially attractive for a full ocean depth vehicle such as JASON.

The same vehicle translational controls could greatly improve performance in offshore and industrial inspection tasks, particularly in high currents and poor visibility. We are working on enhancements to the basic supervisory control system which will allow the operator to command the vehicle in coordinates which are referenced to the environment or task being performed. This reduces the number of degrees of freedom that the operator must manage, improves performance in many tasks, and eases operator workload [2].

How Do We Design an ROV with a Predictable Level of Control Performance?

Path following performance for an ROV is difficult to quantify through analysis. Generally, the speed of response and the tracking precision will be limited by a variety of factors, including sensor performance, disturbances, and the dynamic characteristics of the vehicle. Due to the nonlinear nature of underwater vehicle dynamics, existing linear control system design techniques are poorly suited to providing an understanding of an automated ROV.

Performance may also be measured in ways that have no direct relationship to tracking accuracy or response times. For instance, in the deep ocean application of JASON, quality continuous color video is a high priority. Therefore, a steady camera platform is essential. The characteristic attitude oscillations common to most ROVs constitute poor performance.

Tracking performance limitations for an ROV control system can come from a variety of sources. The available navigation sensors have limited precision and update rates and many have intrinsic time delays. The dynamics of an ROV are highly nonlinear and difficult to model precisely. Finally, the ROV is subjected to many disturbances such as forces induced by currents and a tether. In some cases, computational power may be limited.

We are currently developing control system design tools that project the closed-loop performance of an ROV given simple descriptions of the limiting factors. These techniques reveal how the different limiting factors interact, permitting the designer to concentrate on those elements that affect performance most. The techniques can save both effort and cost by allowing simplified dynamic models to be used for the control system design while guaranteeing stability and achieving a defined level of performance.

The basis for this work is a robust control technique for nonlinear

systems called sliding control. Sliding control theory [3,4] and details of its application to undervater vehicles [2,5,6] can be found in the references.

An outline of the sliding control design procedure is shown in figure 3. There are three inputs to the design process: specification of the desired closed-loop dynamics; approximate dynamic model of the vehicle; and estimates of the uncertainties in the model. The design method not only produces simple controllers that perform well, but also directly provides information about system performance given a description of the limiting factors.

The desired closed-loop dynamics are typically specified to be those of a low-order, linear system (e.g.: first order linear, critically damped linear second-order system, etc.). In each case the desired or "target" dynamics will have a low-pass characteristic with a specified bandwidth. The closed-loop system will not be expected to respond infinitely fast. The bandwidth limit reflects basic limitations of the system and may originate from several sources including navigation system specifications, actuator and power limits, unmodelled vehicle dynamics, and disturbances.

In addition to the desired or target dynamics, the open loop dynamics of the vehicle must also be specified. This model can contain nonlinear terms for the drag effects, and may also include time-varying added mass terms. This control system design technique is completely compatible with the types of models produced by hydrodynamic analysis.

Another input consists of estimates of the uncertainty in the dynamic model. These estimates may also be in nonlinear form and account for uncertainties in model parameters, structural simplifications of the model, and disturbances.

This technique summarizes performance in a powerful way in a nonlinear context. Any control system design technique will allow evaluation of closed-loop bandwidth and disturbance responses, but sliding control provides a single unified metric for each degree of freedom that combines the effect of bandwidth limitations and dynamic uncertainty such as model uncertainty and disturbances.

Sliding techniques permit a nonlinear dynamic model to be used directly to design a closed-loop system with no need for linearization. This suits the ROV control problem well, since the vehicle dynamics are highly nonlinear and there are no obvious operating points about which to linearize the model [7].

ROVs typically move in all directions, so linearizing about values of forward speed is not the best approach. Designing a stable controller using the nonlinear model directly simplifies the design and implementation of the controller and gives more uniform behavior over the entire range of operation.

An error metric and a time-varying envelope of its expected bounds, both integral to the control computations, provide simple confirmation that the controller is operating as expected, and give a direct, continuous measure of controller performance.

Sliding control is a robust design methodology; it takes into account uncertainties in the vehicle model and the disturbances and can guarantee stability and performance bounds, despite these uncertainties. Unlike some robust design techniques, sliding control produces bandwidth limited control action which guarantees that high frequency unmodelled dynamics are not excited. As a result, tracking performance degrades as uncertainty increases. However, experience with both ROVs [2] and high speed manipulators [4] show that performance is very good even with substantial model errors.

The explicit trade-off between dynamic uncertainty and performance permits sliding control to be the primary tool in the design process. It is not necessary to produce the most precise model possible; a simplified model using approximate coefficients can produce a stable controller that performs within guaranteed limits. The desired level of performance can be used to guide the process by which the model is simplified and to determine the level of uncertainty permitted in the coefficients. The relative impact of disturbances and model uncertainty can be quantitatively assessed. For example, knowing drag coefficients to very high precision is meaningless from a control perspective if there are large disturbances. Likewise, the value of new sensors that decrease the dynamic uncertainty can be quantitatively evaluated.

Experimental Results: Pool Test

Trials using the Benthos RPV-430 ROV in a pool demonstrated closed-loop vehicle control in a trajectory tracking task [2]. Those tests used a sliding controller running at 10 Hz. to fly pre-determined paths. A prototype Applied Sonics SHARPS navigation system with repeatability of a few millimeters was used for position feedback [8]. The SHARPS (Sonic High Accuracy Ranging and

Positioning System) consists of a set of hard-wired receivers placed in a net, with a transmitter on the vehicle.

These tests showed that following a trajectory with high accuracy is possible using sliding control. Figure 1 shows desired and measured positions while following a rectangular trajectory in the pool. Errors in position were generally less than two inches. Speeds during this trial were 1.1 feet per second.

Figure 2 shows the error metric, s, for the controller, staying within the "boundary layer", indicating that uncertainties have been adequately bounded. The model used had 50% uncertainty in both drag coefficient and effective mass. A more refined model would be directly reflected in both the metric s and the boundary layer thickness ϕ.

The uncontrolled pitch and roll modes of the RPV, at about 0.4 Hz., were found to limit bandwidth as these modes were coupled to translation. Therefore, the bandwidth of the controller had to be limited to well below 0.4 Hz.

Bandwidth Limits on Controller Performance

Controller performance is restricted by the system bandwidth, which limits how fast the system can respond to both command inputs and disturbances. As the bandwidth of the system is increased, errors caused by disturbances and changes in the desired trajectory will decrease. A primary consideration in the design of any control system is to determine the practical limitations on closed-loop bandwidth. These limitations come from several sources, and must be acknowledged in the bandwidth of the controller.

Navigation System Limits on Bandwidth

In most demonstrations of closed-loop ROVs, the sensor bandwidth limit has been dominant, as low frequency acoustic navigation was employed [9,10]. Most acoustic navigation systems provide relatively coarse information at low update rates, and at long ranges time delays become substantial. A state estimator must be used to filter this data and to provide estimates of the unmeasured states (e.g., velocity). Given reasonable amounts of uncertainty in the plant model, any state estimator will have a bandwidth limit. The

closed-loop bandwidth must then be set several times lower than the bandwidth of the state estimator.

Actuator Limits on Bandwidth

Sluggish motors, delays in motor logic, limited thrust, and any other limits in the thruster portion of the vehicle system restrict bandwidth and typically cannot be compensated for. If this bandwidth limit is less than that imposed by navigation or by unmodelled dynamics, then it will limit control system bandwidth and hence performance.

Unmodelled Dynamics

The bandwidth of the controller must be constrained to remain below the frequency of the lowest unmodelled mode of the vehicle. As noted earlier, the most serious problem encountered in the sliding control demonstration resulted from the coupling between translational thrust and unmodelled modes, pitch and roll of the vehicle. The vehicle responded to a step input in horizontal thrust by pitching upward. The navigation responder, fixed to the bottom of the vehicle, yielded an ambiguous superposition of translation and attitude changes. If the control system bandwidth was set near the natural frequency of the vehicle in pitch or roll, the system became unstable.

This is a classic example of unmodelled vehicle dynamics limiting available system bandwidth. A decrease in the coupling to the mode can reduce the magnitude of the oscillation, but will not increase the frequency. The only ways to increase the bandwidth are to instrument the vehicle in the unmodelled mode and include the mode in the controller, or to increase the frequency of the mode. Instead, the vehicle's natural frequency in pitch and roll has been increased, raising metacentric height by going to a lighter flotation and adding ballast. Coupling between translational thrust and pitch has also been reduced by moving the center of gravity closer to the horizontal plane of the thrusters.

Tanaka, Mochizuki and Oda [11] present a series of simulations in which a large submersible (7800 kg dry weight) with variable metacentric height is commanded with a step input in forward thrust. The simulations vere based on

the results of scale model tests. Some of their results are presented in figure 4. The lowest metacentric height, 0.1 meters, results in oscillations through approximately 25 degrees of pitch with a period of approximately 40 seconds. To control such a vehicle, controller bandwidth would have to be set below this frequency to avoid exciting it, and performance would be abysmal. Alternatively, this mode could be actively controlled, which would require additional sensors, actuators, and a more complex controller.

By increasing metacentric height to .2 meters, the magnitude of the oscillations drops to about 7 degrees and, more importantly, the period falls to about 15 seconds. With the metacentric height at its design value of .299 meters the period is down to about 10 seconds, a more reasonable figure for a large vehicle of this sort, and oscillations are quite small.

Increasing the metacentric height will allow the bandwidth to be increased by a factor of four with no additional actuators or sensors. As position errors decrease with the square of the bandwidth, the result is a 16-fold improvement.

Limitations: Dynamic Uncertainty

Uncertainties in vehicle model arise from two sources: simplifications in the vehicle model and errors in the model parameters.

All vehicle models include simplifications which represent compromises between simplicity and accuracy. Similarly, the accuracy with which individual parameters can be determined can always be improved through more tank testing or more rigorous analysis. However, the accuracy gained often does not justify the effort in terms of stability or performance. For example, a very precise knowledge of drag contributes nothing to performance if there are substantial current or tether forces present.

Refinements or simplifications of the model appear explicitly in the control computations, and their effects on performance can be measured directly from the controller parameters. This feature gives the designer the ability to directly observe the change in performance that an improvement in the vehicle model provides, and allows him to avoid wasting effort or computational power to provide negligible benefit.

On the other hand, sliding control is very forgiving of inaccurate

vehicle models. Models with 50% errors in drag and mass can give acceptable closed-loop vehicle performance using sliding control. Adaptive sliding control [12], which is being developed, promises to make gross approximations in vehicle model acceptable, since the controller itself will be able to estimate vehicle parameters on the fly.

Any form of control must reject disturbances, and thus the design of any controller implies bounds on the expected disturbances. The sliding control design method allows the designer to specify these bounds, and remains stable as long as the disturbances do not exceed their specifications. If the disturbances do exceed their bounds, the s trajectory will exceed its bounds, indicating to the operator that a departure from the expected conditions has occurred. Again, the performance implications of disturbances can be directly understood.

Conclusions: Design Requirements for "Good" Performance

Via sliding control, we have developed some concepts regarding what constitutes "good" vehicle design from a control perspective. Generally, these concepts would also improve vehicle performance using other closed-loop design methods or manual control.

Unmodelled Modes

Perhaps the most important requirement for good performance under any form of control is that a vehicle have uncoupled dynamics and no significant bandwidth limits. This implies that horizontal and vertical thrust vectors should pass near the centers of mass and drag to avoid imparting torques that couple to vehicle attitude. Counter-rotating thrusters also help prevent coupled dynamics. The vehicle should have sufficient metacentric height to ensure that rocking and pitching frequencies are well above the desired control bandwidth. Alternatively, the vehicle may be designed to monitor and actively control attitude and torques. Typically, this will require extra thrusters and more complicated instrumentation and modelling, which may be impractical. In the deep ocean environment for which JASON is being designed, extra thrusters impose unacceptable costs in weight and power, and are not an acceptable alternative to a stable, balanced design.

Thrusters

Thrusters which are underpowered or slow to respond cannot be adequately compensated for by any method. However, sliding control makes the limits imposed by slow thrusters explicit.

Manipulation

Manipulators and manipulation tasks have not been discussed here, and perhaps deserve their own paper. However, our goal of precise manipulation without anchoring is a major consideration behind our desire for high performance vehicle control. Manipulators place their own constraints on the vehicle design, particularly with respect to stability in pitch and roll.

Navigation System

The requirements for a high performance navigation system are self-evident: Low measurement noise, high accuracy and fast updates. These requirements interact and trade-offs must be made. Long ranges imply long time delays and will inevitably degrade performance.

Coarse or infrequent acoustic range and bearing measurements can be supplemented with other measurements to improve the bandwidth of the state estimation process. One possibility under investigation is the use of doppler sonar for measurement of vehicle velocity, either over the bottom or through the water. Preliminary simulation studies with a commercially available unit look very promising. Low-cost inertial sensors could also supplement position measurements. Inherent drift in both such systems requires that they be used in conjunction with a position reference if absolute position is required.

Nonlinear Vehicle Model

A controller based on a simple approximate nonlinear model will usually

lead to better performance than a controller based on a linearized version of a highly detailed model. In formulating a vehicle controller it is often more important to include the nonlinear quality of the vehicle dynamics than to find very accurate values for model parameters. This statement generalizes beyond a discussion only of sliding control.

Application to JASON

These concepts are being employed to make JASON a productive scientific instrument. Components and techniques are being refined in shallow water tests using the RPV-430 vehicle. This summer we expect to test the RPV in high currents to investigate high-bandwidth and adaptive control techniques for both the vehicle and a manipulator.

ACKNOWLEDGEMENTS

This work was sponsored by the Office of Naval Research, Contract No. N00014-84-K-0070, N00014-82-C-0743, N00014-85-C-0410. Material support was also received from IBM and Applied Sonics, Inc., Gloucester Virginia USA.

REFERENCES

1. R.D. Ballard, ROV Development at Woods Hole's Deep Submergence Laboratory, Proc. ROV '84, MTS, 1984.

2. D.R. Yoerger, J.B. Newman, J.-J.E. Slotine, Supervisory Control System for the JASON ROV, to appear, IEEE J. Oceanic Eng., 1986.

3. J.-J.E. Slotine, Tracking Control of Nonlinear Systems Using Sliding Surfaces, Ph.D. Thesis, MIT Dept. of Aero. and Astro., May 1983.

4. J.-J.E. Slotine, The Robust Control of Robot Manipulators, Int. J. Robotics Res., Vol 4, No. 2.

5. D.R. Yoerger, J.-J.E. Slotine, Robust Trajectory Control of Underwater Vehicles, IEEE J. Oceanic Eng., Vol OE10 #4., Oct. 1985.

6. D.R. Yoerger, J.B. Newman, Demonstration of Closed-Loop Trajectory Control of an Underwater Vehicle, Proc. Oceans 85, IEEE/MTS, San Diego, 1985.

7. D.H. Lewis, J.M. Lipscombe, P.G. Thomasson, The Simulation of Remotely Operated Vehicles, Proc. ROV '84, MTS, 1984.

8. D.A. Hahn, G.N. Williams, M. Wilcox, P. Wilcox, A Computerized High Resolution Underwater Triangulation Mapping System, Proc. OCEANS '85, MTS, 1985.

9. G.T. Russell, D.M. Lane, S.C. Wells, Autonomous Submersible Systems, Subtech '83 Proc., Soc. Underwater Tech., London, Nov. 1983.

10. J.C. Jalbert, EAVE-East Sea Trials, Proc. Oceans '84, IEEE/MTS, Washington, Sept. 1984.

11. N. Tanaka, M. Mochizuki and T. Oda, Simulation on the Motion Characteristics of an Unmanned Untethered Submersible, Proc. Fourth International Symposium of Unmanned Untethered Submersible Technology, Durham, NH, June, 1985.

12. J.-J.E. Slotine, J.A. Coetsee, Adaptive Sliding Controller Synthesis for Nonlinear Systems, Int. J. Control, to appear, 1986.

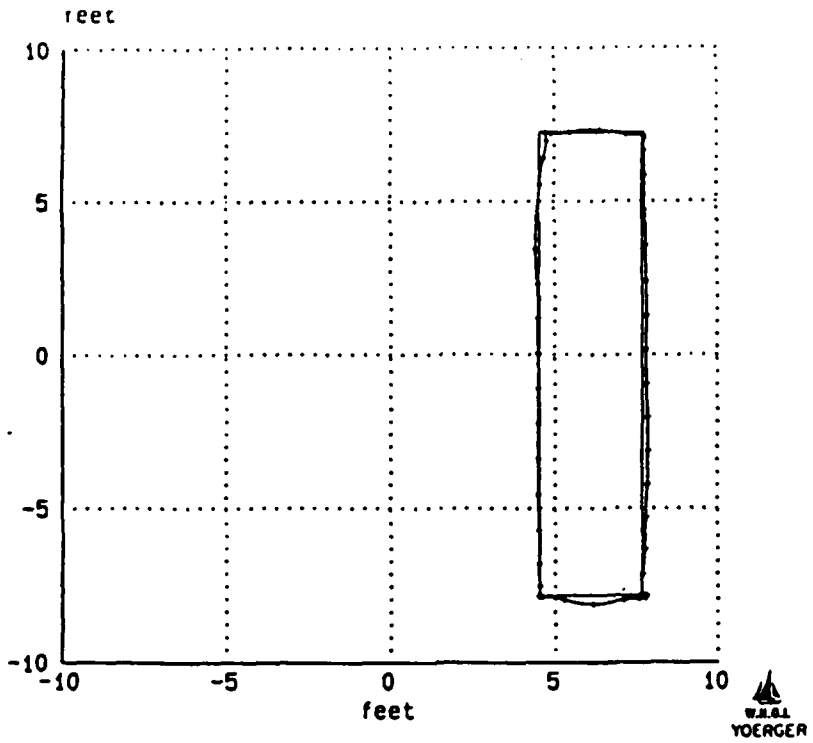

Figure 1. Commanded position (plain line) and measured position (with ticks) from an automatic control test in a pool. X direction is to the right. Position errors do not exceed a few inches.

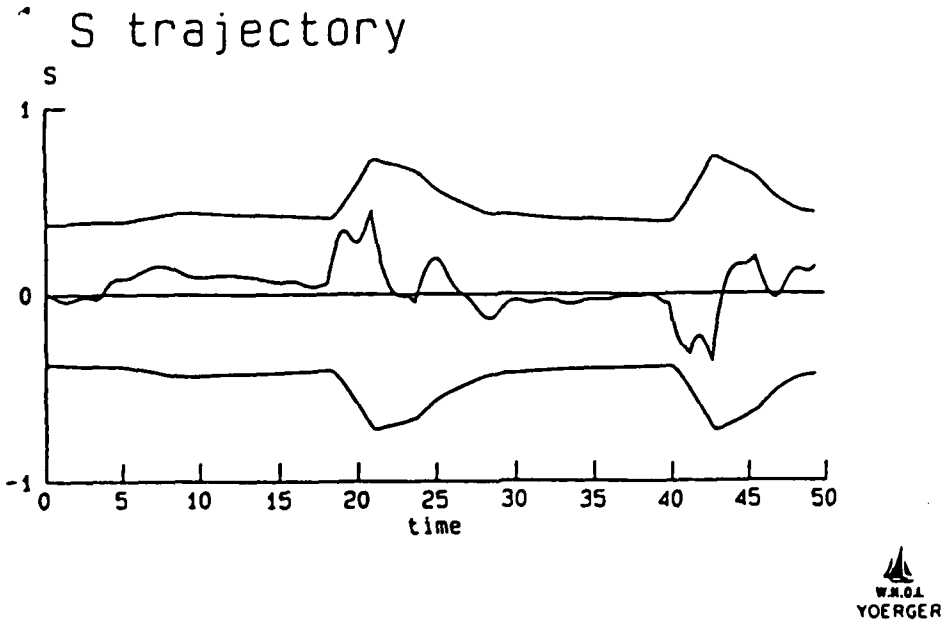

Figure 2. The error metric for the X direction during the automatic control test. A time-varying envelope (called the "boundary layer") is also shown. The error metric (called "s") is guaranteed to remain inside the boundary layer if uncertainty is bounded correctly. The magnitude of the boundary layer (called Φ) can be easily projected from the control bandwidth and estimates of model uncertainty and disturbances.

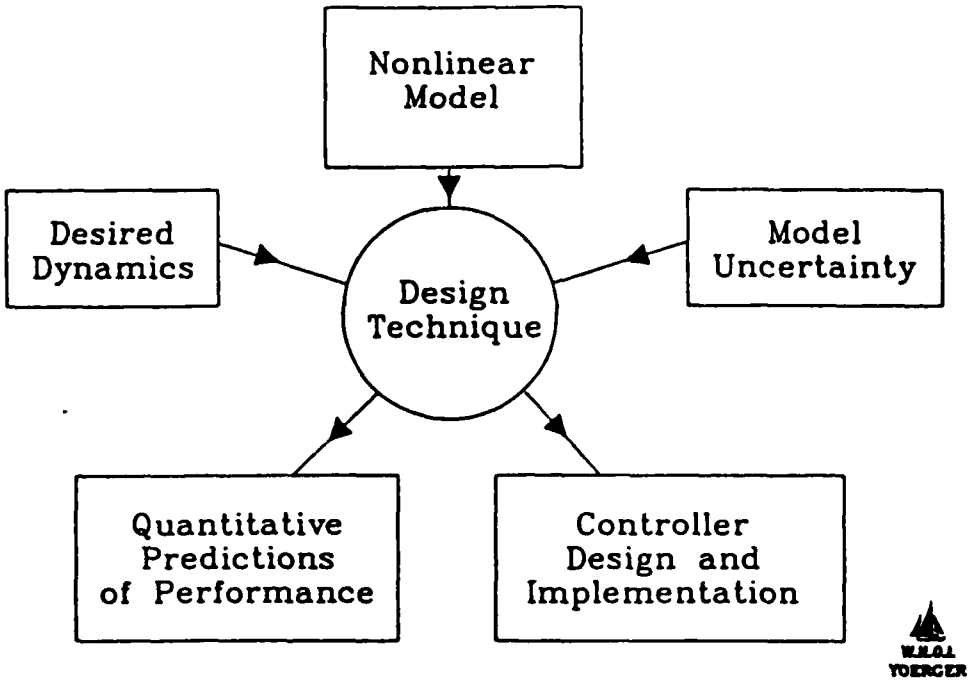

Figure 3. A summary of the sliding control design method. Given an approximate dynamic model of the vehicle, a desired dynamic characteristic, and estimates of model uncertainty, the performance of the closed-loop system can be easily projected.

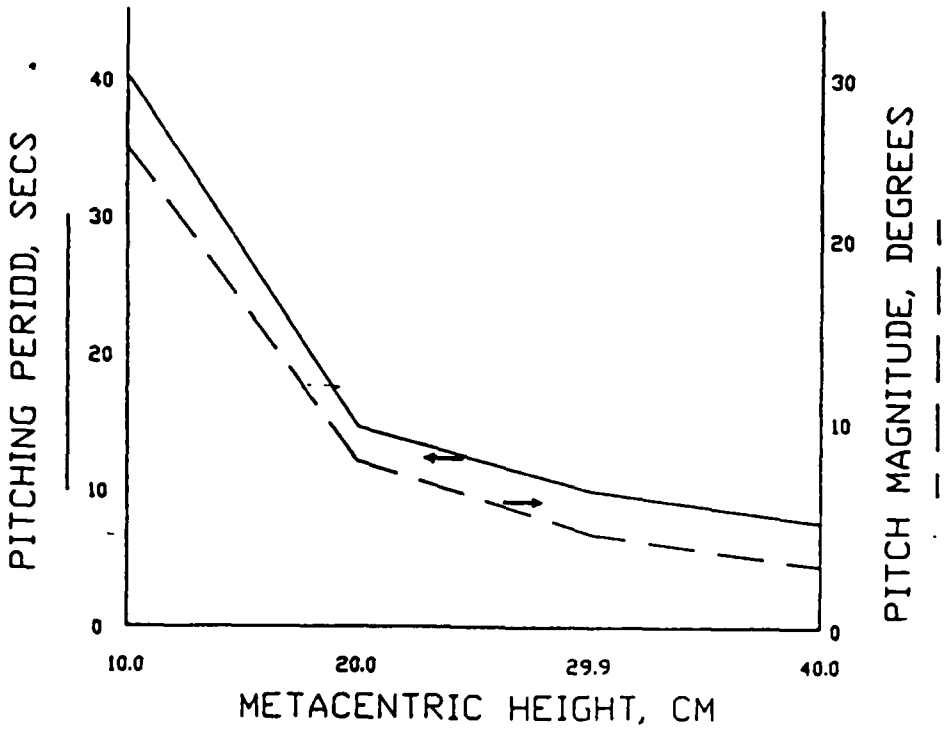

Figure 4. Period and magnitude of pitch oscillations of a large ROV following a large step in forward thrust as a function of metacentric height. The large increase in frequency of this mode will permit greatly improved closed-loop control performance with no additional sensors or actuators. Adapted from Tanaka, et al [10].

Accepted for publication, IEEE J. Oceanic Eng., 1986

SUPERVISORY CONTROL SYSTEM FOR THE JASON ROV

Dana R. Yoerger
James B. Newman
Deep Submergence Laboratory
Dept. of Ocean Engineering
Woods Hole Oceanographic Institution
Woods Hole, MA 02543

Jean-Jacques E. Slotine
Dept. of Mechanical Engineering
Massachusetts Institute of Technology
Cambridge, MA 02139

ABSTRACT

A prototype supervisory control system for an ROV is described and several key elements demonstrated in simulation and in-water tests. This system is specifically designed to fill the needs of JASON, a new ROV under development that will perform scientific tasks on the seafloor to depths of 6000 meters. JASON will operate from the ARGO towed imaging platform, which is currently operational.

Supervisory control is a paradigm for combined human and computer control. Several key elements of the supervisory control system are presented. These include the closed-loop positioning system based on a high resolution acoustic navigation system, a monitoring capability for assessing performance and detecting undesirable changes, and an interface that allows the human operator and the computer system to specify the desired vehicle trajectory jointly.

Reference 7

INTRODUCTION

The Deep Submergence Laboratory of the Woods Hole Oceanographic Institution is currently developing JASON, an ROV for deep ocean scientific applications. JASON will be deployed from the ARGO optical and acoustic imaging vehicle [1], which is now operational. A major emphasis of the JASON program is the refinement of supervisory control techniques that will allow carefully controlled, coordinated movements of both the vehicle and manipulators from high level commands issued by the human operator.

The supervisory control system will be built on closed-loop trajectory controllers. Closed-loop control of manipulator functions is common in the offshore industry today, and servo-controlled arms are available from several manufacturers. However, closed-loop control of vehicle movement is not presently available. Although automatic depth and attitude controls are commonly found on many vehicles, full closed loop control of vehicle translation requires that many difficult problems be solved.

Simultaneous control of both vehicle and manipulator motions can have many important benefits. The need for heavy grabber arms or variable ballast systems that allow the vehicle to park on the seafloor can be avoided by controlling the vehicle movements in closed-loop.

Further, eliminating the need to anchor the vehicle can greatly reduce the amount of time required to perform manipulation tasks. Taking advantage of finely controlled vehicle movements can also reduce the number of manipulator degrees of freedom required to execute a specific task. The resulting reductions in vehicle size, weight, power, and mechanical complexity are especially attractive for a full ocean depth vehicle such as JASON. The same vehicle translational controls could greatly improve performance in offshore platform inspection tasks, particularly in the presence of high current and poor visibility.

An ROV supervisory control system has many elements. The closed-loop control system must insure a high level of performance while being tolerant of poorly known vehicle dynamics and disturbances. The closed-loop systems should contain monitoring features that can provide information to the operator about the state of the system and which can alert him if a problem arises. Finally, the supervisory control system should provide flexible methods for the human operator and the computer system to define the desired trajectory jointly. This allows the human operator to offload portions of the control task to the computer system, while retaining those that require the operator's skill.

This paper describes two important elements of the supervisory control system: the closed loop control of vehicle translation and the interactive trajectory generation. The closed-loop control is demonstrated in pool tests with a prototype vehicle, and the interactive trajectories are demonstrated in simulation trials.

UNDERWATER VEHICLE DYNAMICS AND CONTROL SYSTEM DESIGN

Undervater vehicles present control system design problems that are poorly matched to traditional approaches. The dynamics of such vehicles are described by high-order models that are nonlinear and uncertain. A typical model of an ROV has over two hundred coefficients representing various nonlinear effects [2,3].

Although techniques for producing good models of vehicles are well advanced, the corresponding control methods are not. The linear control techniques which are generally used for control system design cannot take advantage of the detailed, nonlinear models that modern hydrodynamic analysis provides. Detailed information about the dynamics of the system is discarded when the model is linearized unless the system state remains sufficiently close to that about which the dynamics were linearized.

Linear techniques can produce stable designs for high-order nonlinear systems such as vehicles, but a set of many linearized controllers is required for good performance. The use of a single linearized control law will result in inconsistent performance as the velocity of the vehicle changes. For improved performance, a linear controller for a submarine might use several controllers, each designed using a model of the submarine linearized about one value of forward

speed [4]. As the submarine changes speed, the gains will change accordingly.

This approach is impractical for a vehicle that can move in all directions, like many underwater inspection and work vehicles, because there are no obvious operating points about which to linearize. Such a situation could only be handled by a large number of linear controllers designed for different combinations of speed along all axes. However, even if a complex design using many linear controllers were implemented, the stability of such "gain scheduled" systems may be questionable.

A good control system design methodology for underwater vehicles would allow a designer to use a single nonlinear model of vehicle behavior directly, without linearization. This would permit one controller to be used rather than requiring that the controllers change as the speed changed. The methodology should also allow the model upon which the controller is based to be systematically simplified while explicitly preserving stability. The performance implications of all simplifications should also be explicit, so that the designer can preserve the terms that contribute most to performance.

We are pursuing a methodology called sliding control to satisfy these requirements. These techniques have been applied to other difficult nonlinear control system design problems, particularly the trajectory control of high speed robots [6]. The benefits of the sliding methodology for underwater vehicle control have been

demonstrated in simulation [7] and with a test bed underwater vehicle as described later in this paper.

ROBUST CONTROL OF NONLINEAR SYSTEMS USING SLIDING CONTROL

This section describes the basic features of sliding control, with emphasis on the design implications. More complete discussions of the underlying theory and details of implementation can be found in the references [5,6,7].

Specification of the Desired Closed-Loop Dynamics

All closed-loop control system design involves transforming the natural dynamics of a system to dynamics that are more desirable. Although vehicle dynamics are nonlinear, it is reasonable that the target closed-loop dynamics be linear.

Traditional regulators are not sufficient for control of the trajectory of a vehicle or a manipulator; tracking controllers are required. Given a trajectory specified in terms of velocity, displacement, and acceleration, the controller should make reasonable compromises between position and velocity errors. This requires that the target dynamics include both position and velocity error terms.

For a system of order n, the control system design can be simplified considerably by choosing apriori well-behaved target dynamics of order n-1. After such a choice, the controller equations reduce to first order differential equations [4].

For a second order mechanical system, reasonable linear target dynamics would specify a stable first order relationship between position and velocity errors, for example:

$$0 = \dot{\tilde{x}} + \lambda\tilde{x} \qquad (1)$$

where $\tilde{x}$ is the displacement error, $\dot{\tilde{x}}$ is the velocity error, and λ is a constant used to set the break frequency of the desired first order error response.

Linear error dynamics such as this can be represented as a surface in state space that passes through the desired state. For a second order example, this corresponds to a line that passes through the point $(x,\dot{x})$. As shown in Figure 2, this line will move with the desired state. If the system state can be forced to remain on the line, then the target dynamics are exactly achieved and the state will proceed toward the desired state in a manner consistent with the target dynamics. As a result the state "slides" along the line, which is called the sliding surface. As detailed in [5,6], this concept can be directly extended to higher order systems.

In the case where the desired dynamics are not perfectly obtained, the sliding surface also provides a convenient metric of the error. The variable "s" is a measure of the algebraic distance between the sliding surface and the current state:

$$s = \dot{\tilde{x}} + \lambda\tilde{x} \tag{2}$$

The error metric "s" that is used in the feedback term in the feedback control law, is also useful in system monitoring.

The Sliding Control Law

For a single degree of freedom system, the sliding control law consists of two parts. The first part is a model-based or "computed" element, and the second part is a nonlinear feedback component.

$$u = \hat{u} - k(\underline{X};t)\ \mathrm{sgn}(s) \tag{3}$$

where sgn is the sign function:
$\mathrm{sgn}(x) = 1$ for $x > 0$
$\mathrm{sgn}(x) = -1$ for $x < 0$

The computed control $\hat{u}$ uses the available model of the system dynamics and the sliding surface definition to determine a control action that would keep the state on the sliding surface if the model was perfect. The feedback component insures that the state will be drawn to and remain on the sliding surface despite uncertainty in the model and

the resulting imperfection in $\hat{u}$. The function $k(\underline{X};t)$ can be determined directly from Lyapunov stability considerations given the system model, the sliding surface definition, and estimates of model uncertainty and disturbances [5,6]. Generally speaking, $k(\underline{X};t)$ increases as $\hat{u}$ becomes less precise, since a larger discontinuity is required to keep the state on the sliding surface.

This type of control law can guarantee that the system state remains on the sliding surface. In other words, the target dynamics are exactly achieved and tracking is perfect. However, the control action resulting from the discontinuous feedback term will produce control chattering that is unsuitable for most applications, since it may excite high frequency unmodelled dynamics. Structural modes and actuator time delays are potential sources of these unmodelled dynamics.

The control law can be modified to solve this problem. The bandwidth of the feedback portion of the control action can be limited if the control action is smoothed over a "boundary layer" of variable thickness ϕ that lies on each side of the sliding surface (Figure 3). The continuous control law may be written as:

$$u = \hat{u} - k(\underline{X};t)\ \mathrm{sat}(s/\phi) \qquad (4)$$

where sat is the saturation function:

$\mathrm{sat}(x) = x$ for $|x| < 1$
$\mathrm{sat}(x) = 1$ for $x > 1$
$\mathrm{sat}(x) = -1$ for $x < -1$

This interpolation assigns a low-pass filter structure to the feedback and therefore to the closed-loop dynamics. To obtain this

bandwidth-limited control, however, the perfect tracking of theoretical pure sliding control must be slightly compromised. The state will not remain exactly on the sliding surface, yet is guaranteed to remain inside the boundary layer if the uncertainty estimates are valid. In practice, the performance penalty has been found to be slight, and acceptable performance can usually be obtained even with large uncertainty in the model parameters.

This structure can assure stability, guarantee a prescribed level of performance, and insure that high frequency unmodelled modes in the system are not excited. The procedures for composing $\hat{u}$, $W(\underline{X};t)$ and ϕ are detailed in the references [5,6], and their application to underwater vehicles is detailed in [7].

Extension to Systems with Multiple Degrees of Freedom

The nonlinear equations describing the dynamics of a vehicle or a manipulator are often highly cross-coupled, making the control problem more difficult. If such a nonlinear model is linearized, the resulting linear system is also highly coupled. A high-order linear controller must be designed, or important coupling terms will be ignored. Sliding control allows the control system to be decoupled into a set of low-order controllers, one for each axis, while still explicitly accounting for the coupling terms.

For each axis of the vehicle or manipulator, a separate low-order

sliding surface is specified. For most vehicles, each sliding surface can be first order:

$$s_i = \dot{\tilde{x}}_i + \lambda_i \tilde{x}_i. \tag{5}$$

If integral control action is desired, then the sliding surface would be second order.

For a multi-axis system, each axis will have a control law of the form:

$$u_i = \hat{u}_i - k_i(\underline{X};t)\text{sat}(s_i/\phi_i) \tag{6}$$

The model used to compute $\hat{u}_i$ can contain as many cross-coupling terms as are necessary to obtain the desired performance. All modelled aspects of cross-coupling are used to compute $\hat{u}_i$, while uncertainty in the cross-coupling effects contributes to the magnitude of $k_i(\underline{X};t)$. This allows a series of coupled low-order controllers to be used rather than a single high-order controller, producing simpler and more tractable designs.

Implications for Modelling and Parameter Estimation

Models of vehicles are uncertain due to errors in the model structure, errors in the model parameters, or because certain parameters have been dropped completely. The sliding control methodology allows the designer to judge the importance of a given element of the model directly in terms of tracking performance. For a nonlinear vehicle model with several hundred terms, many terms can be discarded in the

model used to design the controller. The controller can be made explicitly robust to the elimination of these terms with only a small performance penalty but with a large reduction in controller complexity. Similarly, if bounds on the disturbance forces can be estimated, their contribution to tracking error can be computed directly.

The quantitative relationship between model uncertainty, disturbances, and performance has important implications for the entire design process. Rather than starting the control system design with a model with very low uncertainty (probably obtained at great expense and possibly more uncertain than one expects), a much simpler model can be used with confidence. Note that this simplification does not mean linearization, but rather the elimination of coefficients whose influence is small.

Large simplifications in the model can be made without jeopardizing stability and often without significantly degrading performance. Any force term can be eliminated, simplifying the structure of $\hat{u}$ and boosting $k(\underline{X};t)$ and ϕ. The increase in ϕ and the resulting change in the performance bounds can be computed drectly. Generally, only a few important parameters are required for each axis, greatly reducing the amount of model testing or analysis required and making the controller easier to implement.

Sliding Control and Monitoring

Sliding control includes important elements for sophisticated monitoring of the status of the closed-loop system. The key is the quantified tradeoff between uncertainty and performance. If the state remains inside the time varying boundary layer ($|s| < \phi(t)$), then the total uncertainty is below that acknowledged in the design of the system. However, if the state goes outside the boundary layer, a problem has arisen. The system can either alert the human operator or signal an autonomous subsystem. The information generated when the system is outside the boundary layer can also be used to improve the model of the system on-line [9].

DEMONSTRATION OF SLIDING CONTROL FOR UNDERWATER VEHICLES

The control technique was demonstrated in a pool using the Benthos RPV-430 vehicle. These tests provided confirmation of the usefulness of the method following simulation studies [7,8].

A prototype navigation system was used to provide high quality position information. The SHARPS (Sonic High Accuracy Ranging and Positioning System) developed by Applied Sonics Inc. provides high resolution (several millimeters) at update rates exceeding 10 samples/second even in high multipath environments. The system consists of a responder placed on the vehicle and a set of hard-wired receivers placed in a triangular net.

Using traditional state estimation techniques, velocity estimates were constructed from the position measurements and the yaw rate measurements from the vehicle. The state estimator was also able to discard bad position fixes caused by vehicle electrical noise.

All functions, including navigation, state estimation, control, data logging and graphic displays, were implemented on an IBM PC-AT, an 80286 based microcomputer equipped with an 80287 math coprocessor. All computations ran at 10 Hz.

A very simple model of the vehicle was used for this test. For each axis controlled by the computer, a single inertia and drag coefficient was determined from simple step response tests using the vehicle and navigation system. Uncertainty estimates were 50% for each term. Due to an unmodelled coupling between translation and attitude of the vehicle, the closed-loop bandwidth of the system was limited to 0.2 Hz.

Figure 4 shows the desired and measured track of the vehicle. Each straight line segment consisted of constant acceleration, constant velocity, and constant deceleration sections. Heading and depth were held constant throughout the test. Position errors are typically less than a few inches at full speed, and very small as the system slows down.

Figure 5 shows the desired and estimated forward displacement of

the vehicle. Errors are very small and transient behavior good despite the extremely low closed-loop bandwidth.

Figure 6 shows s plotted versus time for the forward motion of the vehicle. The boundary layer thickness, ϕ, is plotted as well. Uncertainty increases as the vehicle speeds up due to the uncertainty in the drag coefficient, so the boundary layer expands. Errors (as shown by the value of s) also increase, however, they remain below the anticipated magnitude, indicated by ϕ.

Sliding control provides analytical guidance about how performance can be improved. The boundary layer thickness ϕ corresponds to a time-varying bound on the magnitude of the error metric s. The contribution of the uncertainty of each model element, the disturbances, and the desired closed-loop bandwidth λ to the magnitude of ϕ can each be examined. For a second order system, the maximum position error can be related to the boundary layer thickness ϕ by:

$$|\tilde{x}|_{max} = \phi/\lambda \qquad (7)$$

Figure 7 shows the maximum magnitude of the displacement errors at zero and maximum speed as projected by the boundary layer of Figure 6. This projection can be broken down into components that depend on the following:

- The specified closed-loop bandwidth λ

- The estimated effective mass $\hat{m}$

- The multiplicative uncertainty in the effective mass β

- The additive uncertainty of the drag force $F(\underline{X})$

- The maximum disturbance force γ .

This plot shows the relative importance of these terms, and also indicates how their importance varies with speed. All components are inversely proportional to λ^2, and proportional to the multiplicative uncertainty in the effective mass β. The additive uncertainty of the drag $F(\underline{X})$ and the disturbance magnitude each contribute in an additive fashion. The ability to compare the influence of these factors in a nonlinear setting is extremely useful to a designer and is a unique feature of this approach.

Increasing the closed-loop bandwidth is clearly the best way to improve performance, as translation errors will be reduced by λ^2. In this implementation λ could not be increased beyond 1.4 rad/s (0.22 hz) or the attitude modes of the vehicle would have been excited by translational motion.

The closed-loop bandwidth could be increased if:

- The coupling between translation and attitude could be reduced.

This could be achieved by moving the center of mass closer to the line of action of the horizontal thrusters;

- The frequency of the attitude oscillations were increased. This could be done by increasing the metacentric height of the vehicle.

- The attitude oscillations could be measured and their influence on the position measurements removed. Angular displacement and velocity could be measured and their dynamics included in the vehicle model.

Any of these changes would allow the closed-loop bandwidth to be increased. As shown in Figure 7, any increase in the closed-loop bandwidth contributes strongly to the performance.

Reducing the uncertainty of the effective mass will reduce the maximum displacement error. However, improving the effective mass estimate from the coarse value used here (multiplicative uncertainty of 50%, i.e. $\beta = 1.5$) to a precise value (such as $\beta = 1.1$) would reduce the maximum displacement error by less than 30%. This might not justify the effort required to produce the refined estimate, but in any case the potential improvement from better modelling is quantified.

Reducing the uncertainty in the drag and disturbance forces will have a direct benefit. With little effort, the uncertainty in the drag force could be reduced through more refined testing. However, unless

measurements or estimates of the forces produced by the disturbances are available (such as those produced by a current or the tether), the performance benefits from a very detailed model will not be significant. Likewise, the benefits obtained from instrumenting the tether force or including a current measurement may be much greater.

These techniques provide a much closer coordination between vehicle modelling and control system design efforts. The required model quality and vehicle characteristics can be determined based upon the desired tracking precision. This can lead to reduced modelling and testing as well as a simple control system with known performance.

Interactive Trajectory Definition for ROVs

In the uncertain underwater environment, human interaction with the vehicle is essential for most inspection and manipulation tasks. However, the precision and repeatability of automatic control is desirable. The supervisory control system combines the benefits of automatic control while allowing the human operator to continuously command the desired trajectory. The computer is employed to perform the following tasks: positioning the vehicle and rejecting disturbances; accepting and conditioning the operator's command inputs; and presenting the operator with an informative display to help in system monitoring.

The supervisory control system allows the operator to input movement commands in a reference that corresponds naturally to the

task. This reference may be a particular cartesian frame, a very distorted field that conforms to the environment, or the reference may lock the vehicle into a predefined track while allowing the operator to continuously specify vehicle speed along the track. Five versions of coordinate transformations are considered here: body-reference coordinates; fixed-reference joystick coordinates; cylindrical coordinates; complex coordinates; and pre-defined path or search trajectory coordinates.

A series of simulation trials was undertaken to demonstrate several forms of trajectory definition, and to compare the supervisory control modes to each other and to manual control. These were not controlled experiments, but rather a demonstration of these methods and a qualitative comparison between the control methods. An experienced ROV pilot was used as the subject for the trials.

Body-Referenced Coordinates

In the simplest form of supervisory control considered, the operator's commands are similar to manual control commands; commands are defined in a coordinate frame that moves with the vehicle. The operator may even be unaware of the presence of the computer control, except that the dynamics have become much simpler and disturbances are dealt with automatically. For example, when the operator allows the joystick to return to the center position, this does not correspond to zero thrust but to zero velocity, and the vehicle will actively fight currents or

tether forces to remain at its present position.

Usually, when an operator is flying an ROV manually, he is viewing the world through the vehicle's video camera. Therefore, joystick coordinates fixed relative to the body coordinates of the vehicle are matched to the operator's view of his environment. These body-referenced coordinates are incompatible with a fixed-referenced (i.e. north up) display, and should be matched to a display in which the environment moves while the vehicle remains fixed.

Fixed-Reference Joystick Coordinates

Many tasks are better understood by observing a fixed reference top view or map display of the vehicle and its surroundings. Such a display provides a reference that does not move with the vehicle but is fixed in world coordinates giving the operator a natural coordinate system in which to control vehicle motion. In this case, the joystick commands are compatible with the display. Not surprisingly, controlling the vehicle in a fixed reference frame seems more natural and appears to improve performance when the operator is viewing the map display rather than the vehicle video.

Cylindrical Coordinates

A further development on the coordinate system involves warping

the cartesian reference frame into shapes that match the environment, thus reducing the number of degrees of freedom which the operator must simultaneously supervise. In a cylindrical-coordinate mode the operator can symbolically indicate that the vehicle's workspace centers on a piling or similar upright cylinder. A port or starboard command on the joystick will then result in a translation of the vehicle around the piling, keeping a constant stand-off distance and continuously facing the piling. Forward and aft commands on the joystick will move the vehicle closer to and farther from the piling. The vehicle will remain pointed at the center of the target cylinder at all times. Such a system would be useful, for instance, when inspecting a platform leg, or in guiding a manipulator to a target. Computationally, cylindrical coordinates require only that the vehicle heading be constrained to point at the center of the coordinate system.

A trial of this mode simulated an inspection task where the vehicle was required to fly semicircular paths around a fixed point while keeping the vehicle headed toward the point. In the cylindrical mode this required only simple joystick commands and was performed quite accurately (see figure 8). In the cartesian-coordinate mode the operator had to control two displacements and heading to follow the desired track. In this preliminary demonstration, the cylindrical coordinate mode showed better track following performance and the subject felt the task was made easier.

Complex Coordinates

Another method of conforming the operator's commands to the environment can be used in more complex environments, which are modelled as combinations of simple shapes. An example is shown in figure 9. This would apply to many types of inspection tasks, where the ROV must be manuevered around an offshore structure, ship hull, etc. In this scheme, port and starboard joystick commands cause the vehicle to move along the object to be inspected at approximately constant distance. Forward and aft commands move the vehicle closer to and farther from the barrier. Heading is constrained so that the vehicle always points toward the objects to be inspected.

An inspection or search task can be greatly simplified by the complex constraints on vehicle motion. The operator can easily maintain constant distance from the objects and can rapidly scan the surface for interesting features.

The implementation is similar to a well-known technique for path planning and obstacle avoidance [10,11]. An imaginary "potential field" surrounding each object is defined. The total potential and the gradient of the potential field from all objects are then computed for the current vehicle position. Vehicle heading is then constrained to point up the gradient. Sideways commands move the vehicle along lines of constant potential, while forward and reverse commands move the vehicle along the gradient of the potential field. This results in a coordinate space that conforms around the objects, and provides smooth transitions between objects. The computational burden is small and increases linearly with the number of objects.

The cylindrical coordinate computation is a simplified form of the complex coordinate computation where the only object is an upright cylinder.

Predefined Trajectories

Vehicle degrees of freedom can be further constrained by defining a fixed path for the vehicle to follow. This differs from pre-programmed control by allowing the operator to continuously specify vehicle velocity along the defined track. The operator can fly the vehicle at a comfortable speed, watching for an object of interest, and can stop or even back up, but cannot get off the path or lose track of his absolute position. As in the previous methods, the demands on the operator are shifted so that he can concentrate on that part of the job which only human operators can perform.

Supervisory Control Trials

Simulation trials were conducted in which the vehicle was required to fly a grid search pattern. A steady current corresponding to approximately 10% of full vehicle thrust in a diagonal direction was simulated, and gaussian noise was added to measurements of vehicle position and velocity, which were then filtered.

The operator flew the vehicle in the following modes: pre-defined

trajectory in which he controlled only vehicle speed; full trajectory control with body and world coordinate joystick; and a fully open-loop manual mode.

The operator was instructed to fly straight lines between markers on the graphic display, making smooth turns at the corners and keeping the vehicle facing ahead. This corresponded exactly to the pre-defined trajectory, which the operator ran first (figure 10).

These trials demonstrated that these techniques have been sucessfully implemented and allow preliminary comparisons of performance. Not surprisingly, the predefined trajectory mode showed the best track following and was felt by the subject to be the easiest to use. Fixed-coordinate joystick mode showed better track following than the body-coordinate mode. All supervised modes indicated better track following than open-loop manual control. The supervisory modes also required much simpler, more consistent joystick commands from the operator.

CONCLUSION

A supervisory control system based on reliable, high performance closed-loop control and a properly designed operator interface can make an ROV much more capable. The overall performance of the system can be

improved and the capabilities of the system can be extended to tasks that could otherwise not be performed. Examples of such tasks are those that must be accomplished in lov visibility and high currents. Very carefully controlled, repeatable surveys can be performed without sacrificing flexibility or the ability to respond to the unexpected. Overall, vehicle operations are made more efficient and simpler, with a relatively small investment in complexity and cost.

Elements of such a control system have been implemented and will soon be applied to JASON, an ROV for deep ocean scientific applications. Reliable closed-loop control has been demonstrated in pool tests, and trials with prototype man-machine interfaces have been completed in simulation.

REFERENCES

1. R.D. Ballard, ROV Development at Woods Hole's Deep Submergence Laboratory, Proc. ROV '84, MTS, 1984.

2. D.E. Humphries, K.W. Watkinson, Hydrodynamic Stability and Control Analyses of the UNH-EAVE Autonomous Underwater Vehicle, University of New Hampshire, Durham, 1982.

3. D.H. Lewis, J.M. Lipscombe, P.G. Thomasson, The Simulation of Remotely Operated Vehicles, Proc. ROV '84, MTS, 1984.

4. L.G. Milliken, Multivariable Control of an Underwater Submersible, SM Thesis, MIT Departments of Mechanical and Ocean Engineering, May 1984.

5. J.-J.E. Slotine, Tracking Control of Nonlinear Systems Using Sliding Surfaces, Ph.D. Thesis, MIT Dept. of Aero. and Astro., May 1983.

6. J.-J.E. Slotine, The Robust Control of Robot Manipulators, Int. J. Robotics Res., Vol 4, No. 2.

7. D.R. Yoerger, J.-J.E. Slotine, Robust Trajectory Control of Underwater Vehicles, IEEE J. Oceanic Eng, Vol OE10 #4., Oct. 1985.

8. D.R. Yoerger, J.B. Newman, Supervisory Control of Underwater Vehicles and Manipulators, Proc. ROV '85, MTS, 1985.

9. J.-J.E. Slotine, J.A. Coetsee, Adaptive Sliding Controller Synthesis for Nonlinear Systems, Int. J. Control, to appear, 1986.

10. O. Khatib, J.F. LeMaitre, Dynamic Control of Manipulators

Operating in a Complex Environment, 3_{rd} Symp. Theory and Practice of Robots and Manipulators, Udine Italy, 1978, pp. 267-282.

11. N. Hogan, Impedence Control: An Approach to Manipulation: Part III - Applications, ASME J. Dynamic Systems, Measurement, and Control, Vol. 107, March 1985.

Footnotes

This work was sponsored by the Office of Naval Research, Contract No. N00014-84-K-0070, N00014-82-C-0743, N00014-85-C-0410. Material support was also received from IBM and Applied Sonics, Inc.

D. R. Yoerger and J.B. Newman are with the Deep Submergence Laboratory, Dept. of Ocean Engineering, Woods Hole Oceanographic Institution, Woods Hole, MA.

J.-J. E. Slotine is with the Dept. of Mechanical Engineering, Massachusetts Institute of Technology, Cambridge, MA.

Figure Captions

Figure 1. JASON will be an ROV that can emerge from the towed ARGO platform to perform close-up inspection and manipulation tasks.

Figure 2. For a second order system, a typical sliding surface consists of a line that passes through the current desired state.

Figure 3. The bandwidth of the control action can be limited by interpolating the control action across a "boundary layer". This interpolation produces a trade-off between model uncertainty and performance.

Figure 4. This plot shows the desired and actual trajectory of the vehicle in a pool test. Each trajectory segment consisted of constant acceleration, constant velocity, and constant deceleration sections. Heading and depth were held constant throughout the run.

Figure 5. Desired and estimated displacement in the X direction is shown as a function of time. Performance was very good despite substantial model uncertainty and limited control bandwidth. Evidence of the attitude oscillations can be seen when the vehicle decelerates.

Figure 6. The error metric "s" is plotted along with the time varying boundary layer ϕ. The boundary layer expands when the vehicle

speeds up due to uncertainty in the drag force. The state always remains inside the boundary layer, indicating that dynamic uncertainty is always less than the estimated bound.

Figure 7. The maximum displacement error $|\tilde{x}|_{max}$ can be related to the closed-loop bandwidth λ and the model uncertainty. Components of model uncertainty include the multiplicative uncertainty in the mass β, the additive error in the drag force $F(\underline{X})$, and the maximum unmodelled force γ. The explicit relationship between the components of model uncertainty and performance will often allow the vehicle model to be simplified with a minimum impact on tracking performance.

Figure 8. Semi-circular path trials show better track following cylindrical joystick coordinates than with body reference joystick commands. Figure 8a shows the less precise vehicle path achieved using cartesian joystick coordinates and 8b shows the better vehicle path achieved with cylindrical joystick coordinates.

Figure 9. Figure 9 shows potential fields for an arbitrary barrier. The topmost line represents the barrier itself, made up of two intersecting walls and a vertical cylinder set into one wall. The lines approximately parallel to the wall are lines of constant potential which will correspond to athwartships joystick commands. The lines orthogonal to the constant potential lines correspond to forward and aft joystick commands. Smooth transitions are made at the corners with the radius of the turn increasing as the vehicle track gets farther from the wall.

Figure 10. Figure 10 compares vehicle paths in the search trajectory trials. Figure 10a shows vehicle path in body reference joystick coordinates using supervisory control (solid line) and with manual control (dashed line). Figure 10b shows vehicle path using predefined trajectory definition (solid line) and fixed reference joystick coordinates (dashed line). The corners on the predefined trajectory path are rounded because constant accelerations in both directions were imposed during the supervised transition phases. Qualitative comparisons indicate that the more sophisticated forms of trajectory definition produce better track following as well as reduced operator workload.

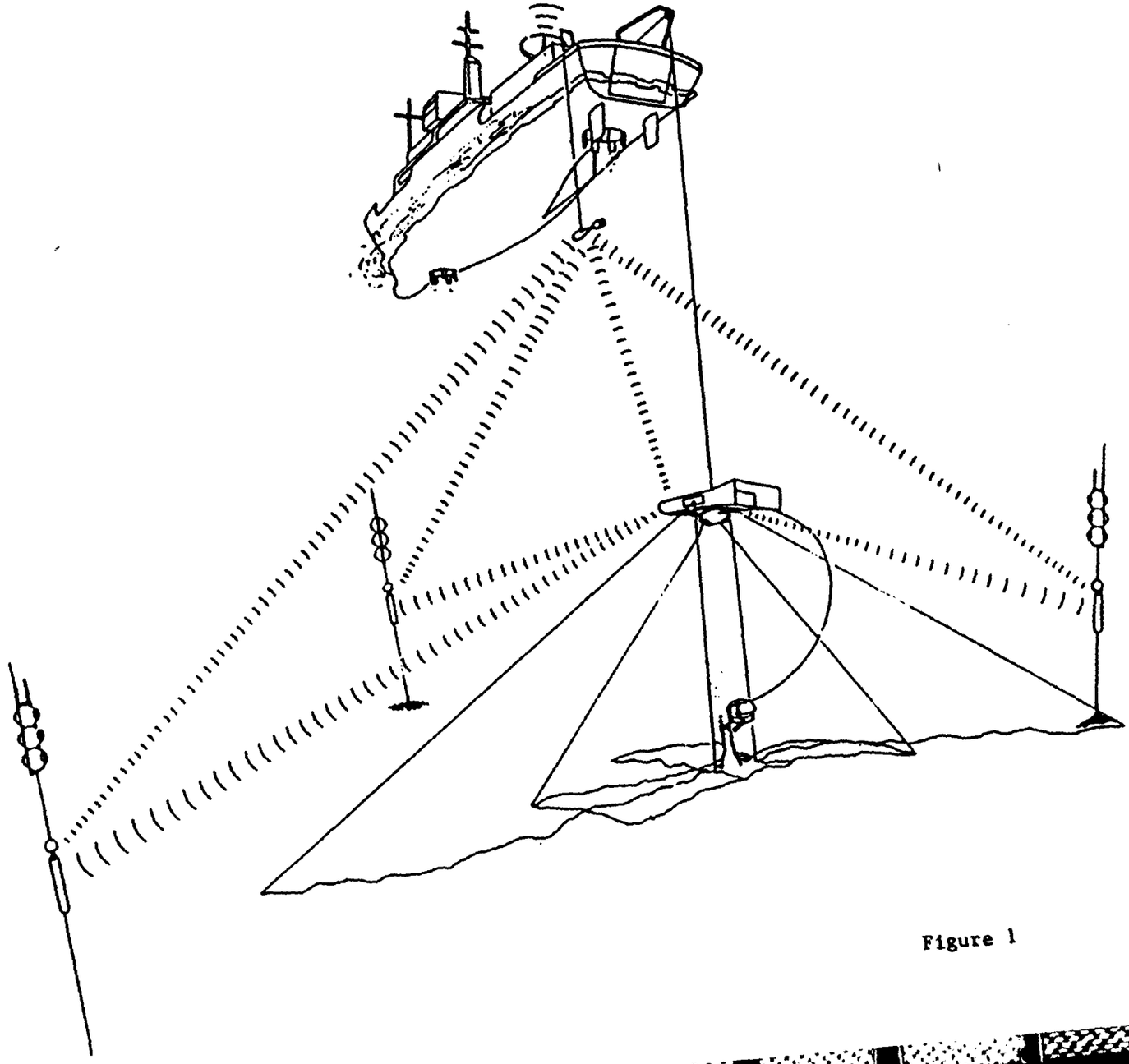

Figure 1

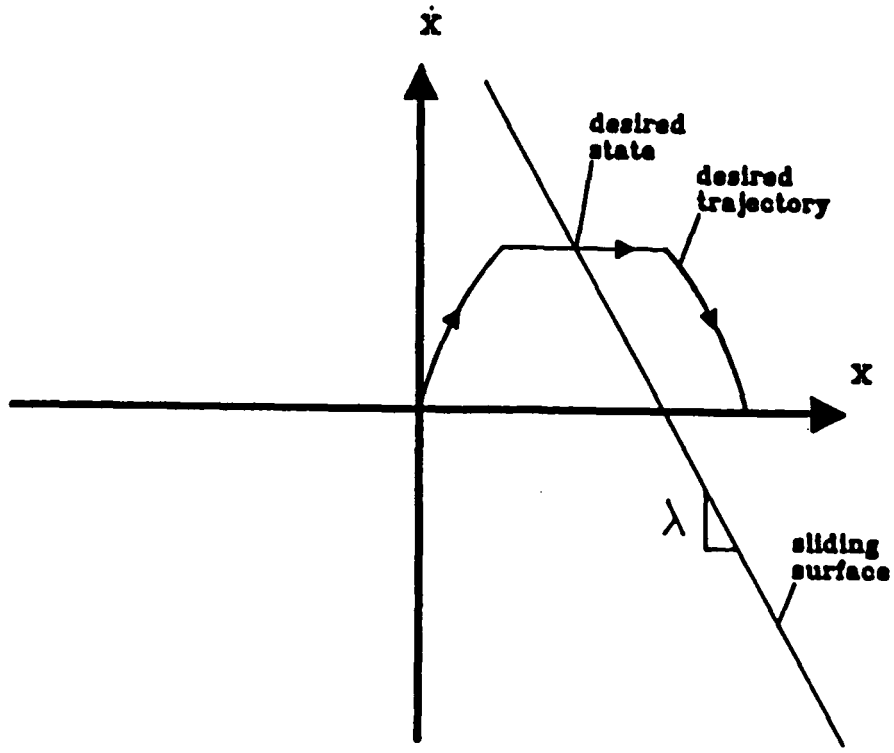

W.H.O.I.
YOERGER

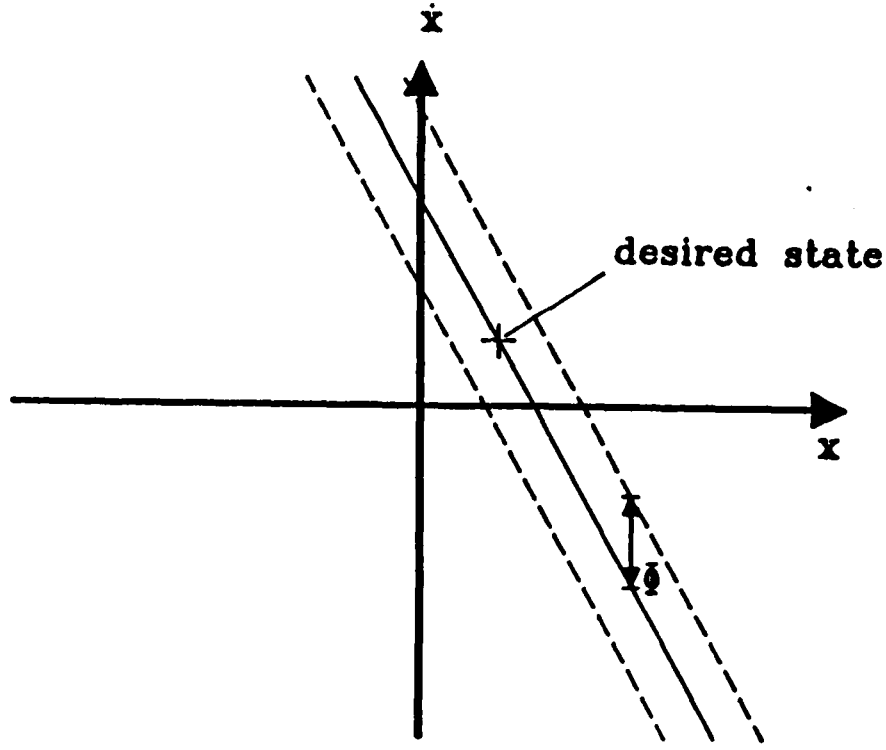

W.H.O.I.
YOERGER

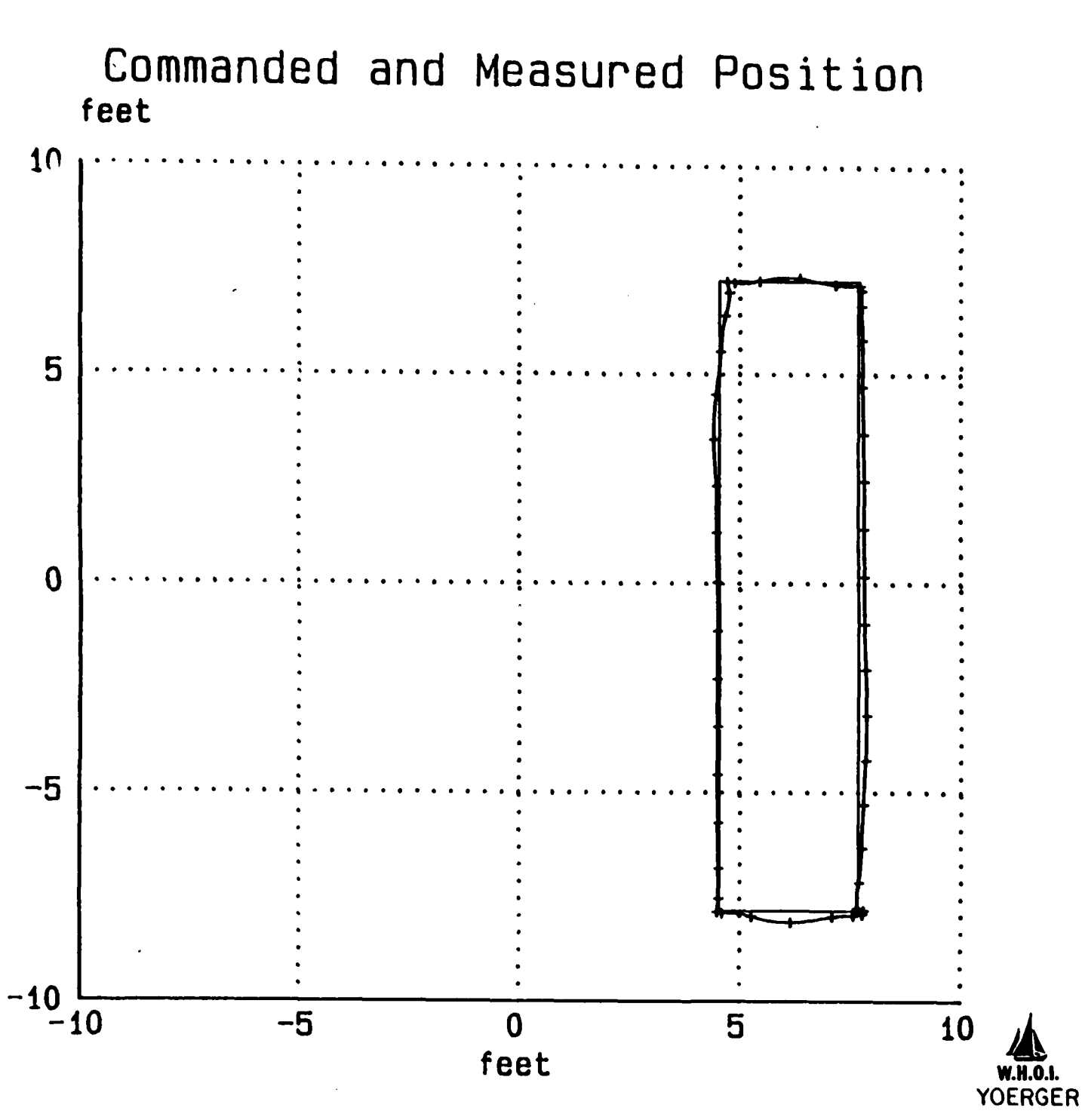
Commanded and Measured Position
feet
10
5
0
-5
-10
-10
-5
0
5
10
feet
W.H.O.I.
YOERGER

Desired and Actual Displacement

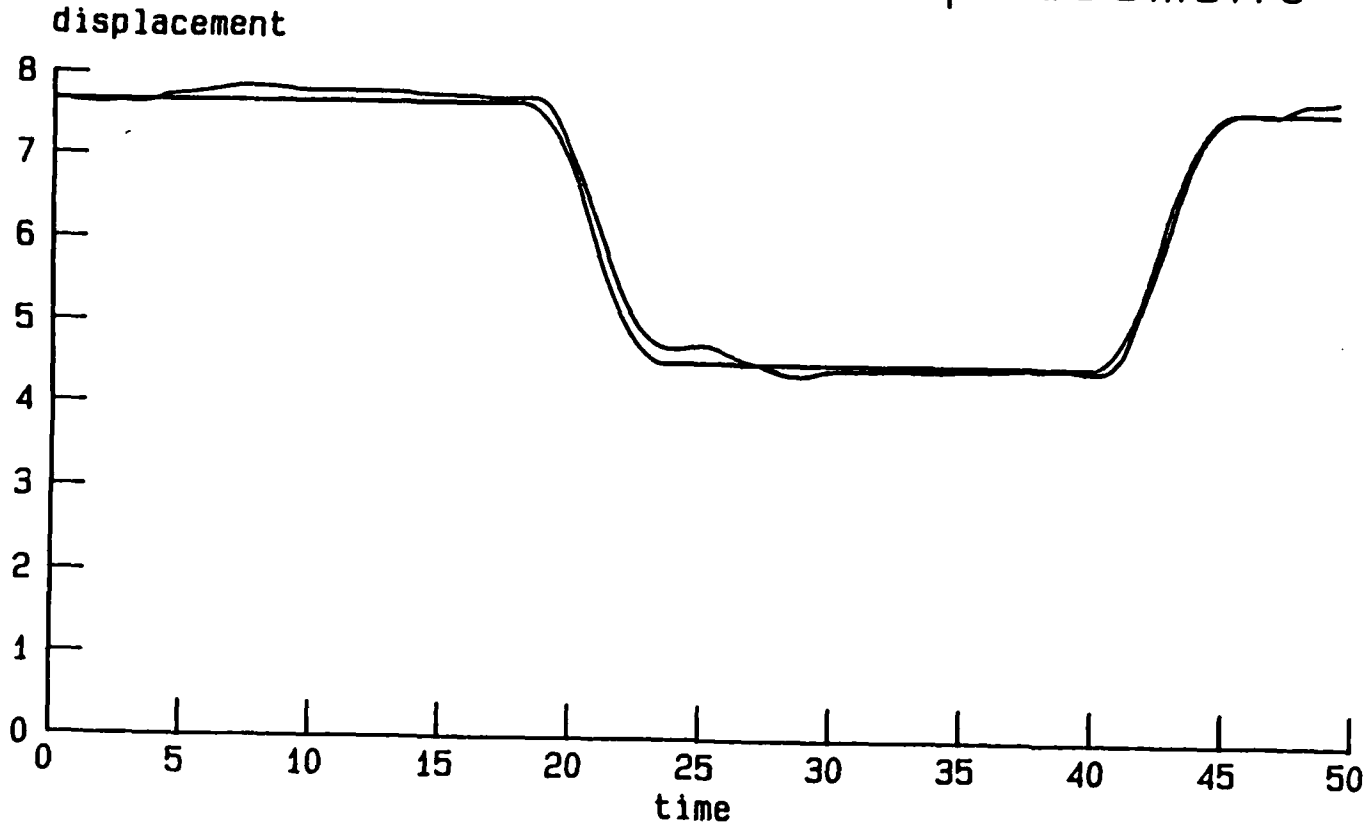

W.H.O.I.
YOERGER

S trajectory

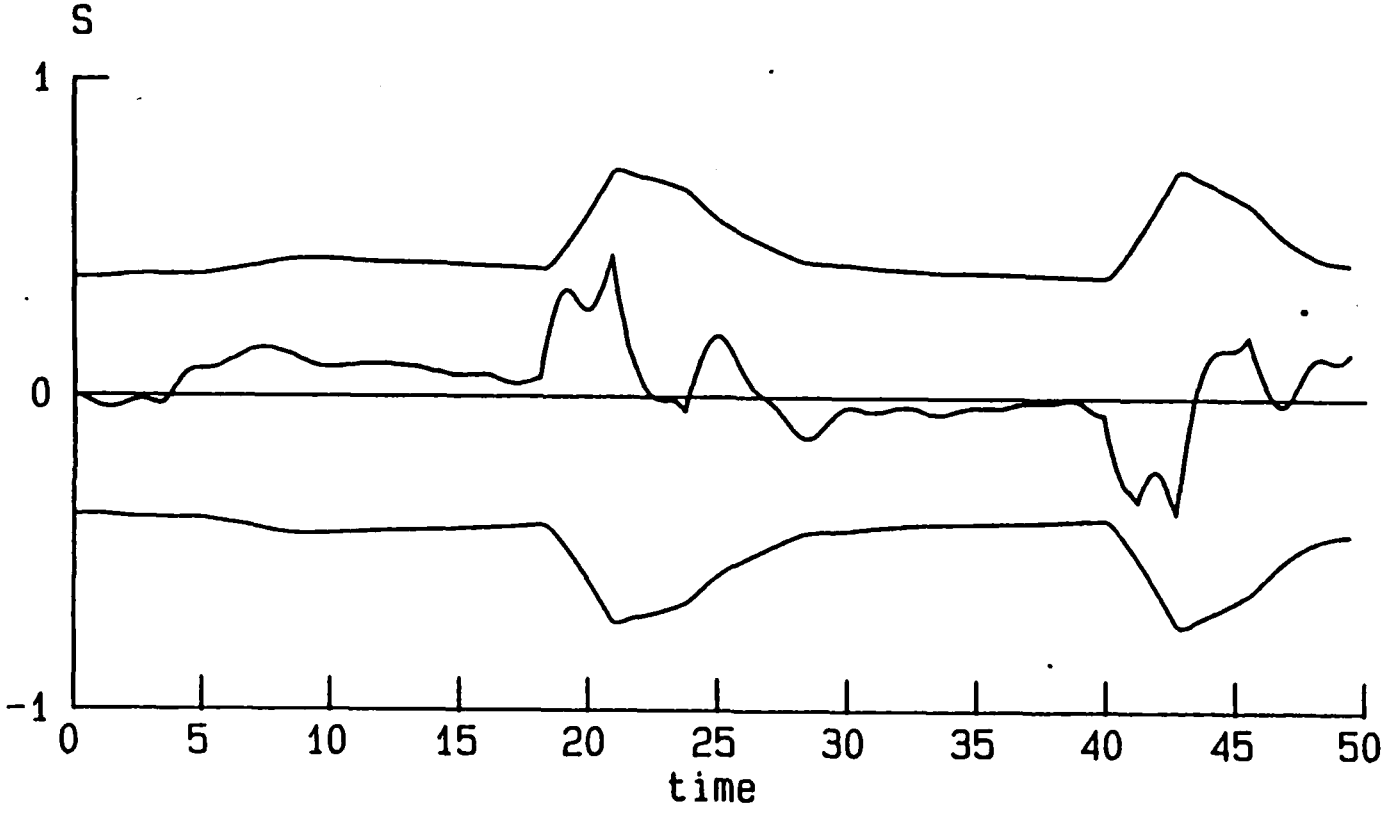

W.H.O.I.
YOERGER

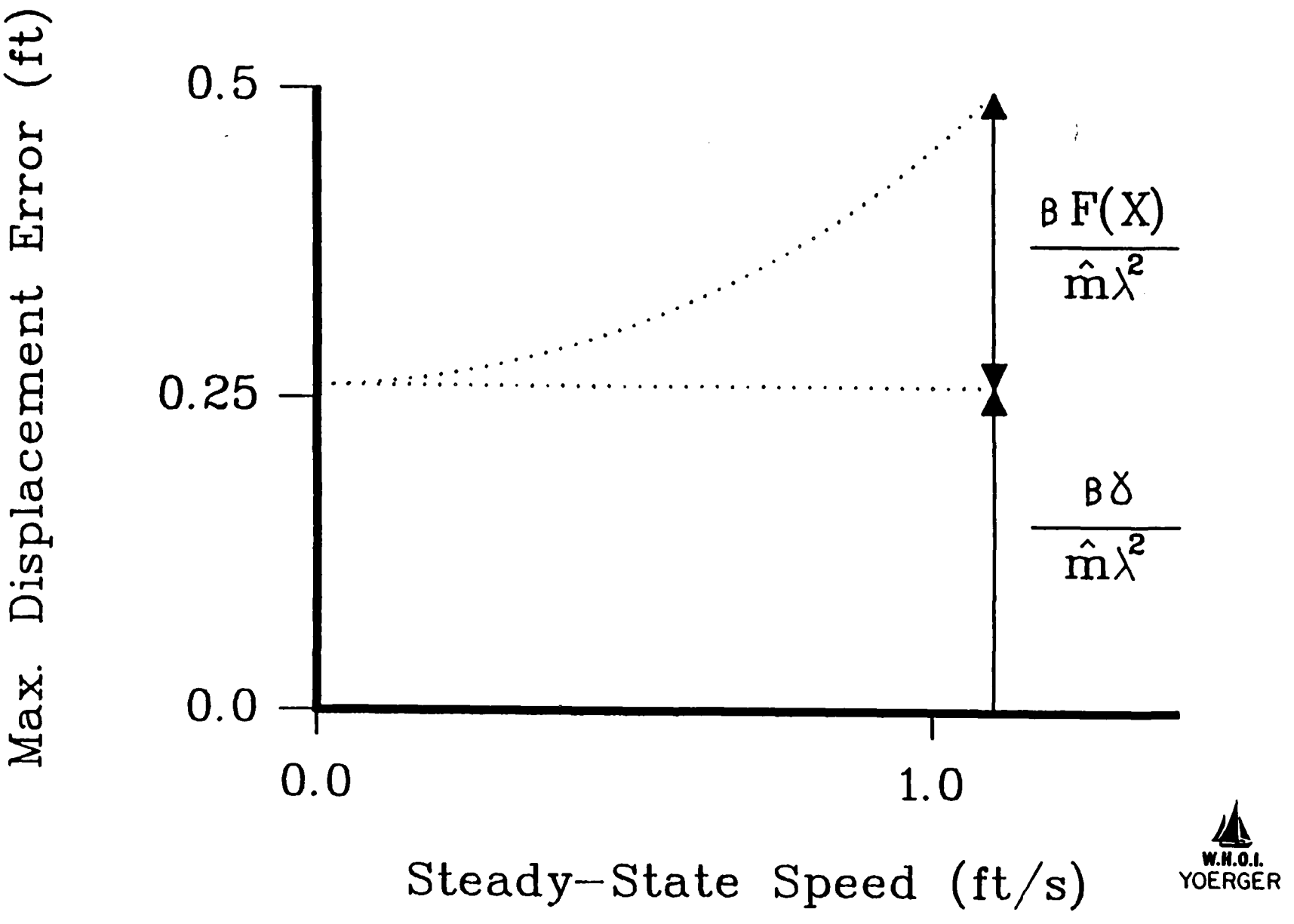
Max. Displacement Error (ft)
0.5
0.25
0.0
0.0
1.0
Steady–State Speed (ft/s)
$\frac{\beta F(X)}{\hat{m}\lambda^2}$
$\frac{\beta\delta}{\hat{m}\lambda^2}$
W.H.O.I.
YOERGER

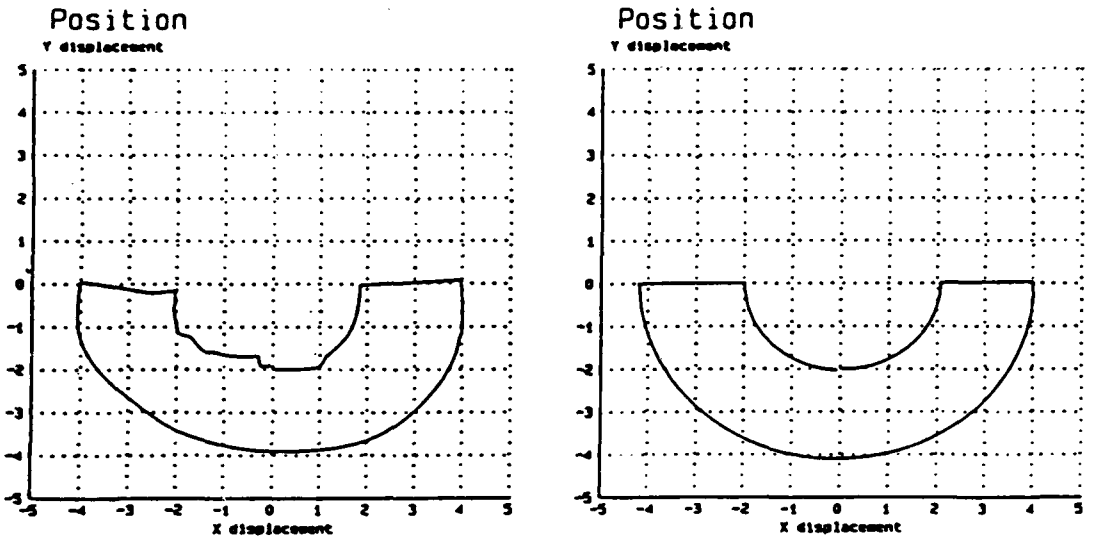
Position
Y displacement
X displacement
Position
Y displacement
X displacement

Figure 8

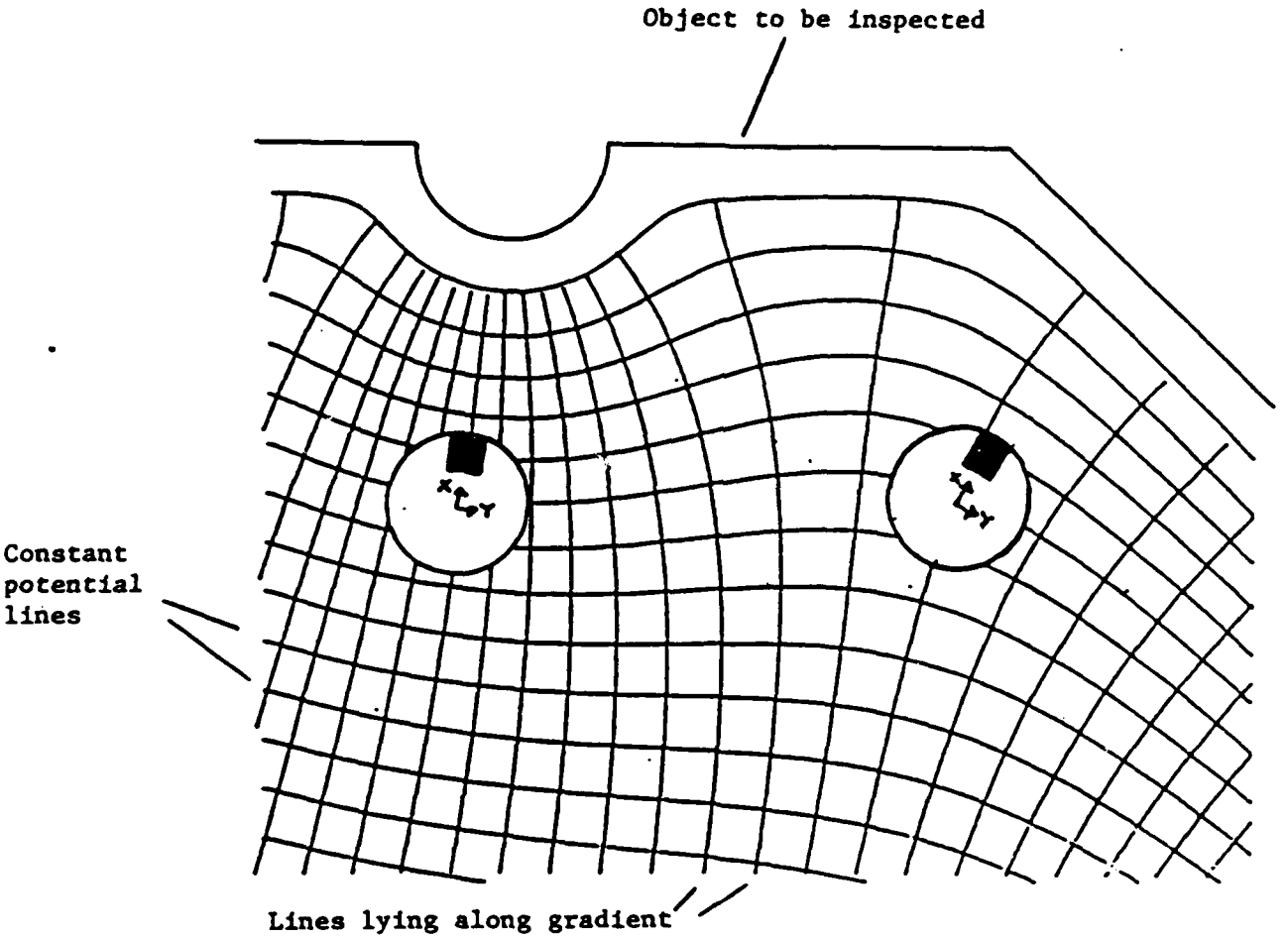

Figure 9

Figure 9: Barrier With Potential Fields

AD-A171 681 ARGO DEVELOPMENT PROGRAM(U) WOODS HOLE OCEANOGRAPHIC INSTITUTION MA DEEP SUBMERGENCE LAB JUN 86 N00014-82-C-0743 2/2

UNCLASSIFIED F/G 13/10 NL

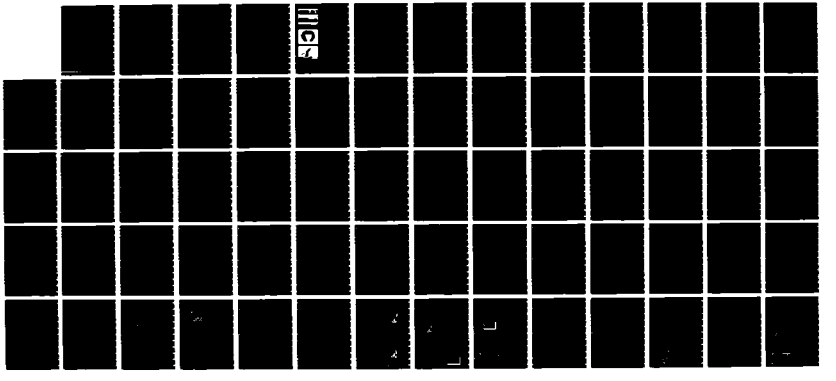

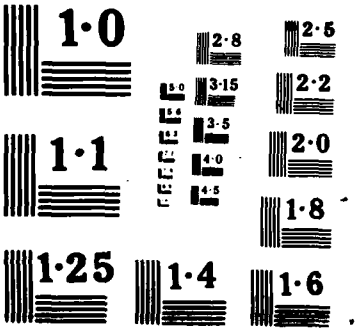
1·0
1·1
1·25
1·4
1·6
1·8
2·0
2·2
2·5
2·8
3·15
3·5
4·0
4·5

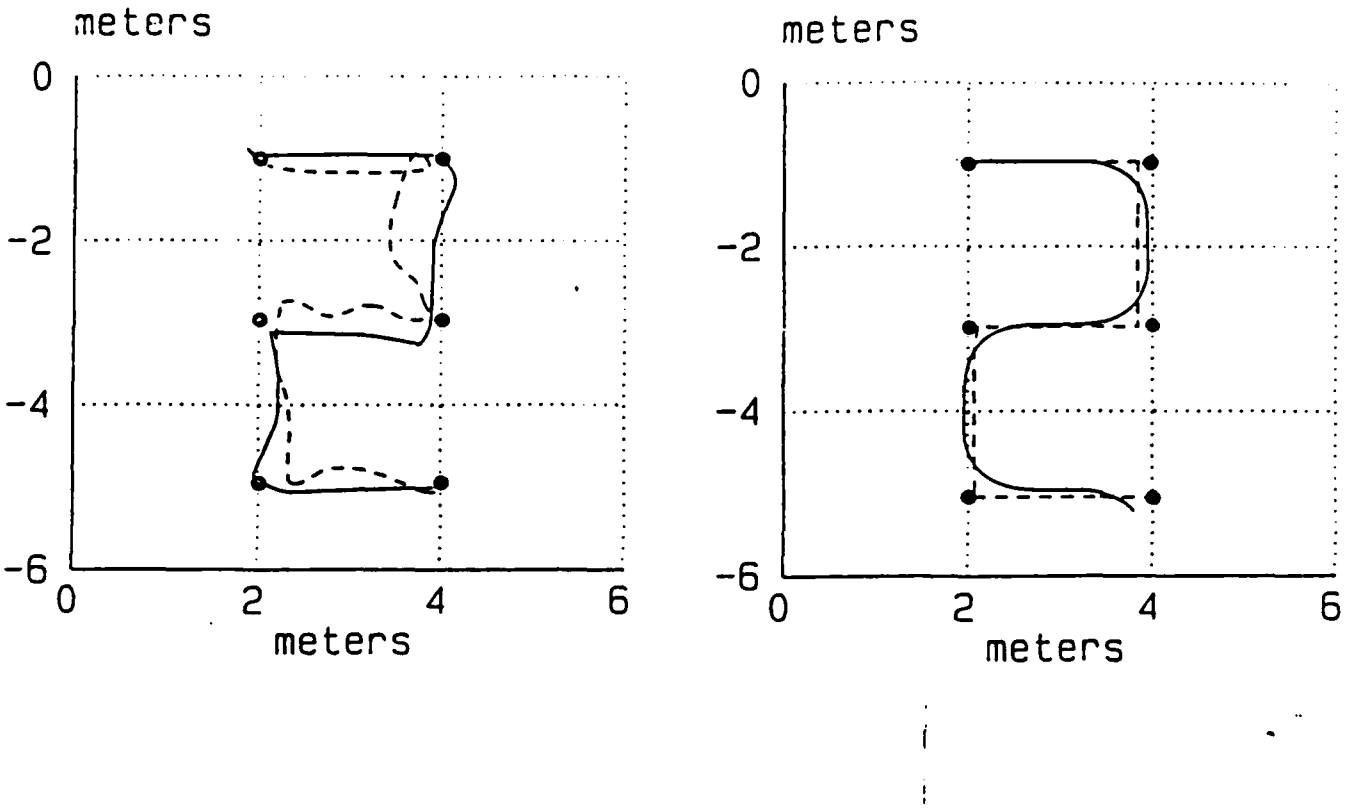

Figure 10

'ROV '84 Conference, Proceedings MTS/IEEE, San Diego, April 1984.

AN ADVANCED OBSERVATION AND INSPECTION ROV FOR 6,000 METER OPERATIONS

William K. Stewart

Woods Hole Oceanographic Institution [1]
Woods Hole, MA 02543

ABSTRACT

The Deep Submergence Laboratory of the Woods Hole Oceanographic Institution is developing an enhanced version of the Advanced Maneuverable Underwater Viewing System. The small, highly maneuverable observation and inspection ROV was designed to operate from a manned submersible to a depth of 6000 meters. The reconfigured system will be controlled from ALVIN or other manned vehicle, from a surface vessel as a towed body subsystem, or from a stand-alone laboratory development console. Analog and discrete subsystems are being eliminated in favor of digital architecture and integrated circuits. Microprocessor-based telemetry and control contribute to a compact, economical design, and a software control scheme offers flexibility and improved performance. Particular attention is given to operator interactions with the system. Keyboard, joystick, and voice recognition and speech synthesis peripherals are being assessed for contributions to control performance.

1. INTRODUCTION

To support the U.S. Navy's deep submergence activities, the Advanced Maneuverable Underwater Viewing System (AMUVS) was designed to deliver real-time video from underwater areas inaccessible by existing observation techniques. Deployed and controlled from a manned submersible, the tethered vehicle's small size and maneuverability suited it to surveys of submerged structures or to close-up inspection in confined spaces. The vehicle and outboard components have an operating depth range to 6000 meters.

Since becoming operational in the early 1970's, AMUVS-1 was used intermittently over the years following. Pressure induced failures and excessive maintenance demands precluded much active service. In October 1982, the Deep Submergence Systems Division of the Office of the Chief of Naval Operations transferred AMUVS to the Deep Submergence Laboratory (DSL) of the Woods Hole Oceanographic Institution (WHOI). Under a contract from the Office of Naval Research, DSL was to evaluate the system and offer recommendations for its future disposition.

As the result of an investigation and shallow water test program in 1983, DSL concluded that the AMUVS-1 concept was sound, but recommended a redevelopment effort to take advantage of progress in electronics and systems technology. With an emphasis on modular design and attention to compatibility issues, the enhanced AMUVS-2

AMUVS-2
OPERATING CONFIGURATIONS

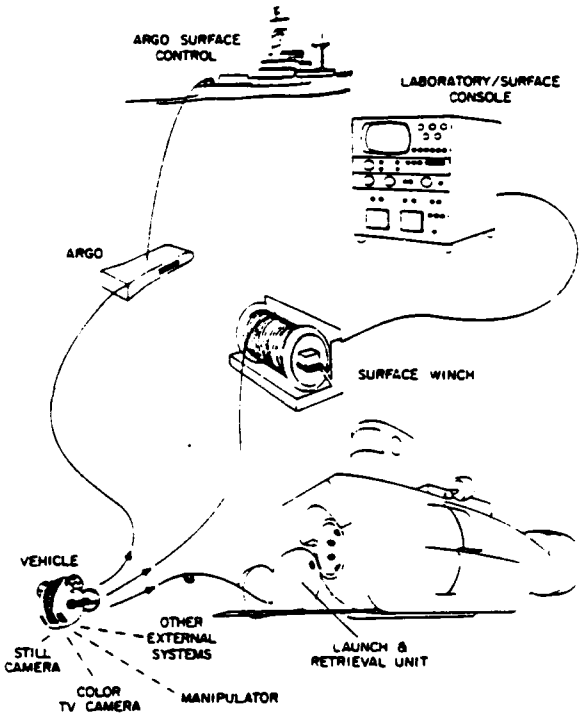

Figure 1. AMUVS-2 Operating Configurations

1. Ken Stewart, a Ph.D. candidate in the Massachusetts Institute of Technology/Woods Hole Oceanographic Institution Joint Program, is an ONR Fellow pursuing underwater applications of Artificial Intelligence and Robotics.

could serve also as a development test bed for deep ROV systems, or as an alternative vehicle for ARGO/JASON[2] (Figure 1.).

2. SYSTEM DESCRIPTION: AMUVS-1

Reduced to near essentials, AMUVS is a roving underwater eyeball. To escape the agonies of positioning a viewing device on a cable several kilometers long, the camera was deployed from a free-swimming manned submersible. The operator's senses, or vision, at least, were extended beyond his cumbersome life support apparatus. Gravity stabilized in pitch and roll, the vehicle can be propelled in forward and reverse, up and down, or left and right translations; rotated to port or starboard; or maneuvered in any combination of the four directions simultaneously.

Toward an understanding of the system's architecture and capabilities, AMUVS may be characterized by its functional subsystems and main equipment groups (Figure 2.).

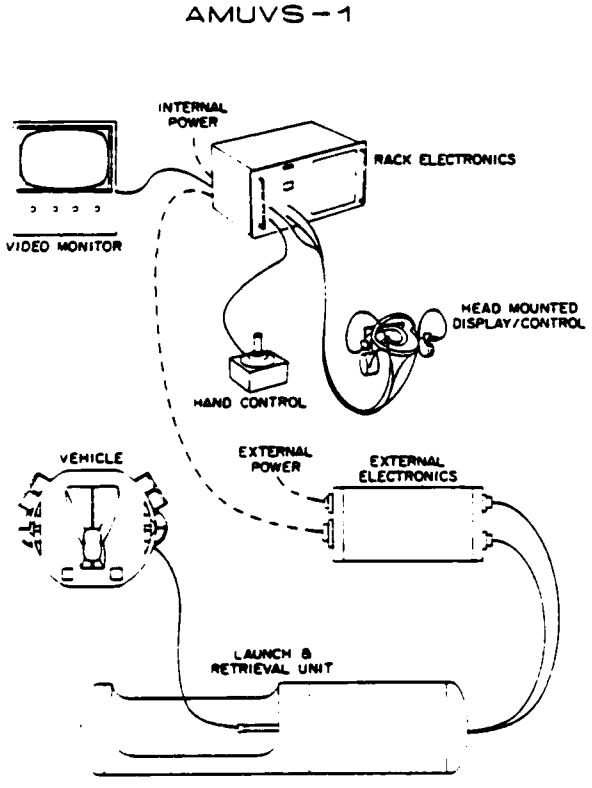

Figure 2. AMUVS-1 Equipment Groups

Functional Subsystems The four functional AMUVS subsystems are power, launch and retrieval (L/R), vehicle control, and viewing.

From dc sources aboard the support vessel, the power subsystem supplies the electrical requirements of all other components. The AMUVS-1 power subsystem was designed for TRIESTE II and requires both internal and external battery supplies.

The launch and retrieval subsystem enables an operator to release the vehicle from or secure the vehicle in a protective housing during submerged operations. It also provides for the paying out or winching in of the umbilical cable.

The vehicle control subsystem includes a platform (body) to support the camera and lights, propulsion for maneuvering the platform, and electronics for precise control. Depth and heading servos permit operation in manual or automatic feedback modes.

At the core of the AMUVS concept, the viewing subsystem includes a low-light-level SIT camera, two submersible lamps, signal conditioning electronics, and a video monitor. A secondary video output supports another monitor or video recorder.

Equipment Groups Hardware realization of the functional subsystems also falls into four groups or units: control station, external electronics, launch and retrieval, and vehicle.

The control station (console) group includes the rack electronics assembly, hand controller, video monitor, and associated cabling. Fed by a 28 V battery source, the rack electronics houses console power supplies and all internal control electronics. The hand controller is a small, portable unit with joystick and other controls for manual or automatic maneuvering of the vehicle. A head-coupled controller governing camera pitch and vehicle heading was originally included but later discontinued.

The external electronics unit contains the power control, power converters, motor drivers, and launch and retrieval control. Housed in a titanium cylinder, the unit is mounted near the L/R package outside the support vessel's pressure hull. Power for the external electronics (and vehicle) is delivered by a 115 V external battery supply.

The launch and retrieval unit comprises a fiberglass housing, umbilical winch and handling assembly, slip rings and signal control unit, and vehicle clamp (Figure 3.). Mounted to the exterior of the support vessel, the L/R unit secures the vehicle during support vessel operations and handles the umbilical during deployment.

The vehicle's roughly spherical, 56 cm (22 in) diameter, syntactic foam body supports

---

2. See "Development Status: ARGO Deep Ocean Instrument Platform," Stewart E. Harris, William M. Marquet, and Robert D. Ballard, ROV '84 Proceedings.

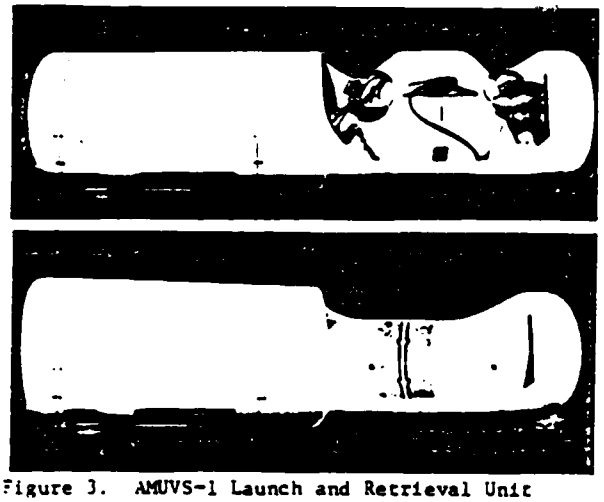

Figure 3. AMUVS-1 Launch and Retrieval Unit

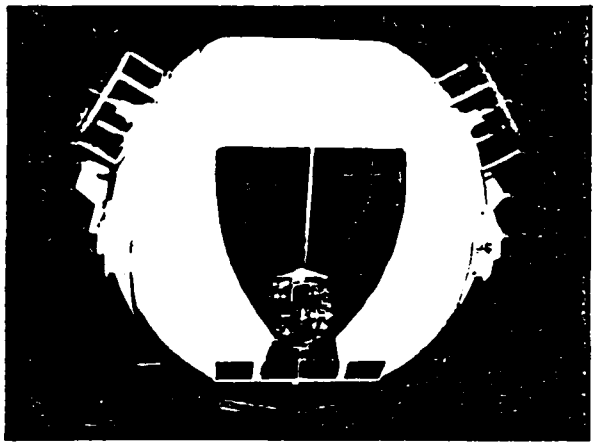

Figure 4. AMUVS-1 Vehicle and Pressure Housing

the thrusters and encloses a titanium pressure housing containing the camera and electronics (Figure 4.). A spherical glass envelope and precision pitching optics allow the viewing angle to be varied between plus and minus 90 degrees from horizontal. The thruster assemblies use oil compensated dc motors, two longitudinal, and two VERTRAN (combined vertical and transverse).

3. INVESTIGATION AND SHALLOW TESTING

During the summer of 1983, after a period of familiarization with the AMUVS and a preliminary investigation of its previous failures, the control station and external electronics were altered for use as a stand-alone system. Elimination of the external electronics unit required new motor control and signal paths, and power modifications to operate from regulated dc supplies. The reconfigured control station was assembled in a portable development console and a modified hand controller was designed and constructed.

Beginning with a completely dismantled vehicle, electronics subsystems were consecutively diagnosed, then repaired or modified until operational in the laboratory. The vehicle and underwater components next were assembled and tested in DSL's shallow water tank (1.2 m deep, 6 m diameter). After several iterations of troubleshooting and repair, the system approached full performance. At this point, the testing became more operational, and AMUVS' capabilities were evaluated in the DSL tank and in the waters of Vineyard Sound.

Concurrent with operational testing, DSL implemented computer control of AMUVS as a step toward development of more sophisticated systems. Using an RCA Microdisc Development System with an 1805 microprocessor "piggybacked" on the console, the vehicle could be operated manually, under direct software control, or by a combination of the two methods. Voice recognition and speech synthesis peripherals linked through an IBM-PC added an option for operator voice control; computer generated speech verified correct interpretation of commands.

As a final part of testing and evaluation, it was necessary to address the issue of AMUVS' compatibility with the ALVIN submersible. Such obvious considerations as power distribution and hull penetrations presented no insurmountable difficulty, but there remained some questions of mutual interference between two electrically noisy systems. After small changes to use a combination of shore power and battery supplies, the vehicle and L/R unit were mounted at ALVIN's bow, the console and power supplies inside ALVIN's pressure sphere. During two days of testing, AMUVS was operated and evaluated from within the semi-submerged ALVIN.

4. TEST RESULTS AND EVALUATION

After reviewing the program results, we concluded that AMUVS' general design philosophy and much of its hardware were well-conceived and executed. Through discussions with Navy operations personnel, the original equipment manufacturer[3], and other suppliers, there emerged a consensus that AMUVS could be made to work reliably at depth. However, there were significant problems to be overcome, mainly associated with the thrusters, umbilical, and high packaging density.

To reduce the camera platform size, which greatly influences the scale of other components, two important design tradeoffs originally were made. First, the video signal was modified to carry vehicle sensor and control signals. Some reduction in telemetry circuitry was realized but at the cost of an interdependency between the two functions. The choice resulted in some degradation of the picture, in an incompatibility with other cameras, and in cable length constraints because of video synchronization requirements. Second, vehicle control functions, notably the motor drivers, were located as much as possible in the console or external electronics unit. This prescribed four pairs of umbilical conductors for motor control. To deliver enough power, the cable diameter grew. The pulse width modulated armature current further degraded the baseband video signal.

Though the vehicle's spherical shape and VERTRAN thruster arrangement have disadvantages, the tradeoffs against compactness, omnidirectional maneuverability, and simplicity of design appear to be good ones. Cable forces, low damping, and proximity of the centers of mass and buoyancy contribute to unsteady camera positioning, but the viewing defects are acceptable. To propel the vehicle in translation (forward/reverse) and rotation (port/starboard), the longitudinal thrusters are located most efficiently on the vehicle's periphery. For the two other translations (left/right, up/down), this arrangement is not possible. However, the propulsion inefficiencies of the VERTRAN configuration are less objectionable than the scaling effects of a fifth motor or the complexity of steerable thrusters.

The vehicle's brush-commutating dc motors were subject to problems typical of the species. Compensating fluid breakdown caused by commutator arcing was accelerated by brush hydroplaning and high ambient pressure. A conductive, particulate breakdown product reduced the fluid's dielectric strength, leading to increased arcing in a self-feeding process. A second, gaseous byproduct remained in solution at depth, but motors suffered the "bends" when returned to the surface. Worn gearboxes decreased motor efficiency and created a large deadband; at low-torque operation, sensitive manual control was difficult, and some instability was introduced in the azimuth servo.

To realize neutral buoyancy in a 90 mm (0.35 in) cable, the umbilical design employed copper-clad aluminum conductors (five pairs and one coaxial), a solid-core synthetic strength member, and polypropylene jacket. Because of significant stiffness and memory, the cable took the set of the spool creating a "watch-spring" effect. Besides hindering free movement of the vehicle, the helical cable tended to kink during retrieval. Leaks were a problem around connectors since the polypropylene jacket was not readily bondable.

High packaging density in the vehicle and external electronics created a noisy electromagnetic environment and a marginal ability to dissipate waste heat. Problems included premature component failures in the motor drivers and vehicle heat sink assembly. Incorporated in the laboratory console, the original drivers worked well for several weeks but eventually failed. For lack of spares, repair efforts ceased and testing was completed by modifying the control electronics to use power amplifiers from DSL's Benthos RPV-430. The remainder of the vehicle electronics, though sensitive to handling, were reliable once working properly and installed in the pressure housing.

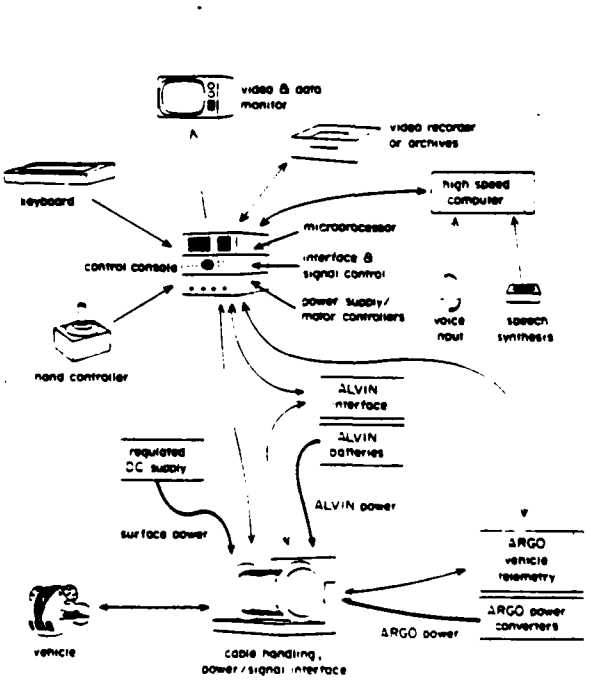

FIGURE 5. AMUVS-2 Equipment Groups

3. Originally developed by Oceanographic Engineering, Inc. Later became Hydro Products, Inc., which now markets an improved, shallow-water version of AMUVS, the RCV-225.

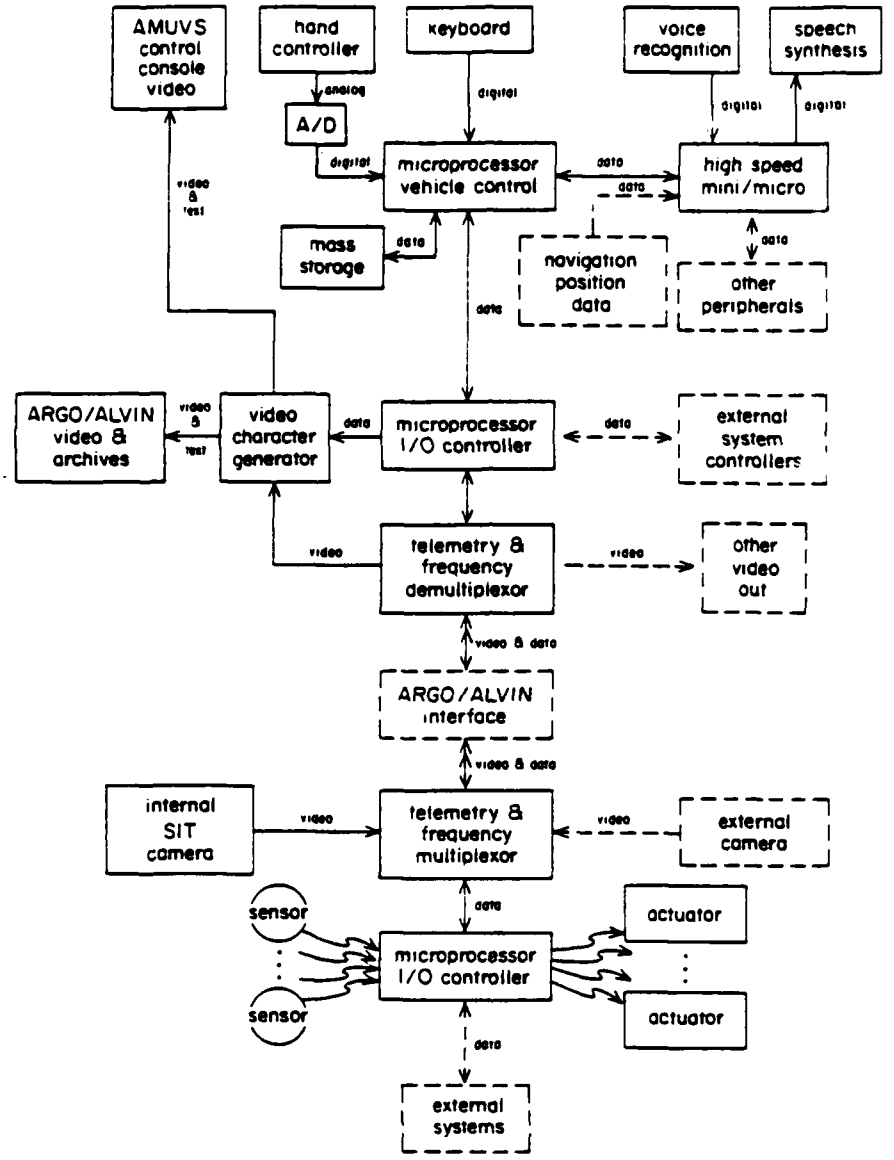

Figure 6. AMUVS-2 Telemetry and Control

Other more general problems arose in dealing with an older, one-of-a-kind system. Because of rapid progress in electronics technology during the last decade, some parts were difficult to replace. Also, the control station and vehicle electronics had been extensively repaired and altered over the years. Unfortunately, the documentation had failed to evolve with the system. Seemingly minor repairs or modifications often had unpredictable results.

5. DEVELOPMENT CONSIDERATIONS: AMUVS-2

Finding the general AMUVS conceptual design to be excellent, DSL is using the original configuration as the basis for a two year development program (Figure 5.). Fundamental concerns are video quality, the vehicle's small size, and maneuverability. Since the system was intended primarily as an observation device, DSL will focus initially on AMUVS-2 subsystems which

most influence that function. To the extent possible, the size and weight reductions of more efficient vehicle components will be put toward some payload capacity. An external color camera will augment an improved SIT, and a small manipulator package or other external sensors will expand the system's functions.

AMUVS-2 will incorporate some AMUVS-1 hardware including the vehicle's syntactic foam body, titanium pressure housing, and much of the launch and retrieval unit. However, the core of the redevelopment program entails the upgrade of console and system electronics to a microprocessor-controlled design (Figure 6.). The main reason is that advances in electronics technology argue for the replacement of analog and discrete subsystems with cheaper, more reliable integrated circuits. A low component count will contribute to a compact, efficient, and maintainable system. A second impetus is the need to separate telemetry and video into two separate subsystems. FM modulation of the video signal will reduce motor driver interference, and software control will enhance performance and offer more flexibility in future development.

The external electronics bottle will be eliminated, and a new power supply/motor controller unit incorporated in the console. A reduction in pressure exposed components, cable, and connectors will help simplify the system and improve its reliability. The interface with other systems is eased, and elimination of the heavy, external housing makes it more reasonable to install on ARGO or on ALVIN. In contrast to TRIESTE II, these have limited space and payload. With modifications to the vehicle L/R unit, AMUVS-2 will use ALVIN's 30/60 Vdc battery supplies more efficiently.

The overriding consideration in a new umbilical design for AMUVS is the need to realize the smallest cable diameter possible. Cable forces significantly affect the vehicle's stability and mobility, and limit the possible excursion radius where curents are present. A development effort with the Naval Oceans Systems Center shows promise for a new umbilical of the same diameter which will circumvent the previous deficiencies. For now, cable size will be dominated by the requirement of four conductor pairs delivering power to the thrusters. On the horizon, we hope, is a brushless motor design integrating commutation and control electronics within the motor housing. With such an arrangement, motor control signals would be telemetered along with other data, and motors would operate from a common power bus to eliminate the eight conductors. At that point, the use of an optical fiber to further reduce cable size begins to make sense.

In the meantime, thrusters will be upgraded to more efficient, brushless dc motors from Hydro Products, Inc. The gassing problem will be avoided and fluid breakdown reduced. Operating at lowered rpm, a gearbox is obviated, and viscous and mechanical losses are diminished. For the same weight and volume as the originals, the newer, 1/3 hp motors are rated at three times the shaft torque. When delivering a comparable thrust, the motors work at an easier pace to prolong the life of ALVIN's batteries.

Software efforts will focus on improving the operator's control of and interactions with the vehicle. Along with the development of new hardware, including the console and improved hand controls, other aspects of the operator interface will be addressed. Voice recognition and other control software will be developed and assessed. Computer modelling of the vehicle's hydrodynamic characteristics will be used to investigate vehicle stability and dynamics. This will lead eventually to the development of different bodies using more modern, low-density foam.

6. FUTURE DEVELOPMENT

During the first two years of the AMUVS-2 program, our emphasis will be on fulfilling the original design goals for a working observation and inspection device. The first deep-water testing to ALVIN's 4000 meter (13,000 feet) depth is scheduled for the beginning of 1985.

Also under consideration is a plan to adapt AMUVS-2 for use with early versions of DSL's ARGO platform. The system's compact size and reconfigured power and telemetry make it suitable for preliminary trials of an ARGO/JASON system. With the larger, more capable JASON vehicle still in the first stages of design, AMUVS-2 offers an immediate alternative for testing ARGO/JASON concepts. Later, this "JASON JR." could be used as an optional, second vehicle to suit specific mission requirements.

At a later program phase, a simple manipulator will be added to extend the AMUVS-2 capabilities beyond those of a passive viewing device. The primary use of such a function would be in clearing away sediment, marine growth, or other small obstructions which prohibit the system from completing its observational mission. Also, some manipulative ability would permit an operator to deal with a fouled tether or to carry out light tasks or recovery without recourse to a larger work package.

In keeping with the Deep Submergence Laboratory's mission to develop advanced underwater systems, AMUVS-2 will serve to explore more advanced aspects of vehicle control[4]. A particular area of interest is in improving the

---

4. See "Man-Machine Interface and Control Concepts for the JASON Program," Dana R. Yoerger, ROV '84 Proceedings.

interface between operator and system. Though AMUVS-2 presents a relatively uncomplicated control problem, more sophisticated ROVs, such as JASON, will strain an operator's ability to manage large degree-of-freedom systems. Consideration will be given to developing a "smart" ROV which can augment the operator's skills.

Integrated positioning and control is one example of such an application. Input from the operator and sensor data from the vehicle, support vessel, or surface devices may be combined by the system to "learn" about its environment and to build an internal model of it. Communicating with the operator through speech, graphics, and video overlays, the computer supervisor may relieve some burden on its human counterpart by sharing or trading control. Hands-off stationkeeping, automatic compensation for changing environmental conditions (currents, for example) or self-adaptation to varied vehicle loading would be advantageous.

7. CONCLUSIONS

As with ALVIN, ANGUS, and others of WHOI's proved deep submergence devices, AMUVS-2 is intended as a fully-functional working system. In support of oceanographic research, AMVUS-2 must withstand its harsh environment during extended periods at sea. But along with ARGO/JASON and others of DSL's family of vehicles, AMUVS will be an open-ended development tool to incorporate and evaluate conceptual and technological advances in deep submergence systems. As the marine community's interest in the deeper ocean regions continues to expand, AMUVS-2 will enhance an ability to project our human senses and capabilities there.

ACKNOWLEDGEMENTS

This work is funded under ONR Contract No. N00014-82-C-0743.

EVOLUTION OF Sea MARC I

Dale N. Chayes

Reprinted from 1983 IEEE PROCEEDINGS OF THE THIRD WORKING SYMPOSIUM ON OCEANOGRAPHIC DATA SYSTEMS

EVOLUTION OF Sea MARC I

Dale N. Chayes

Lamont-Doherty Geological Observatory of
Columbia University
Palisades, N.Y. 10964.

ABSTRACT

Sea MARC I (Sea-floor Mapping and Remote Characterization) is a deep towed acoustic swath mapping system used primarily in the deep ocean. The present state of the system is the evolutionary product of a continuing cooperative development effort between Lamont-Doherty Geological Observatory (LDGO) and International Submarine Technology, Ltd. (IST). The vehicle has a bilateral side scan sonar (27 and 30 kHz), a CHIRP subbottom profiler (1 to 5 kHz sweep or fixed frequency), a three-axis flux-gate magnetometer, pitch and roll sensors, a frequency agile (7-14 kHz) navigation responder, a two-axis electromagnetic speed log, and a pressure gauge. A self-recording Aanderaa current meter is mounted on the vehicle. In real time, Sea MARC I displays slant-range-corrected, orthorectified side scan images representing a 1,2, or 5 km wide swath; a pressure-depth-corrected seafloor and subbottom profile; computer generated plots of vehicle altitude, vehicle depth, water depth, vehicle heading, pitch and roll and total magnetic field. Sonar data, vehicle parameters, and navigation data are stored on computer tape for post cruise analysis. The vehicle is stabilized using a two body tow scheme with a passive depressor and a neutrally bouyant instrument package.

INTRODUCTION

Sea MARC I is an acoustic swath mapping system using medium frequency (27 and 30 kHz) side scan sonar and a versatile CHIRP subbottom profiler. Although initialy built to search for the Titanic, Sea MARC I was designed as and is primarily operated as a flexible research tool for scientific investigation of the sea floor. Sea MARC I has proven most powerful for investigating features on the scale of tens of meters to tens of kilometers including slumps, slides, and debris flows (Ryan, 1982), submarine canyons (Farre et al., 1983), spreading centers and transform faults (Malahoff et al., 1982), and seamounts (Fornari et al., 1983). The five kilometer swath width is wider than Deep Tow (Spiess and Tyce, 1973) and narrower than either GLORIA, (Laughton, 1981) or Sea MARC II (Blackinton et al., 1983). Table I is a list of Sea MARC I cruises to date.

The Sea MARC I system is a significant addition to the suite of available tools for mapping the ocean floor in several unique ways. First the intermediate range coupled with high resolution (Kosalos and Chayes, 1983) fills a gap in the existing range of obtainable survey tools. Second, the improved vehicle stability derived from the two body towing arrangement provides significantly better data quality than is available with single body systems. Third, careful attention to maintaining high dynamic range in the sonar and telemetry subsystems coupled with very low cross-talk and minimal system noise result in high quality sonar images.

Initial funding for the system was made available by Titanic 1980, Inc. in April of 1980. Following three months of frenetic effort at LDGO and IST, sea-trials began in July. Since the initial cruise, the system has evolved to its present configuration as the result of a sequence of additions, deletions, and modifications based on scientific requirements and operational constraints modulated by the availability of manpower and money.

For the purposes of this paper the system will be discussed as the following components: Ship, Operations van, Deck machinery, Tow system, and Electronics, each of these will be discussed in terms of its evolution, its interaction with the rest of the system, and its impact on the quality and quanity of data collected.

SHIP

At the very least we require a ship which is capable of manuvering at slow speeds (1-2 knots) and has sufficient deck space for the operations van and the deck equipment. Although Sea MARC I is flexible enough to operate from a broad range of ships (Table 1), the handling and sea keeping characteristics of the ship have a significant impact on the quanity and quality of data which is collected. On larger more stable ships such as the Surveyor and the Hudson, the system will continue to produce good quality side scan data in sea states up to 5; on smaller ships vehicle motion increases drastically and data quality deteriorates significantly in sea states worse than 4. Slow towing speeds, the high drag of the tow cable in wind, current and waves may conspire to make it impossible for a small or less manuverable vessel to achieve the desired course. Bow thrusters, active rudders, acts of God, twin screws, a towing crane (see "Deck Machinery" below),shallow water (with resulting shorter cable), and experienced personnel increase the chances of successfully carrying out a desired survey track.

OPERATIONS VAN

For the first seven cruises all of the computers, electronics, facsimile recorders, winch remote controls and monitoring equipment, test equipment, manuals and spares associated with the system were installed in each ship's lab prior to each cruise and removed at the end. This laborious task took about ten person days, and was hard on tempers and equipment. In the summer of 1982 all of this equipment was built into an ISO standard twenty foot shipping container. Although the van is configured as a laboratory there are no external fittings

CH1926-5/83/0000/0103$01.00©

TABLE 1. Sea MARC I Cruises

SHIP	DATE	LOCATION	FUNDING
H.J.W. Fay	Jul. 1980	Titanic 1980	Titanic '80
RV Gyre	Aug. 1980	US East coast canyons	USGS
RV Gyre	Sep. 1980	SE US coast Cont. Slope	USGS
MV Pacific Seal	Feb. 1981	Mississippi Trough	Shell
MV Pacific Seal	May. 1981	New Jersey Cont. Slope	Shell Consort.
RV Gyre	Jul. 1981	US East Coast Cont. Slope	USGS
CSS Hudson	Jul. 1982	Nova Scotia Cont. Slope	Can. Govt.
OSS Surveyor	Sep. 1982	Juan de Fuca Ridge	NOAA
RV Robert D. Conrad	Dec. 1982	Mississippi Fan	JOI
RV Thomas Washington	Jan. 1983	East Pacific Rise	NSF
CSS Hudson	Jun. 1983	Laurentian Fan	Can. Govt.
RV Robert D. Conrad	Jul. 1983	Titanic 1983	Titanic '83

which might preclude its being shipped sea freight as a container.

During Sea MARCing the van is the operations center as well as the place where the sonar data are displayed. It is staffed 24 hours a day by a watch-leader who has overall responsiblity for data quality,navigation, and safety and a fish-flyer whose responsibility is to monitor the depth and altitude (height above the sea floor) of the vehicle, the operation of the winch and deck equipment, and to remotely operate the winch so that the vehicle altitude remains within the range specified by the watch leader. All of the data necessary to the operation and control of the Sea MARC electronics and winch are displayed in the van. This includes display of processed sub-bottom profiler data showing the vehicle depth and altitude, slant range corrected side scan sonar images, status of the data logging computer, vehicle and ship navigaion parameters, a plots of the ship position, and plots of vehicle speed through the water, magnetic field and vehicle attitude, and television monitors showing the deck equipment.

The van is equiped with a power distribution and lighting system, air conditioning and ventilation, fire extinguishers, a watertight hatch and an emergency exit. Storage for expendables, manuals, and spare parts is provided in built-in cabinets, shelves and lockers. A steel container was chosen over aluminum or fiberglass to provide some measure of electromagnetic shielding, and for ease of installing the hatch, emergency exit, and penetrators. The van was framed internally with two by fours and insulated to R-19 to reduce the air conditioning load and to provide acoustic insulation. Half-inch plywood over the insulation provides the foundataion for mounting light equipment and shelves. Three nineteen-inch electronics racks on a hydraulically movable frame carry the bulk of the electronics. Terminals, plotters, and a desktop computer are installed on table tops. Facsimile recorders are mounted in a cabinet behind plexiglass windows with forced ventilation to reduce noise, odor and particulate matter in the air.

DECK MACHINERY

Deck machinery includes the tow winch, level-wind, slip ring, tow crane or "A"-frame, accumulator, and launch and recovery equipment. Although not particularly exciting when it is working normally, deck machinery is probably the biggest single cause of lost ship time in deep towing. While it is not unusual to spend man-years engineering the instrument package , many pieces of deck equipment are acquired without adequate analysis of their impact on the overall system performance. Towing operations require line speeds of one to five meters per minute, emergency speed of about 100 meters per minute, and line tension as high as 7,000 kg. Of the ships from which Sea MARC I has operated, only the Hudson and the Washington came equipped for deep towing. On the Fay, and the Gyre, all of the deck machinery including a Western Gear traction winch, ,spring accumulator, sheaves and towing crane were leased from the Marine Physical Laboratory (MPL) of Scripps Institution of Oceanography. On the Pacific Seal the MPL winch, sheaves, and accumulator were used but a small "A"-frame was used instead of the towing crane.

After several problems with the winch caused the loss of ship time and damage to tow cables we evaluated what type of winch would be best suited to our application. Jay Ardai of LDGO in conjunction with LeBus International developed a design for a direct pull diesel-hydraulic deep sea towing winch with LeBus grooving and a LeBus Fleet Angle Compensator with Positive Sheave Control. A diesel-hydraulic power plant was chosen over an electro-hydraulic plant in order to be independent of the ship's power and because there was a surplus diesel available at Lamont. For a permanent installation, electro-hydraulic power might be preferable . A closed loop hydraulic drive was chosen over electric drive for ease of control and simplicity of repair.

The draw works and the level wind were built by LeBus as separate pieces for easier shipping, and the compact diesel-hydrualic power unit was built at the Lamont Machine Shop from readily available commercial components wherever possible. A GM in-line 6-71 diesel driving a Sundstrand PV-25-2074 variable displacement axial piston pump in the power unit drives a Sundstrand MH-187-JG fixed displacement radial piston pump and integral 4:1 planetary gear reducer which is directly coupled to the drum in the draw works. The winch has been used on the Surveyor and Conrad cruises with very little down time. A similar design has been developed by Whitman Ben (Mills,1982) for the Atlantic Geoscience Centre and built by Timberland Equipment.

Although small and relatively inexpensive the top-side slip ring can be the source of major difficulties which are often time consuming to isolate. A mercury-wetted design from Meridean Laboratory was chosen for its very low noise, sealed stainless steel construction, and small size.

Sheaves, and accumulators are important especialy as they directly influence the the life of the tow cable (Gibson, 1982). Wire life can be measured as the number of bending cycles to failure under load so it follows that reducing the total number of sheaves in an installation will increase wire life. Snap loading is not a problem while the vehicle is deployed but can be

serious during launch and recovery operations in heavy weather when it is possible for the wire to go slack on the deck. A good accumulator can significantly damp snap loads. Care must be taken in the installation and in the design of the sheaves and fair-leads that a slack wire can not jump a sheave or snag.

Two-thirds of the Sea MARC I cruises have used a HyHoe crane, specially modified by MPL for use as the tow point as well as for launch and recovery. The HyHoe was originally a diesel powered articulated, hydraulic excavator. The tow cable runs into the base of the crane through a vertical flag block and over three more sheaves out the boom and through the snout. The snout contains a locking mechanism for launching and recovering instrument packages on the the end of the wire, as well as motion damping for the package while in the air. While towing, the HyHoe is free to rotate about its base. The ability to effectively rotate the ship under the HyHoe is a substantial asset for manuvering the ship in heavy weather. Although the HyHoe adds at least three more sheaves than would be required with a conventional "A"-frame the added advantages in manuverability and its utility in launch and recovery make it preferable to an "A"-frame.

TOW SYSTEM

The "tow system" includes the contra-helically armored coaxial tow cable, the cable termination, the depressor, the umbilical, and the neutrally bouyant vehicle. The primary reason for using this relatively complicated two body tow scheme illustrated in Figure 1 is to passively stabilize the instrument platform minimizing vehicle pitch and yaw which degrade the quality of the side scan data. The neutrally bouyant instrument package is towed behind the dead weight depressor by the neutrally bouyant umbilical. Vehicle height above the sea floor ranges from 100 to 1000 meters depending upon swath width, and is maintained by changing the length of tow cable deployed. Significant decoupling of the instrument platform from ship-induced motions is achieved with this arrangement. Measurements of pitch, roll and yaw show the vehicle to be very stable in roll (less than 0.1 degree peak to peak) and pitch and yaw amplitudes range from 0.5 degrees to 3 degrees peak to peak depending on changes in sea state, winch operation and ship motion. The period of vehicle pitch is a function of sea state and ship size and ranges from five to ten seconds.

The tow winch and level wind as well as the system electronics are designed for 0.680 inch diameter contra-helically armored coaxial tow cable which was pioneered by the MPL Deep Tow (MPL, 1980) group and is rapidly becoming accepted as the standard in the deep towing community. The length of cable required is approximately 1.5 to 1.7 times the water depth.

In any over-the-side tethered operation the failure of the termination is catastrophic. An electro-mechanical termination developed by the Deep Tow Group at MPL (Fisher and Mundy, 1973) has proven satisfactory for use with the system. The MPL termination incorporates a mechanical swivel and an oil compensated electrical slip ring in a proven design.

In our implementation, the termination is connected to a passive depressor (900 kg. in air) which serves as the transition between the tow cable and the neutrally bouyant tether. The depressor is also occasionally used as the attachment point for a self-recording Aanderaa thermistor chain which is towed vertically below the

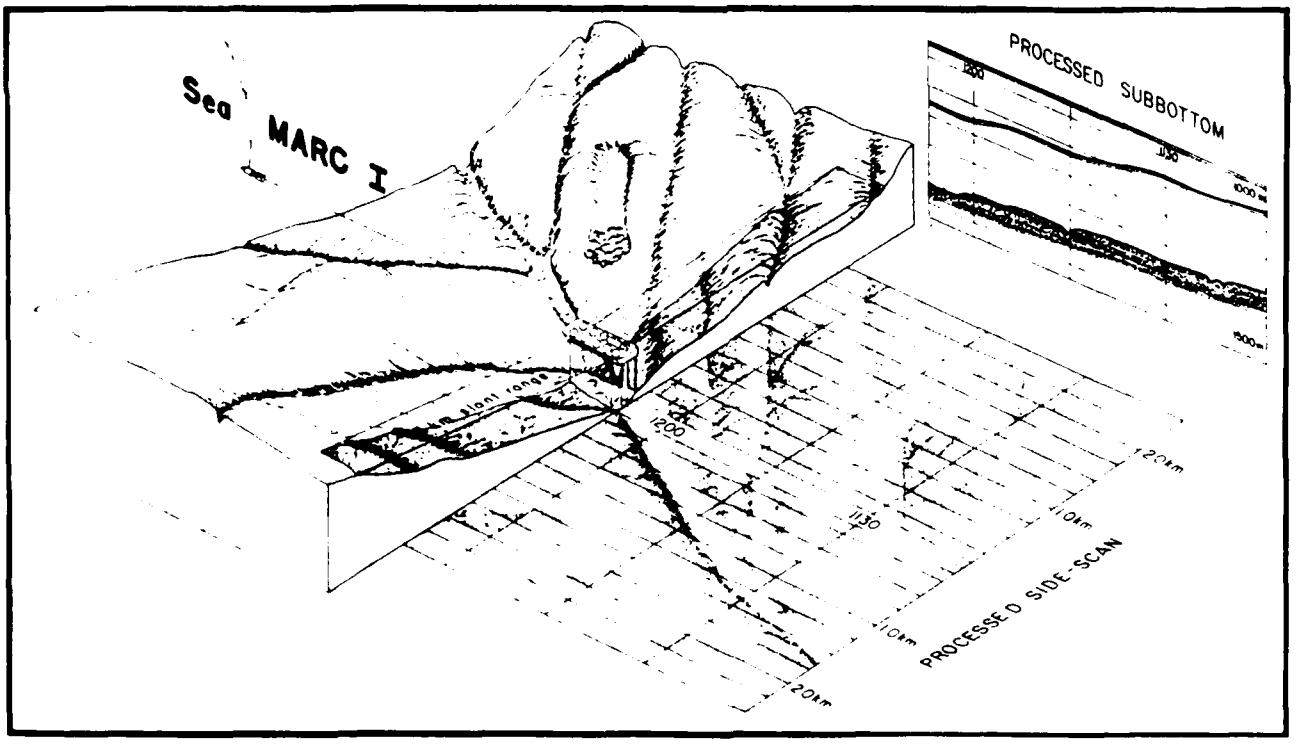

FIGURE 1. Sea MARC I TWO BODY TOWING SCHEME AND DATA PRESENTATION
Pictoral representation of the Sea MARC I vehicle being towed up a canyon. The representations of processed side scan and processed subbottom data illustrate the real-time facsimile recorder output from Sea MARC I.

depressor. The vehicle is towed behind the depressor by a neutrally bouyant umbilical. We have used umbilicals 80 and 100 meters long. The umbilical or tether uses a Kevlar strength member six millimeters in diameter along which is loosely taped an RG-213 coaxial cable. The strength member and electrical conductor are inside of sixteen millimeter hollow braid polypropelene rope which provides abrasion protection. While rather crude, this type of umbilical has proved quite serviceable. Most of the problems associated with the umbilical seem to be caused by over-stressing the coaxial cable at the connections to the depressor and the vehicle.

There have been three different Sea MARC I instrument packages. The first vehicle, refered to as the "blue fish" was a heavy single body system used during sea trials and for the first Titanic search. In retrospect using a single body tow fish was a good idea in the early stages when there were numerous recoveries for repair and testing. After that cruise the electronics, sensors, and transducers were switched to the neutrally bouyant vehicle illustrated in Figure 2. The aluminum structure of the vehicle was too robust and considerable effort went into lightening it before it was replaced. The integration of the CHIRP in 1983 added a second pressure case forcing the replacement of the old vehicle. The new vehicle is a welded tubular frame construction fabricated from 6061-T6 aluminum and uses twelve 43 cm. diameter glass spheres for floatation. Non-magnetic materials are used throughout so as not to

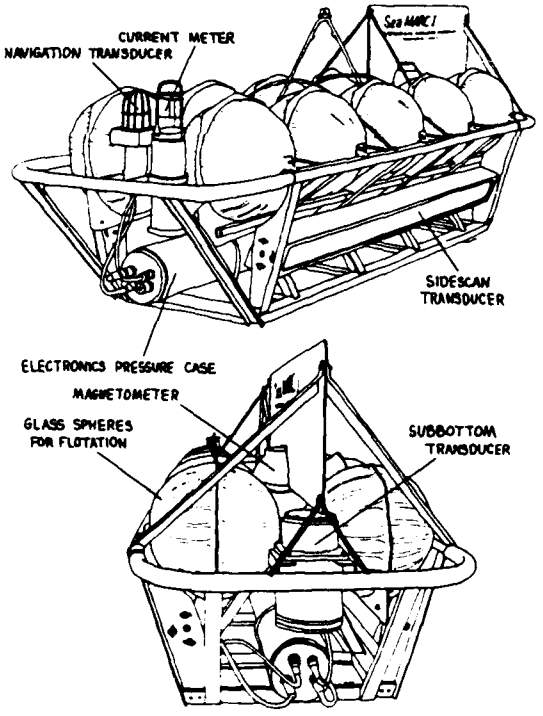

FIGURE 2. Sea MARC I VEHICLE
Line drawings of the first neutrally bouyant Sea MARC I vehicle showing all of the principle components.

intefere with the magnetometer and compass. Glass floatation was chosen for both of the neutral vehicles primarily because deep ocean syntactic foam is prohibitively expensive and at low tow speeds the extra hydrodynamic drag from a non-streamlined package is not a serious penalty.

ELECTRONICS

This section will present a description of the current state of the Sea MARC I electronics (Table 2) followed by discussion of some of the evolutionary process.

The Sea MARC I vehicle is powered by one and one-half amps of clean direct current from a power supply in the operations van. The required voltage ranges from 100 volts for a short wire and no CHIRP to more than 300 volts for a full length wire and CHIRP. In addition to carrying power to the vehicle, the coaxial tow cable carries two Frequency Shift Key (FSK) telemetry channels for low speed data transfer at 600 bits per second and five analog channels for high data rate information transfer between the surface and the vehicle. Control data such as pulse length and reciever gains are sent to the vehicle (down link telemetry) on one FSK channel while vehicle parameters including depth, heading, and magnetometer data are sent up on the other. At the surface, the vehicle parameters are displayed and transferred to the Hewlett-Packard 9845S navigation computer over an RS-232C serial interface at 600 baud. Data from the five sonar channels (port side scan, starboard side scan, subbottom, navigation receiver, and low frequency receiver) are transmited to the surface on five spectrally separate, high dynamic range (nearly 70 dB) analog channels. At the surface, each side scan channel is digitized, corrected for beam pattern variations, slant range corrected, formatted, displayed on facsimile recorders in real time and buffered in the computer interface. Subbottom data is digitized, corrected for vehicle depth, formatted, displayed in real time on a facsimile recorder and buffered in the computer interface. Raw (not digitized) side scan, subbottom, navigation, and low frequency receiver data are available for output to facsimile recorders.

The Sea MARC computer interface double buffers processed side scan, processed subbottom and the FSK telemetry data and makes it available on a 16 bit parallel interface at a 75 kHz transfer rate with a through-put of 32,768 bits per second. An HP-1000XL computer is used to acquire the data via Direct Memory Access (DMA), reformat it, display some of the vehicle parameters, and log all of the data on nine-track tape. This data logging computer also controls a few bits of down link FSK telemetry which are used to control the output of the CHIRP transmitter, and to select either flux-gate magnetometer data or pitch and speed log data to be digitized in the vehicle and sent to the surface.

The TRANS I acoustic navigation transceiver is flexible enough to work in nearly any acoustic navigation scheme. There are eight crystal-controlled transmit frequencys (presently set at 8.0, 9.5, 10.0, 10.5, 11.0, 11.5, 12.0, and 14.0 kHz) and a broad-band (7 to 14 kHz) receiver. The TRANS I listens and transmits at the vehicle but pulse length (1, 5, or 20 milliseconds) and transmit frequency are controlled manually or by computer from the surface. Provision exists to synchronize with an external short or ultra-short base line navigation processor.

TABLE 2. CURRENT Sea MARC I SPECIFICATIONS

GENERAL		
	Operating depth	7000 meters
	Tow cable	Double armored 0.68 inch dia. 10,000 meter long coax
	Depressor	Dead weight 900 kg in air
	Umbilical	Neutrally bouyant 100 meters
	Tow vehicle	Neutrally bouyant passively stabilized 3 X 1.2 X 1 (meters)
	Surface electronics	Minimum: Two 19" racks Normal: One 8'x8'x20' ISO container fitted out as a lab
	Power requirements	Three phase/three wire 220 or 440 VAC 30 A. max
SWATH MAPPING SONAR		
	Beam pattern	Vertical plane: 50 degrees Horizontal plane: 1.7 deg
	Frequency	Port 27 khz Starboard 30 khz
	Swath width	Slant range corrected: 1,2,5 km total Time domain: 1,2,4 seconds each side
SUB-BOTTOM SONAR		
	Beam pattern	Conical 30 degrees
	Frequency	4.5 khz
	(Subbottom and CHIRP are mutually exclusive)	
CHIRP SONAR		
	Beam pattern	Conical 30 degrees
	Frequency	1 to 5 kilohertz
	Pulse Length	1 cycle to 100 milliseconds
	Power	Test, 300,1000,2500 watts
	Mode	Sweep freq. or tone burst type, duration and freq. selectable from the surface
COMPASS		
	Type	Endeco fluxgate (mag north only)
	Resolution	0.1 degree
	Sample rate	Once per second
MAGNETOMETER		
	Type	Three axis fluxgate
	Resolution	approx 2 gammas (each axis)
	Sample rate	All axes every second
DEPTH		
	Type	Semiconductor strain gague
	Resolution	0.1 meter
	Sample rate	Once per second
PITCH		
	Type	Fluid damped pendulus pots
	Resolution	0.1 degree
	Sample rate	Once per second
RESPONDER		
	Transmitter	Two hundred watt, omni-directional pulse,timimg,& frequency slectable from surface
	Reciever	7 khz to 14 khz band

Pressure is measured with a bulk semiconductor strain gauge which is installed in the endcap of the main pressure case. Pressure is converted to depth and used for navigation and true-depth profiles.

A low frequency (40 to 1000 hertz) preamplifier and telemetry channel was installed to listen near the sea floor to a water-gun towed near the surface. A short deep water hydrophone array on loan from the University of Washington was used but the signal to noise ratio was very near unity. Additional testing will be required to fully evaluate the potential of this concept.

The CHIRP (Mayer and Leblanc, 1982) transmitter can transmit in either of two modes :fixed amplitude variable frequency (CHIRP) or fixed amplitude fixed frequency (tone burst). Output power level of 7, 200, 1000, or 2000 watts is selectable from the surface with transmit pulses up to 100 milliseconds long. Seven CHIRP and eight tone burst code tables are stored in EPROM on the CHIRP controller board in the vehicle. An NSC-800 microprocessor uses data received from down link telemetry to decide what type of transmit to generate. CHIRP data is sent to the surface on the subbottom telemetry channel. This uplink data contains a current monitor of the transmit pulse along with the received reflections. Logging of CHIRP data has progressed to the point that a small amount of data has been digitized and stored in real time.

The flux-gate magnetometer is housed in a glass sphere and contains three orthogonally mounted Schoenstadt RAM-5B sensors and interface circuitry. Vehicle pitch is measured with a Humphery CP-17-0607-1 viscously damped pendulous pot. Speed of the vehicle through the water is measured in the forward and up directions with a Marsh McBirney two-axis electromagnetic log. A multiplexer controlled from the surface allows either the three flux-gate sensors or two speed log outputs and the pitch pot to be digitized and sent to the surface. The digitizer has three channels which sample simultaneously once per second with a resolution of one part in seventy-thousand.

Evolution of the electronics has been driven by modifications to improve the mean time between failures, replacement of lost or damaged subsystems, and additions of new hardware.

During the first cruise the tail of the heavy vehicle was torn off carrying with it the glass sphere containing the three axis flux-gate magnetometer. An Endeco compass and pendulous pots for attitude sensing were installed to replace the magnetometer in 1981.

In 1982 the pitch sensor was moved inside the main pressure case and a new three axis flux-gate magnetometer was acquired. At the same time a multiplexer was added which allowed the input to one of the analog to digital converters in the vehicle to be switched between the vertical flux-gate sensor and the pitch sensor to be selected from the surface. During the 1982 Hudson cruise the original navigation responder which was housed in a separate pressure case was destroyed when the pressure case leaked. Subsequently the TRANS I responder was installed in the main pressure case.

In 1983 the speed log was added to the vehicle, and the single channel multiplexer was expanded to three channels and the CHIRP transmitter was installed in place of the 4.5 kilohertz subbottom transceiver.

FUTURE DEVELOPMENTS

Real-time data processing and display of the CHIRP data is currently under development in a cooperative effort with the University of Rhode Island, Department of Ocean Engineering and Dalhousie University. Potential enhancements to the existing system could include precision vehicle navigation relative to the surface ship, a telemetery channel to bring the thermistor chain data to the surface and hardware to display it in real time, and a digital multi-channel receiver for CHIRP.

ACKNOWLEDGEMENTS

Development and operation of this system is the result of a dedicated effort on the part of innumerable people including engineers and technicians at International Submarine Technology, the Lamont Doherty Geological Observatory Machine Shop and the Marine Physical Laboratory and the officers and crews of the Fay, Gyre, Pacific Seal, Hudson, Surveyor, Washington, and Conrad, and all of the support people who make these ships and organizations possible. I owe a special debt of gratitude to Bill Ryan for organizing this project in the first place and for having the patience to put up with it and me, to Jack Grimm for paying the first bills and to Fred Spiess for introducing me to deep towing in 1976 and for leading us through our first and most trying cruise. Sea MARC I development has been funded by Titanic 1980,1981,and 1983 Inc., the National Ocean Survey, Atlantic Geoscience Centre , the United States Geological Survey, Shell Development Co., Canterra Energy Co. , the National Science Foundation, Joint Oceanographic Institutions, and the Office of Naval Research. Kim Kastens' critical review drastically improved the manuscript.

REFERENCES

Blackinton,J.G., Hussong,D.M.,and Kosalos, J. G.,1983, First results from a combination side-scan and seafloor mapping system (Sea MARC II). Proc. Offshore Technology Confrence, May 1983, Vol. 1, p.307.

Farre,J.A., McGregor,B.A. ,Ryan,W.B.F., and Robb,J.M., 1983, Breaching the shelf break: passage from youthful to mature phase in submarine canyon evolution, in SEPM Spec. Pub. No.33, p25-39, June 1983.

Fornari,D.J.,Ryan, W.B.F., and Fox,P.J., 1983, High resolution side-scan sonar imaging of a linear seamount group near the crest of the East Pacific Rise at 9° 53'N., Abs. in EOS, Vol.64, No.18, May 3,1983.

Fisher, F.H., and Mundy,C.S.,1963,Uniclamp, a load bearing termination for oil-well logging-type cables. J. Mar. Res.,Vol. 21, No. 2,p-125-128.

Gibson,P.,1982, Wire rope and cable operational characteristics, in Handbook of Oceanographic winch, wire, and cable technology. ed. A. Driscol, Oct. 1982

Kosalos,J.G., and Chayes,D.N.,1983, A portable system for ocean bottom imaging and charting. Oceans '83, in press.

Laughton,A.S.,1981, The first decade of GLORIA, J.G.R., Vol. 86, No. B12, pp. 11,511-11-534, Dec 10,1981.

Malahoff, A., Embley,R., Hammond,S., Ryan, W.B.F., and Crane,K.,1982,Juan de Fuca and Gorda Ridge axial ridge morphology and tectonics from combined Seabeam and Sea MARC data. Abs. in EOS, Vol. 63, No. 45, Nov. 9,1982.

Marine Physical Laboratory, 1980, Specification No. 3070 double aromored submarine coaxial cable, March 1980, Modified July,1980.

Mayer,L.A., and LeBlanc,L.R., 1982, The CHIRP sonar: a progress report, Nov. 1982.

Mills,R.G. ,1982, Tow winch investigation, Prepared for Bedford Inst. Oceangr. by Whitman, Benn Assoc., Jan. 20, 1982.

Ryan, W.B.F., 1982, Imaging of submarine landslides with wide-swath sonar in MARINE SLIDES AND OTHER MASS MOVEMENTS, de. S. Saxov and J.K. Nieuwenhuis.

Spiess, F.N., and Tyce, R.C., 1973, Marine Physical Laboratory Deep Tow instrumentation system: Scripps Inst. Oceaogr. Ref 73-4, pp.1-37.

TRIP REPORT

for

CSS HUDSON Cruise

85-010

to

Kane Fracture Zone

(April 27, 1985 - May 27, 1985)

by

Kim C. Benjamin

June 4, 1985

TABLE OF CONTENTS

LIST OF FIGURES

I. Purpose of Oceanographic Research

Briefly, the purpose of this cruise was to select a suitable drill site as near as possible to the Kane Fracture Zone (KFZ) where researchers from Texas A&M University could, on a latter cruise, deploy a new deep ocean rock drilling system and thereby retrieve hydrodynamically, unaltered oceanic basalts. Using Sea MARC and a towed camera system, the scientists aboard were able to locate three suitable drill sites.

The purpose of my attendance on this cruise was to become familiar with the various aspects of the Sea MARC side scan SONAR system, which involves:

a. deployment, flying, and recovery of the two body towed system;

b. acoustic, hydrodynamic, and navigational data acquisition;

c. electronic and acoustic troubleshooting;

d. interpretation of raw and processed acoustic data; and finally,

e. to make recommendations which would improve system performance.

II. Selection of Drill Site

The requirements for the drill site were: seafloor surface slope less than 20 degrees, and surface roughness less than 1 meter.

Previous research in this area included a SEABEAM bathymetric survey and several magnetometer transits. Figure 1 depicts a crude map of the Sea MARC survey area. This diagram, unfortunately, does not show the locations of the three selected drill sites; however, if anyone is interested, I would be happy to obtain that information from Larry Mayer.

23° 35' N
45° 10' W

23° 35' N
44° 45' W

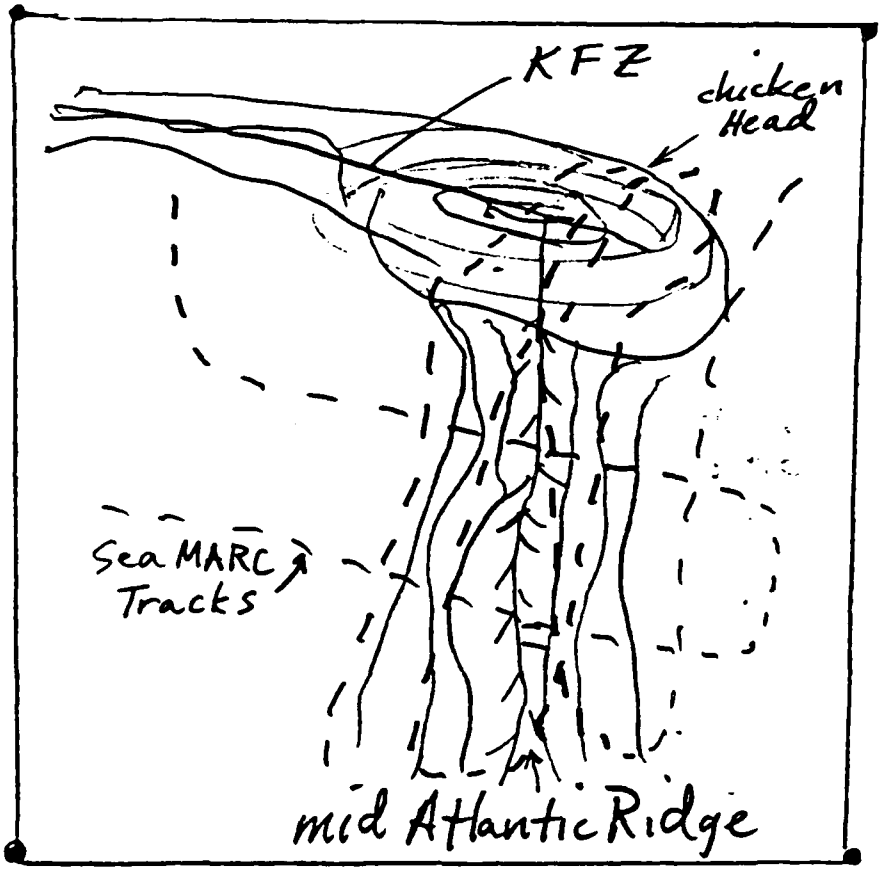

22° 45' N
45° 10' W

22° 45' N
44° 45' W

Figure 1. Sea MARC Survey Area

III. Familiarization with Sea MARC

In this section, I will first describe what was done, my understanding of it, and where applicable, how it could be improved.

The following Sea MARC issues will be addressed sequentially:

1. Deployment and Recovery
2. Data Acquisition
3. Navigation and Positioning
4. Electronic and Acoustic Troubleshooting
5. Data Interpretation

1. Deployment and Recovery

The CSS HUDSON was adequately rigged to deploy and recover Sea MARC safely in seas up to sea state 2 (i.e., waves 2-3 feet). The fantail (or quarterdeck) provided enough workspace (approximately 12 x 12 m) for deployment and recovery of the towfish and depressor weight. The ship was equipped with a LIBUS winch system. Besides good spooling characteristics, the system had only two sheaves which adds to the life expectancy of the cable. A crane having a telescopic boom was used to lift Sea MARC into and out of the water. This crane had two steel posts (or legs) which could be anchored at the stern rail to support the crane boom. Thus, it provided a sort of "A" frame which relieved the towing stresses on the crane boom itself.

The deployment of Sea MARC on this cruise was performed, in my opinion, in a very dangerous manner and if attempted in say sea state 2, could result in personal injury or damage to the Sea MARC towfish. The first recovery was also performed rather dangerously, but subsequent recoveries were made safely.

The Sea MARC towfish weighs approximatey 1600 lbs. Raising it more than six inches above the deck gets dangerous if the ship decides to roll or pitch. One safe way to deploy it would be to orient the ship into the wind where she would experience waves at some oblique angle to the fore and aft direction causing her to roll more than pitch. Next, using a crane (or "A" frame), slighty raise (or drag) Sea MARC out over the stern; once clear, lower away. Sea MARC is deployed using a QUICK RELEASE which lifts the vehicle from the center. It is recovered by lifting it from the towing bridal (see Figure 2). Therefore, on recovery one would raise the vehicle 3/4 to 7/8 above the level of the fantail and then using the crane, swing it in and down (never losing contact with the deck). The Sea MARC towfish is equipped with wooden runners. On this trip they were made of pine. I would suggest either a hardwood or a tough polymer.

The individuals from Lamont used syntactic foam to trim the fish. When this proved inadequate, they moved the two pressure cans which had a large effect on the pitch. However, they left these odd sized pieces of syntatic foam attached which only served to increase the towfish drag. They should be removed.

2. Data Acquisition

The available raw data from Sea MARC are:

a. The 4.5 kHz sub-bottom signal,

b. Port and starboard side scan signals at 30 and 27 kHz,

c. Pitch,

d. Roll,

e. Depth,

f. Altitude, and

g. Speed (soon to be operational).

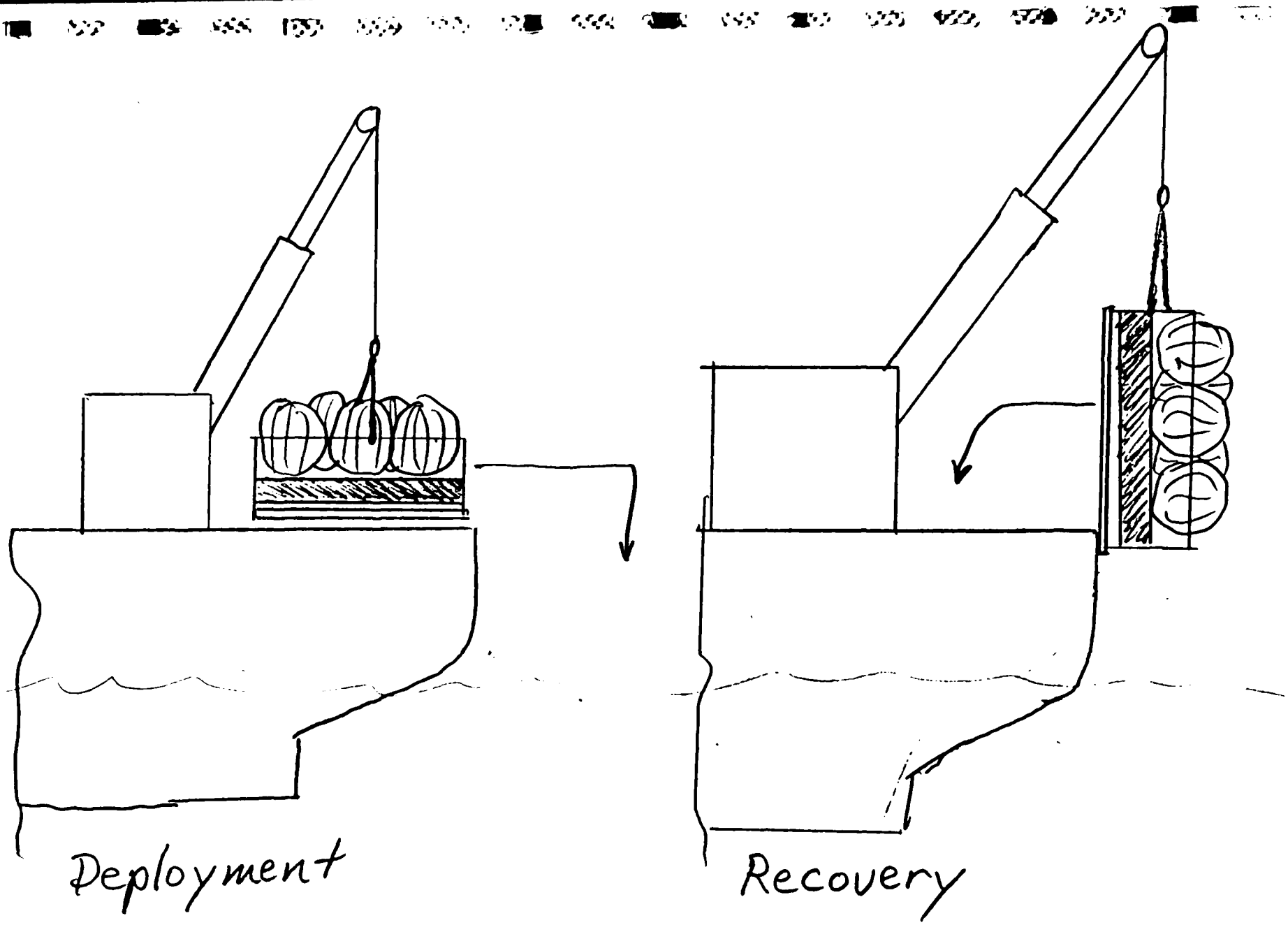

Figure 2. Sea MARC Deployment and Recovery

a. 4.5 kHz Sub-Bottom

The sub-bottom signal was used exclusively for altitude detection. None of the EPC recorders were displaying the sub-bottom acoustic data, and therefore I haven't any idea how well it measures sub-bottom features. It is clear that the sub-bottom transducer characteristics are important for accurate altitude detection which in turn is crucial for making accurate slant range corrections. The present sub-bottom transducer configuration consists of a cylindrical piezoelectric transducer having an omnidirectional beam pattern at 4.5 kHz. Altitude detection is accomplished by measuring the two-way travel time of the pulsed sub-bottom signal. A Time Varied Gain (TVG) is applied to this signal to account for spherical spreading and absorption. There were several instances where bad altitude detection, caused by towfish pitch, resulted in erroneous slant range corrections. One relatively simple solution would be to optimize the sub-bottom transducer characteristics. This can be accomplished by mounting a moderately directional, longitudinal vibrator on gimbals such that it always points toward the bottom regardless of towfish pitch. The specifications of one such transducer are presented in Appendix A.

b. Port and Starboard Side Scan

Each side scan array is composed of two continuous line arrays top and bottom which are connected in parallel with a jumper wire. One side operates at 30 kHz and the other side at 27 kHz. Interferometric swath bathymetry is possible with these arrays provided an additional pressure can of hardware is obtained from IST (price unknown at this time). Please note that the Sea MARC II

system, which has this capability, operates at 12 kHz in order to achieve better range performance. The longer wavelengths imply the following trade-off. Poor altitude (or bathymetric) resolution is traded for a lesser 2 -ambiguity.

c. and d. Pitch and Roll

These signals are provided by the towfish's gyro. They worked well.

e. Depth

The actual depth of the towfish was obtained using a static pressure transducer. This also worked well.

f. Altitude

This was already addressed in the section "Sub-Bottom."

g. Speed

This is planned for the future and will provide the towfish's speed through the water using some sort of mechanical current meter.

In closing this section, it seems appropriate to briefly discuss fish flying. The altitude of the depressor weight and towfish above the ocean floor are highly dependent on the ship's speed, the weight of the depressor, and the viscious drag of the fish. Increasing the weight of the depressor pig would cause it to follow the ship's track more closely. Flying the fish is conceptually like flying a plane (less complex, of course), in that it is a highly reactive system. I suggest that the MS flight simulator (which I have on floppy disc) be used as a trainer for prospective fish flyers.

3. Navigation and Positioning

The CSS HUDSON has a short baseline acoustic positioning system consisting of three transducers and an Oceano interface. This provided the x-y and y-z position of a transponder with respect to a mobile coordinate system with its origin located at the center of the ship. The system worked very well.

4. Electronic and Acoustic Troubleshooting

There were roughly six days of Sea MARCing. During that period there was only one serious electronic problem with Sea MARC. This involved the premature firing of one of the side scan arrays. Evidently, one of the enable signals was being set high by some extraneous noise in the circuitry. D. Chayes and R. Terry worked on this problem for about 1 1/2 days. They changed a potentiometer and resoldered a DIP socket, neither of which exhibited a definite failure. After that, Sea MARC worked well.

A functional block diagram for Sea MARC is given in Appendix B. The main two timing signals are FRAME SYNC and XMIT KEY. FRAME SYNC occurs every 500 milliseconds, and XMIT KEY occurs at every 500ms, 1s, 2s, or 4s depending on the range setting, (4s, for 5km swath). During one FRAME SYNC period all the key enables, pulse lengths, gains, and transmit power levels are set for the next transmit-receive cycle which begins on the next FRAME SYNC or XMIT KEY. Aside from a set of wiring diagrams, most of the electronics and timing information is contained in the head and various notebooks of D. Chayes. I urge that Woods Hole obtain this information on paper so that the electronics portion of Sea MARC is well understood before it is taken to sea. Furthermore, it may be useful to obtain the services of Mr. Rick Terry from NORDCO who has worked extensively with the Sea MARC electronics.

1 byte = 8 bits
(0 - 255)

Figure 3.

...e Backup Functional Diagram

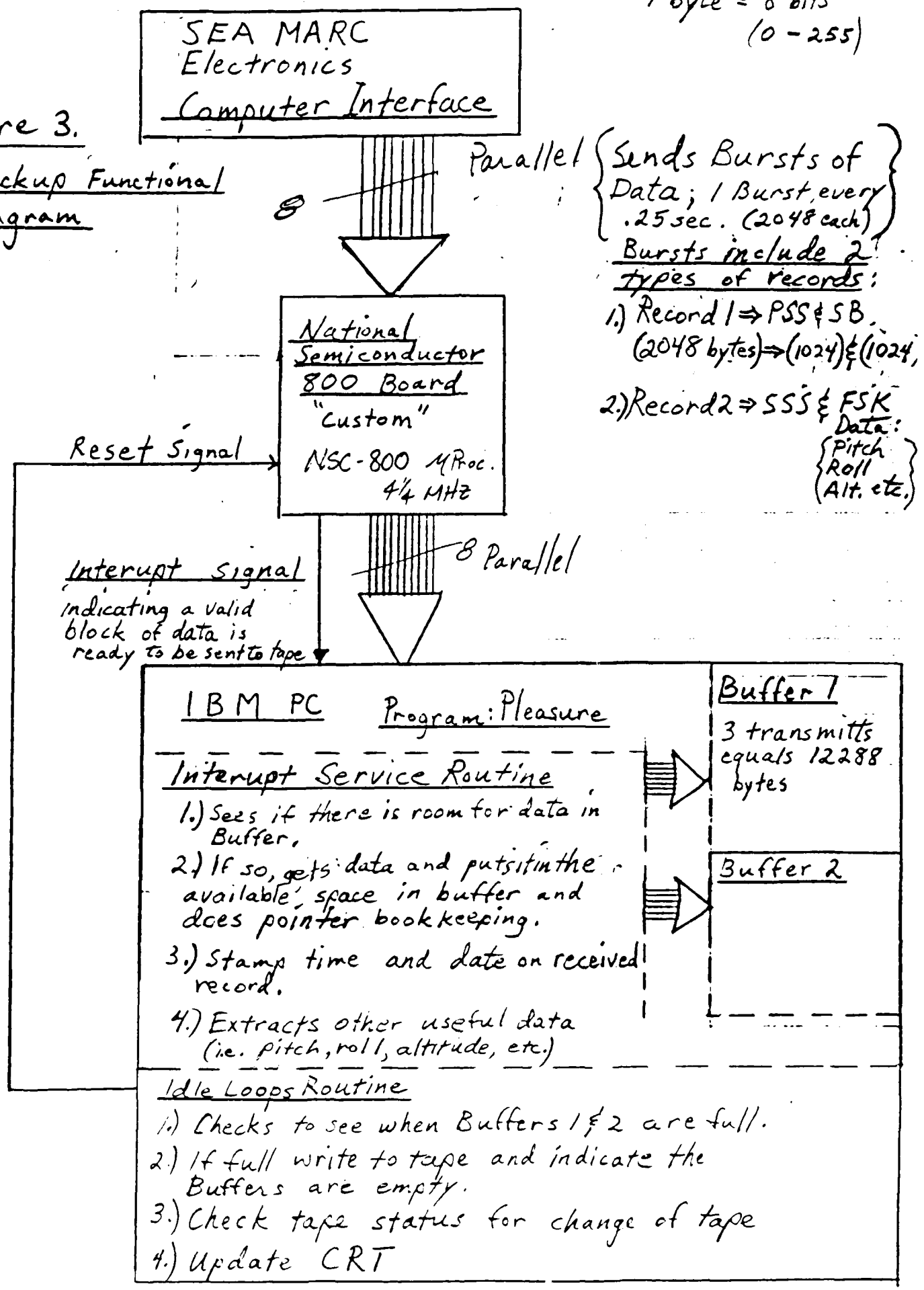

Figure 3 shows a functional block diagram of the tape back-up system. An NSC800 microprocessor-based, parallel interface is used to transfer data from Sea MARC to an IBM personal computer. The PC runs an IDLE LOOPS routine which waits for an interrupt from the NSC800, at which time an interrupt service routine obtains the data and stores it in a buffer. The data is then written to tape by the IDLE LOOPS routine. Some data is lost on the fastest XMIT KEY rep rate.

A transducer is a solid state electromechanical filter. They usually never completely fail or lose their piezoelectricity. If abused, however, their performance will degrade. The most effective way to ascertain the transducer's health is to measure its impedance as a function of frequency and power about resonance.

This can be done using a swept frequency, complex impedance bridge. A neater, more sophisticated tool would be a spectrm analyzer. Although these instruments are expensive (approximately the cost of funding a graduate student for one year), a good spectrum analyzer with an HPIB interface will facilitate development work, and therefore is eventually pays for itself.

5. Data Interpretation

The interpretation of the Sea MARC data this cruise was greatly facilitated by SEABEAM bathymetric data obtained on an earlier trip. Without apriori knowledge of the local bathymetric contours, there is no way of knowing if Sea MARC I is imaging a concave or convex surface. I strongly recommend the purchase and development of the Sea MARC II swath bathymetry capability. I would also recommend the development of an acoustic sonar imaging simulation program which would be similar to UNCLES in that the images are manipulated in the spatial and spatial frequency domains. Much of the analysis in UNCLES would carry over for acoustic wave propagation.

TR-109 Specifications

Frequency	3.5 kHz
Bandwidth	1.0 kHz
3 dB Beam Width	90° to $\pm$ 10°
Impedance	105 to 150 Ω $\pm$ < 10°
Maximum Acoustic Power Out	
CW	
200 Watts	194 dB
Pulsed @ 30% Duty Cycle	
600 Watts	198 dB
Receive Sensitivity	-173 dB re 1V
Cost for a Quantity of 2	$1,495.00 each

VEHICLE

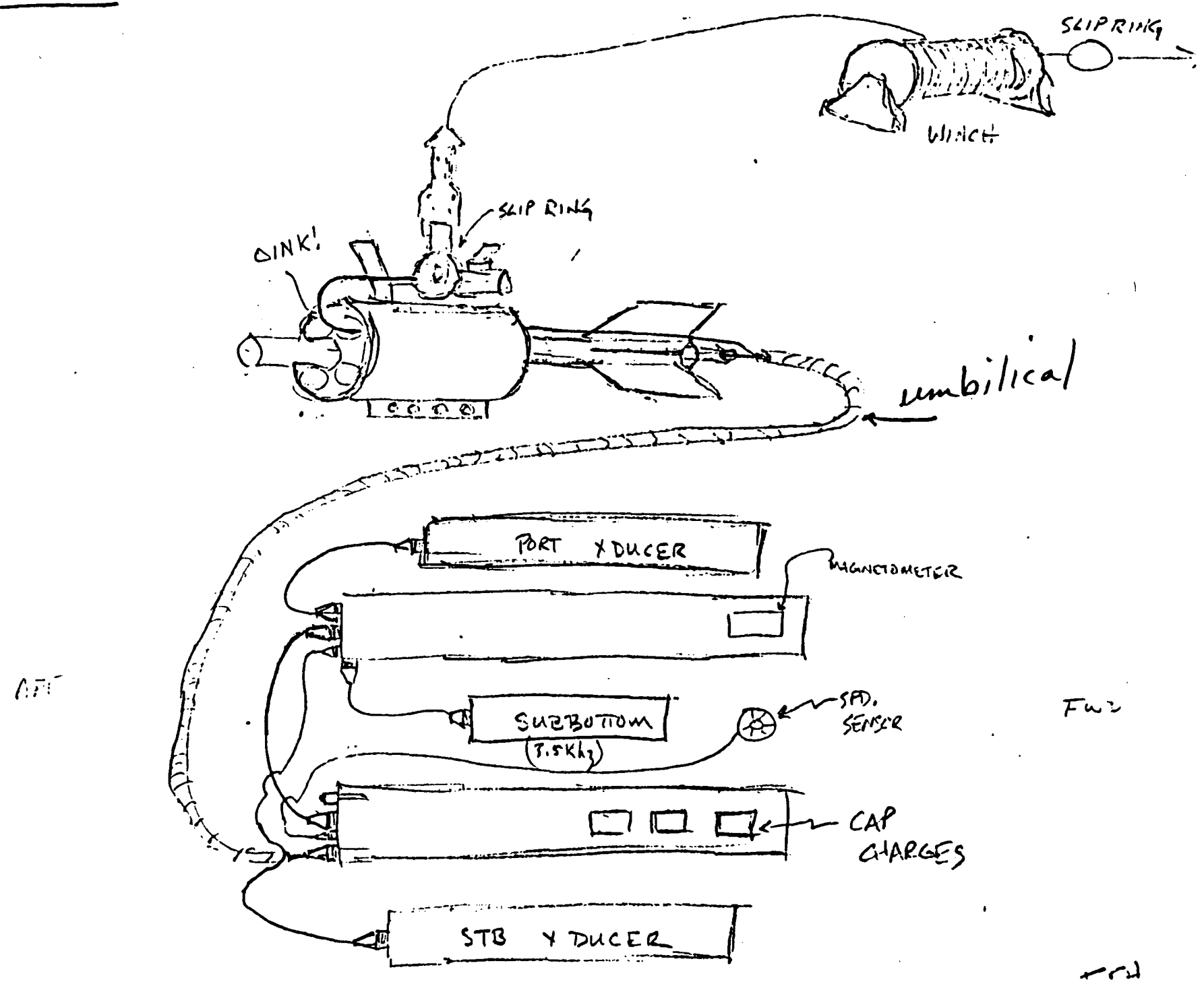
SLIP RING
WINCH
SLIP RING
OINK!
umbilical
PORT XDUCER
MAGNETOMETER
AFT
SUBBOTTOM
(7.5KHz)
SPD. SENSOR
FWD
CAP CHARGES
STB XDUCER

SURFACE ELECTRONICS

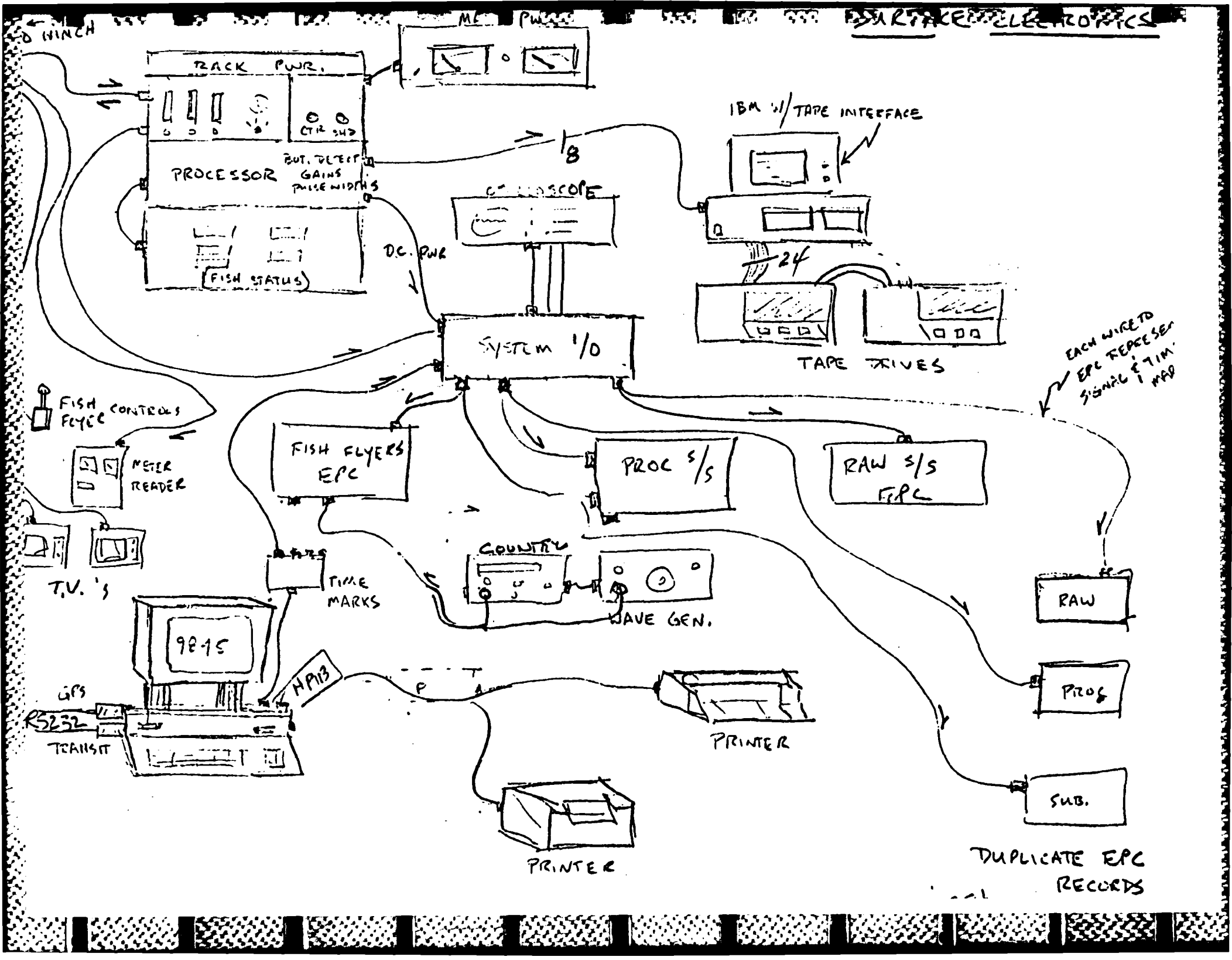

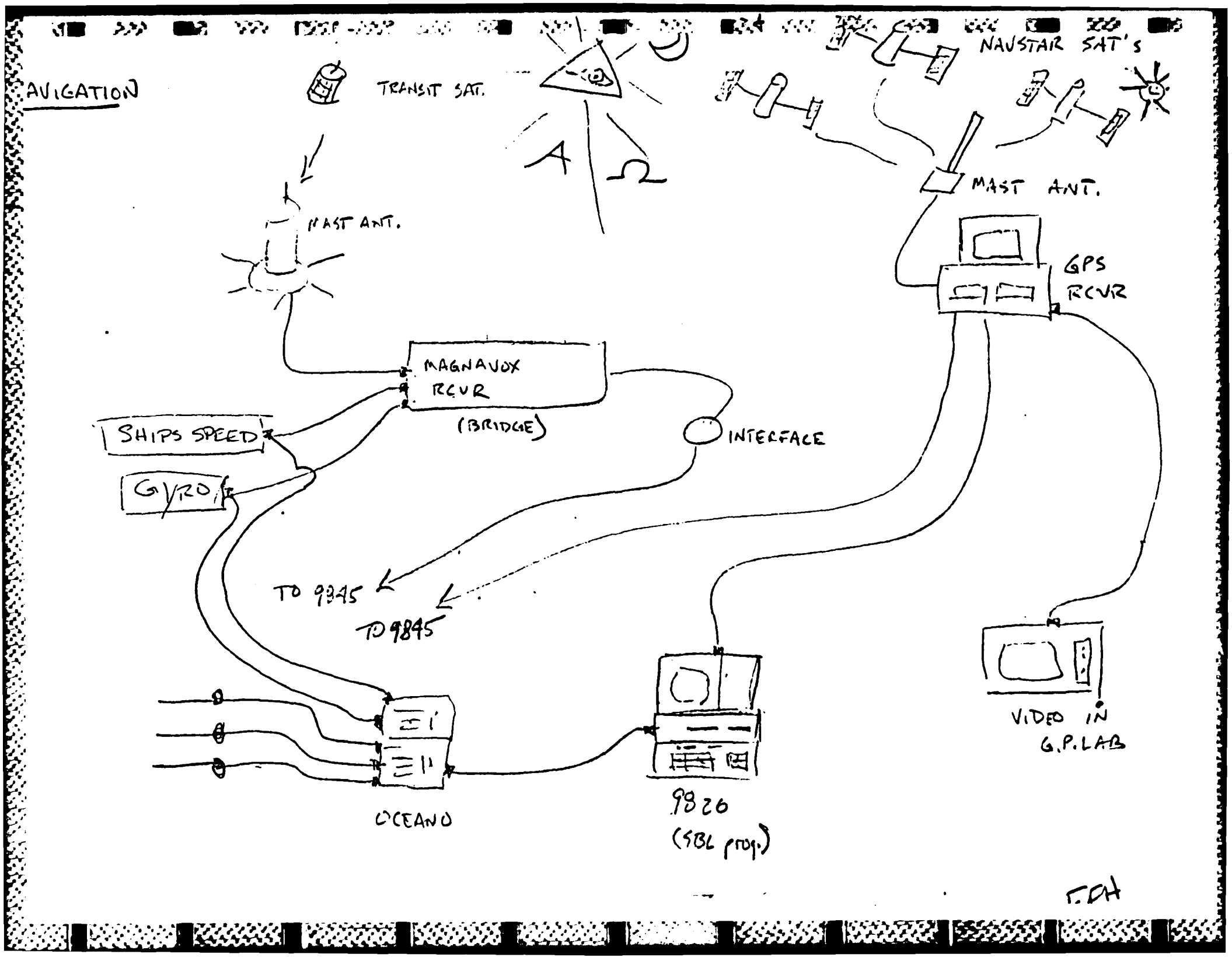
AVIGATION
TRANSIT SAT.
NAVSTAR SAT's
MAST ANT.
MAST ANT.
GPS
RCVR
MAGNAVOX
RCVR
(BRIDGE)
SHIPS SPEED
GYRO
INTERFACE
TO 9845
TO 9845
VIDEO IN
G.P.LAB
OCEANO
9826
(SBL proj.)
F.DH

NAVAL OCEAN SYSTEMS CENTER
Hawaii Laboratory

Ser 533/05-85
10 Jan 1985

MEMORANDUM

From: George Wilkins, Code 533
To: File, "Deepsea E-O Tether"

SUBJ: DESIGN RECOMMENDATIONS FOR AMUVS E-O TETHER CABLE

Ref: (a) My Memo Ser 533/032-84 of 1 August, 1984

Encl: (1) APPENDIX (A): "Modification and 'Optimization' of RG-174U Coax Cable"
(2) APPENDIX (B): "'Optimization' of AMUVS Electro-Optical (E-O) Cable"

1. BACKGROUND. Reference (a) described a series of operating and system constraints that were being placed on a pair of electro-optical (E-O) tether cables by the Deep Submergence Group at Woods Hole Oceanographic Institution (WHOI). The constraints, updated to include more recent information passed on to me by Ken Stewart of that Group, are repeated here in Table (1).

AMUVS — A small, deepsea, tether vehicle now nearing completion at WHOI. It will operate directly from the ALVIN manned submersible at the end of a 200-foot tether cable. ALVIN supplies AMUVS with electrical power and command signals, and receives a high quality TV signal plus a series of instrumentation data.

JASON — This vehicle should be similar to AMUVS, but will operate at the end of a somewhat longer tether from ARGO---a deepsea, unmanned, tethered system.

2. I have agreed to analyze and recommend design approaches for the E-O tether cables which are to support these two vehicles. This memorandum reports on the results of the AMUVS analyses.

3. Design form closely follows system function in the AMUVS tether. That form is particularly sensitive to the constraints shown below.

(a) The AMUVS cable must contain a dedicated coax---but this coax can also carry DC instrumentation power.

(b) The cable must contain separate and independent line pairs to supply power to AMUVS' motors and instrumentation.

(c) Motor/instrumentation supply voltages are relatively low, and in-line voltage drop fractions are not allowed to exceed 0.25. Power transfer at this loss factor is much less efficient than if an optimum (50%) drop were allowed.

Parameter	Value For AMUVS	Value For JASON
1. Maximum Telemetry Frequency	5 MHz	5 MHz
2. Maximum Cable Length	200 ft	500 ft
3. Maximum Power To Instrumentation	115 W	300 W
a) Voltage (at supply end)	115 VDC	115 VDC
b) Allowed Line Drop	5 VDC	5 VDC
c) Nominal Current	1 amp	2.5 amp
4. Main Motor Power Delivered	1000 W	1650 W
a) Voltage (at supply end)	150 VDC	440 VAC
b) Type of Circuit	2-Cond.	3-Cond.
c) Allowed Line Drop	37.5 VDC	60 VAC
5. "Optimum" Cable O.D.	0.35 in	0.35 in
6. Neutral Buoyancy Required?	Yes	Yes
7. Is Cable Highly Stressed?	Only In Survival Mode	
8. Tether Carried By:	ALVIN	ARGO

NOTES
(1) Fiber optic telemetry is a backup to a coax in both cables.

(2) WHOI is willing to superimpose DC instrumentation power on the AMUVS coaxial conductors.

(3) In both systems, motor supply power must be on separate (dedicated) conductors.

Table (1). Power/Telemetry Constraints For AMUVS/JASON Tethers.

Ser 533/05-85
10 Jan 1985

(d) The cable must be neutrally buoyant (in deep seawater). I have arbitrarily fixed this parameter at 1.027 (or somewhat less) in order to compensate for differential compression of the cable at hydrostatic pressures.

(e) To fit an existing winching system, the diameter of the AMUVS tether is fixed at 0.350".

4. The AMUVS cable's geometry is overwhelmingly shaped by the need for a conductor troika---i.e., two power conductors plus a separate coax. The cross section shown in Figure (1) represents the most efficient form fit I can recommend.

(a) It contains (and serves together as a helix) two dedicated motor power conductors and a dedicated coax. For symmetry, these three subcable units are constrained to have the same diameter.

(b) The value of that common diameter is also constrained to never be less than the 0.100" diameter of an RG-174U coax. (See Appendix A).

(c) To reduce the possibility of pinholes, conductor insulation thickness is fixed at a value of 0.020". This keeps voltage stress very low, while not crowding the 0.35"-diameter limit of the AMUVS cable.

(d) The coax is the cable's dedicated (full duplex) telemetry link. It is also the dedicated DC power line for support of AMUVS instrumentation.

(e) The three open channels defined by the assembly helix are used to contain and protect three optical fibers---a data link, a command link and a spare. (Alternatively data and commands can be full-duplexed on one fiber, and the other two fibers used as spares or backups).

(f) The cable jacket is fabricated as a [illegible] extrusion. It contains (sandwiched [illegible]) [illegible] KEVLAR-49 or---as a higher [illegible] alternative---Allied Chemical's new lightweight fiber "A-[illegible]".

5. Table (2) defines a set of "Baseline" constraints which were selected to begin the AMUVS design analysis. The conductor wires are a copper-clad-aluminum composite---with the copper fraction [illegible]

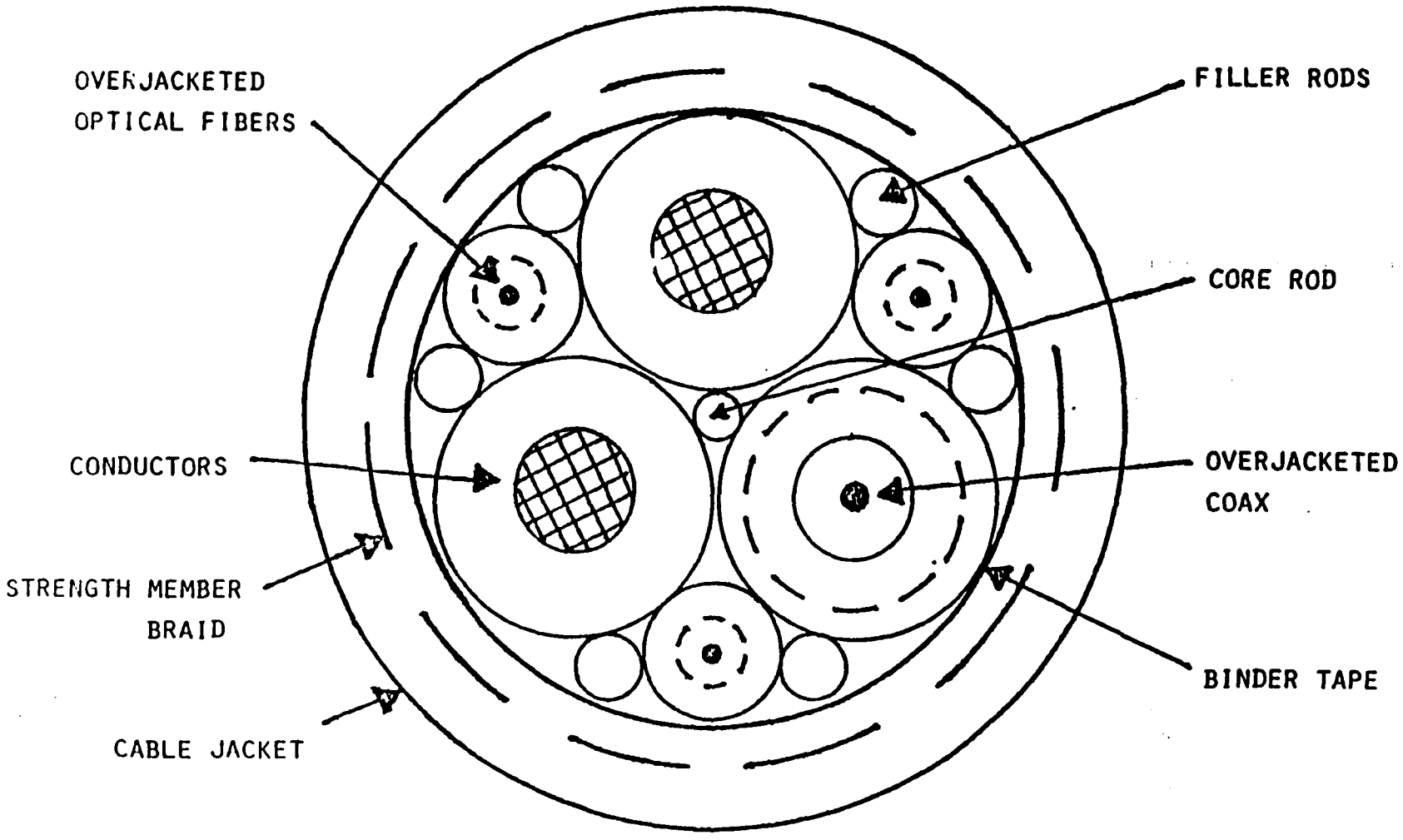

FIGURE (1). CROSS SECTION OF CANDIDATE AMUVS TETHER.

Ser 533/05-85
10 Jan 1985

	Design Parameter	Baseline Values
Vo	Supply Voltage For Motors (VDC)	150
K	Fraction of Vo Lost In Cable	0.25
L	Cable Length (ft)	200
V1	Supply Voltage For Instruments (VDC)	115
K6	Fraction of V1 Lost In Coax Cable	0.25
D1	Diameter of Wires In Power Conductor (in)	0.01003 (AWG 30)
D9	Overall Cable Diameter (in)	0.35
Ti	Cable Assembly Angles (degrees)	
	T0 = First 6 conductor wires	10.0
	T1 = Next 12 conductor wires	19.3
	T2 = Cable Core Assembly	15.0
	T7 = Strength Member Braid	20.0
N	Wires Per Power Conducctor (0-6-12 unilay)	18
A	Volume Fraction of Copper In The Conductor/Coax Cu/Al Wires	1.0
C	Wire Conductivity (re IACS)	f(A)
S1	Wire Specific Gravity	f(A)
Specific Gravities Of Other Cable Components:		
S0	RG-174U Coax Cable Unit	f(A)
S2	Conductor/Coax Jackets (polyallomer)	0.90
S3	Filler- And Core Rods (polyallomer)	0.90
S4	Void Filler In The Braided Shield (Vistanex)	0.925
S5	Cable Assembly Binder Tape (polyester)	1.375
S6	Final Cable Jacket (polyallomer)	0.90
S7	Optical Fiber O'Jacket (polyallomer)	0.90
S8	(20-mil) Buffered Optical Fibers	1.248
S9	KEVLAR-49 Strength Member	1.44

Table (2). Baseline Values For Design Variables----SMUVS Tether.

6. COAXIAL CABLE. Appendix (A) describes a computer program which evaluates the effects of material choices on the AMUVS coax's specific gravity, and on its electrical and telemetry performance. This Appendix also contains a copy of Military Specification Mil-C-17/119F, a general description of the RG-174U miniature coax.

7. The RG-174 coax was chosen for AMUVS because of its excellent performance in other deepsea tether cables (such as RUWS). Its 0.100" diameter gives both low RF attenuation and a close match to the cross section of the insulated motor power conductors.

8. The coax geometry used in the AMUVS design is essentially identical to the one described in Mil-C-17/119F. One fundamental change has been a substitution of copper-clad-aluminum for the copper/steel wires in that specification. This was done to help reduce the RG-174 coax's high specific gravity (2.35) to a more workable value.

9. Page (A-6) presents the results of the coax computer program for values of A = 1.0 and A = 0. Note that the simple conversion from copper- to aluminum wires caused coax specific gravity to be reduced from 1.970 to 1.138. This sensitivity closely follows the linear relationship;

$$SO = 1.1390 + 0.8307*A$$

10. Page (A-6) tabulates the RG-174 coax's RF attenuation at frequencies from 0.5- to 10.0 MHz---but only for the cases of pure copper and pure aluminum conductors. Even at the latter extreme, the coax has quite low attenuation in an AMUVS short-tether application. For $0 < A < 1.0$, RF attenuation in the coax's small wires will be difficult to predict because of skin-depth effects.

11. OVERALL CABLE PERFORMANCE. Appendix (B) describes a computer program which evaluate the effects of material choices (and other parameter changes) on total AMUVS cable performance. The design summary on Page (B-13) is a program output for the "Baseline" parameters listed in Table (2).

12. Tables (3) and (4) summarize the effects of a succession of material substitutions on four AUVS performance parameters. These are listed generally in order of increasing risk and/or complexity---with the safest modifications at the top.

Design Condition	Value Of Performance Parameter:			
	Motor Power P1 (W)	Instr. Power P2 (W)	Cable Weight (lb/kft)	Cable Specific Gravity
1. Baseline Design (D1 = 0.01003")	1703	217	53.70	1.288
2. A = .1. (Copper fraction is 0.1)	1105	141	43.60	1.045
3. A = 0. (Conductors are pure aluminum)	1038	132	42.48	1.018
4. S3 = 0.83. (Filler- & core rods are TPX)	"	"	42.38	1.016
5. S5 = 0.90. (Tape is polypropylene)	"	"	42.10	1.009
6. S2 = 0.83. (Cond/coax jackets are TPX)	"	"	41.70	1.000
7. S6 = 0.88. (Cable jacket is TPR)	"	"	41.24	0.989
8. S9 = 0.97. (Str. member is A-900.)	"	"	40.14	0.962

Table (3). Effects of Successive Material Changes On AMUVS Tether Performance--Baseline For Table (2).

Design Condition	Value Of Performance Parameter:			
	Motor Power P1 (W)	Instr. Power P2 (W)	Cable Weight (lb/kft)	Cable Specific Gravity
1. Baseline Except D1 = 0.008928"	1349	217	51.49	1.234
2. A = .1. (Copper fraction is 0.1)	875	141	42.94	1.029
3. A = 0. (Conductors are pure aluminum)	823	133	41.99	1.007
4. S3 = 0.83. (Filler- & core rods are TPX)	"	"	41.89	1.004
5. S5 = 0.90. (Tape is polypropylene)	"	"	41.61	0.998
6. S2 = 0.83. (Cond/coax jackets are TPX)	"	"	41.19	0.988
7. S6 = 0.88. (Cable jacket is TPR)	"	"	40.73	0.977
8. S9 = 0.97. (Str. member is A-900.)	"	"	39.63	0.950
9. F = 0.352. (Small upward adjustment)	1001	"	39.63	0.950

Table (4). Effects of Successive Material Changes On SMUAS Tether Performance Embodiment With D1 = 0.008928".

13. Entry (1) in Table (3) identically represents the set of "Baseline" design constraints in Table (2). The resulting design is described more completely on Appendix Page (B-13). Entry (1) in Table (4) also represents "Baseline" conditions, except that the copper wires are slightly smaller (AWG 31).

14. RECOMMENDATIONS: Two points are made eminently clear by Tables (3) and (4).

FIRST — The switch from pure copper to pure aluminum conductors is---BY ITSELF---sufficient to reduce specific gravity for either candidate design to less than 1.027.

SECOND — Even in combination, the other changes shown in these Tables cannot accomplish this objective.

15. Therefore, I see no choice but to recommend that all metal conductors in the AMUVS E-O tether cable be pure aluminum. (This follows our successful experience with the RUWS vehicle tether. The aluminum should be work hardened to a high temper---at least to a full hard condition, and (preferably) to some degree of spring temper. I am ruling out copper-clad-aluminum alternatives on the grounds that it is difficult to control either electrical conductivity or (more important) elastic-limit strength for this composite metal.

16. Other design recommendations are shown in Table (5) which duplicates the format of Table (2). Note that the cable assembly angle has been decreased slightly, while the wire serving angles in the motor conductors have been increased. This was done to increase the optical fiber radius of curvature to a value greater than 1.0", while maintaining cable elastic compliance. Table (6) summarizes performance to be expected from the recommended cable.

17. JASON TETHER CABLE. I have not yet started design work on this cable but---based on the AMUVS results---am making the following predesign recommendations.

(a) The JASON cable should have the same general geometry shown in Figure (1) here.

(b) The JASON cable should NOT contain a coax. Today's optical fibers are more rugged under high cyclic tensile stresses than any lightweight coaxial cable. Also, optical telemetry can easily be given noise isolation from other electrical functions in the payload. This freedom removes much or all of the need to separate motor- from intrumentation power.

	Design Parameter	Baseline Values
Vo	Supply Voltage For Motors (VDC)	150
K	Fraction of Vo Lost In Cable	0.25
L	Cable Length (ft)	200
V1	Supply Voltage For Instruments (VDC)	115
K6	Fraction of V1 Lost In Coax Cable	0.25
D1	Diameter of Wires In Power Conductor (in)	0.01003 (AWG 30)
D9	Overall Cable Diameter (in)	0.35
Ti	Cable Assembly Angles (degrees)	
	T0 = First 6 conductor wires	12.5
	T1 = Next 12 conductor wires	23.1
	T2 = Cable Core Assembly	11.50
	T7 = Strength Member Braid	20.0
N	Wires Per Power Conducctor (0-6-12 unilay)	18
A	Volume Fraction of Copper In The Conductor/Coax Cu/Al Wires	0
C	Wire Conductivity (re IACS)	0.610
S1	Wire Specific Gravity	2.67
Specific Gravities Of Other Cable Components:		
S0	RG-174U Coax Cable Unit	1.139
S2	Conductor/Coax Jackets (polyallomer)	0.90
S3	Filler- And Core Rods (polyallomer)	0.90
S4	Void Filler In The Braided Shield (Vistanex)	0.925
S5	Cable Assembly Binder Tape (polyester)	1.375
S6	Final Cable Jacket (polyallomer)	0.90
S7	Optical Fiber O'Jacket (polyallomer)	0.90
S8	(20-mil) Buffered Optical Fibers	1.248
S9	KEVLAR-49 Strength Member	1.44

Table (5). Baseline Values For Design Variables --AMUVS Tether.

AMUVS TETHER CABLE STUDY

CONSTRAINTS ON MOTOR POWER SYSTEM

A	= 0	C	= .60965
V0(VDC)	= 150	K	= .25
D1(IN)	= .01003	N	= 18
P0(W)	= 1000	L(FT)	= 200

PERFORMANCE OF INSTRUMENTATION POWER SYSTEM

V1(VDC)= 115	K= .25
R1(OHM/KFT)= 73.6923	R2(OHM/KFT)= 18.7597
P(W)= 134.107	I(AMPS)= 1.55486

PERFORMANCE OF MOTOR POWER SYSTEM

R (OHM/KFT) FOR EACH CONDUCTOR = 10.2116
P (W) = 1032.83 I (AMP) = 9.1807

RG-174 ATTENUATION (DB/KFT) VS. F (MHZ) & C---A = 0 OR 1

ATTENUATION = (8.99*SQR(F/C) + .0042*F)/COS(T2)

DIAMETERS (INCHES) OF MAJOR CABLE COMPONENTS

CONDUCTOR STRANDS= .048144		JACKETED CONDUCTORS= .1	
FILLER RODS	= .0241335	AXIAL CORE ROD	= .0154701
JACKETED FIBERS	= .046267	ASSEMBLED SERVING	= .21547
BINDER TAPE	= .21947	JACKETED CABLE	= .35

SPECIFIC GRAVITY OF CABLE COMPONENTS

CONDUCTOR WIRES	= 8.87	COND. JACKETS	= .9
COAX CABLE CORE	= 1.13903	COAX OVERJACKET	= .9
BINDER TAPE	= 1.375	FILLER CORE/RODS	= .9
VOID FILLER	= .925	CABLE JACKET	= .9
OPTICAL FIBERS	= 1.248	FIBER O'JACKETS	= .9
STRENGTH MEMBER	= 1.44		

COMPONENT WEIGHTS (LB/1000')

COND. WIRES	= 3.58174	COND. JACKETS	= 5.04728
COAX CABLE	= 3.95788	COAX OVERJACKET	= 5.82505E-07
OPTICAL FIBERS	= .531619	FIBER OVERJACKETS	= 1.84952
FILLER RODS	= 1.13018	AXIAL CORE ROD	= .0733391
VOID FILLER	= 1.44822	BINDER TAPE	= .214618
STR. MEMBER	= 3.38457	OVERALL JACKET	= .814518

CABLE IN-AIR WEIGHT (LB/KFT) = 27.4624
CABLE SPECIFIC GRAVITY = 1.01651

1ST COND. STR. ANGLE T0 (DEG) = 13.4992
2ND COND. STR. ANGLE T1 (DEG) = 23.4595
CABLE ASSEMBLY ANGLE T2 (DEG) = 11.5073
FIBER HELIX ANGLE T5 (DEG) = 16.4257
[illegible] HELIX ANGLE T6 (DEG) = 15.241
[illegible] ANGLE T7 (DEG) =

Table (6)
Recommended Design

(c) Instead, the JASON tether can contain three conductors, and these can support either 3-phase AC power transmission or an unbalanced DC transmission.

18. FINAL COMMENTS ON AMUVS. I believe the information shown in Tables (5) and (6) can allow any competent cable company to (a) critique and modify my design as appropriate, and (b) submit a contracturally complete and detailed statement of design, cost and performance for the AMUVS cable.

19. WHOI should plan to procure this cable in at least 1000-foot lengths (preferably even longer). At the 200-foot operational length planned for AMUVS, setup charges will completely dominate in determining cable costs. The cost of a 1000-foot cable length will be very much less than 5-times the cost of 200 feet.

20. If several of the elastomer substitutions shown in Table (3) are made, it is possible for the AMUVS cable to be neutrally buoyant at a diameter appreciably less than 0.350". This might be an advantage to AMUVS/ALVIN. For example, substitutions 3, 4 and 5 in Table (3) allow cable diameter to shrink to 0.325" at a specific gravity of 1.027. If changes 3 through 8 are effected, then cable specific gravity can be slightly less than 1.00 at a diameter of 0.300".

George Wilkins

GEORGE WILKINS

Copy To:

53
531
532
534
946 (Steve Cowen)

WHOI (Skip Marquet)
BENTHOS (Andy Bowen)

EVALUATION OF AMUVS ENGINEERING DIVES AND DEVELOPMENT PRIORITIES FOR OPERATIONAL USE

8 September 1985

Deep Submergence Laboratory

Woods Hole Oceanographic Institution

Reference 12

SUMMARY

Following a two-and-a-half year R&D effort by the Deep Submergence Laboratory, the AMUVS/ALVIN OPS-85 provided a comprehensive test of the prototype system. Mounted externally on the manned submersible ALVIN, AMUVS made six engineering test dives in July of 1985 to a depth of 2000 m. The vehicle was remotely operated from inside ALVIN and returned with color video footage of the submersible and thermal vent communities. The engineering trials were largely successful, revealing no major flaws in the design, and was invaluable in evaluating the AMUVS/ALVIN interface and in gaining operational experience with the system.

In general, the prototype system is too bulky, heavy, and complicated for routine ALVIN operations. ALVIN batteries and internal wiring constrain an inefficient power system and inadequate isolation among floating systems degrades system performance. The vehicle flotation and weight distribution affords marginal stability in pitch and roll, limiting payload options. Color camera performance is adequate but operating near the limits of sensitivity. Most problematic is the original launch and retrieval system because of poor cable handling characteristics and of excessive weight. Without a reduction in external weight, an operational system on ALVIN will be severely constrained by sea state.

In preparation for AMUVS/ALVIN OPS-86, the focus of development efforts will be to consolidate and refine the system with an emphasis on video imaging quality and operational reliability. The proposed ALVIN upgrade to 120 V battery supplies presents an opportunity to simplify the AMUVS power system and reduce external weight. The streamlined AMUVS system would be suited to SEA CLIFF or ARGO operations and could support other options including high frequency positioning, scanning sonar, or mini-manipulator.

ENGINEERING EVALUATION

Video Subsystem

Performance of the color video system is adequate for close work and can be improved substantially with little more than adjustment. The Osprey camera and Hydro Products CCD show comparable resolution and color rendition though the Osprey's more sensitive tube and wider angle lens have an advantage at underwater light levels. The lens's greater depth of field requires no manual focus to distract the operator and assures image sharpness.

The Hydro Products camera was also more prone to interference from the telemetry system, the poor signal to noise ratio under lower scene illumination further degrading video quality. The Colmek video multiplexor performed well with the better isolated video signal from the Osprey, though the color burst signals passed from the two cameras was sensitive to frequency adjustment.

Vehicle Subsystem

In most respects the vehicle performed satisfactorily but was labor intensive to assemble and disassemble. The external and internal wiring harnesses were too bulky and the system's tight packaging and curved shape made for awkward handling.

Operationally, the vehicle was only marginally stable in pitch and roll. Despite a 2% gain in buoyancy (3.1 lb) at depth, the reserve buoyancy amounts to only 13 lb, mostly distributed around the vehicle for proper trim. Without enough righting moment, the low-damping spherical shape makes the vehicle sensitive to disturbances from cable forces and thrust imbalances.

From limited testing and field operations the newly developed Kollmorgen motors may be considered a qualified success, final judgment to await more pressure cycles. Two failures during prototype testing resulted from human error. The only other failure, spurious command signals to the motor, occurred during the dive series and the motor was replaced by a spare. Other motors experienced this problem to a lesser degree because of

ground faults in the ALVIN interface. The failed motor works normally in the laboratory but shows some isolation breakdown between housing and electronics, suggesting a greater susceptibility to ground loop problems.

The control resolution of the motors was lessened by the large deadband and mismatched scaling of the current controller. Kollmorgen reports that these controller characteristics were chosen at the factory to match their estimates of desired performance and can be modified through a change of resistor values. Kollmorgen's project engineer, Stu Dalton, states that the deadband can be reduced or eliminated and output matched to propeller characteristics with highly linear performance over the full range.

Microprocessor Control Subsystem

System control hardware is equal to processing demands and the two vehicle and console microprocessor systems performed without failure despite abusive shipping and handling. Though there were no hard disk problems, the potential exists for this kind of failure to cripple the system. A delay of several seconds to allow disk spinup also prevents prompt resets after power failures, potentially dangerous in critical situations.

There was no observable EMF/RF interference between the AMUVS and ALVIN systems other than ground faults discussed later. The cramped quarters inside ALVIN's pressure sphere were strained to accommodate AMUVS rack-mounted equipment and peripheral devices. Under these conditions the separate keyboard and hand controller were awkward to handle and there was no convenient placement for the operator display.

Though most control software was adequate, servo loops were not tested since the azimuth sensor was not functional and depth sensor was not calibrated. The main bottleneck to control performance is the serial communications protocol implemented by the Hydro Products microcontroller which has a worst case performance of ten command and status bytes to uplink one data byte. This scheme is adequate for the RCV-225 system but the added downtraffic for AMUVS motor commands causes delays and mushy vehicle response.

Power Subsystem

The prototype power system, though flexible in meeting the unknown system requirements, was bulky, heavy, and inefficient. Though the load on ALVIN's science bus (50A at 30V) never exceeded 45A, the battery output resistance and ALVIN wiring losses caused excessive voltage drops at the inverter input terminals. The resulting power brownouts degraded the video signal and caused frequent microprocessor power-up resets.

Early ground fault problems resulted from faulty ALVIN wiring, a shorted choke casing in the AMUVS pressure housing, and the normal filter capacitors in the regulated power supplies. The obvious problems were eventually corrected, but intermittent faults occurred throughout the dive series. Besides the more severe faults, there was a substantial leakage caused by the high humidity in ALVIN's sphere. The most noticeable effect of ground loops on the AMUVS electronics was a spurious biasing voltage at the motor signal inputs causing unwanted motor velocity.

Launch/Retrieval Subsystem

From an operational perspective, the L/R system, including the basket and external components, was far too heavy and the wiring needlessly complex. Though no failures of the electrical contactors occurred, problems with the offload camera package and a history of ALVIN contactor problems suggest a latent problem. The DSL designed clamp mechanism performed satisfactorily but some adjustment of the linkage is needed for a more secure grip on the vehicle.

Though the spooler functioned well during pre-dive testing, problems occurred in the field. The mechanical drive jammed during one dive and the friction dependent slip rollers could not maintain enough traction in a muddy, oily environment. At locations on the cable where severe slippage occurred, significant abrasion was observed in the soft TPR cable jacket. Use of the spooler was discontinued after the cable failures occurred to help reduce the risk of further cable damage.

The interim cable produced by Vector suffered two failures during the dives and a third back at the laboratory. Dissection of the cables showed in all three cases severe Z-kinking of the co-ax center conductor and shield. This kind of failure normally results from overstressing the cable under high tensile loading.

The first failed cable is not thought to have sustained enough loading during use to cause such a problem. The second failure occurred in a spare cable assembly which had never before been used. This suggests that the Z-kinks formed during manufacture, migrated through the soft dielectric during normal use, and shorted to the shield. George Wilkins supports this view, and postulates that too large a back-tension on the woven KEVLAR could compress the cable conductors and cause the kinking when the tension is relaxed.

Since the external assembly's air weight exceeded the rating of ALVIN's basket release, auxiliary cables or block and tackle were used to reduce the load during launch and recovery. This stop-gap measure is dependent on calm seas for deployment operations since wave-induced accelerations on the surface could develop enough force to damage the release or cause the loss of the basket. A change in weather during a dive could jeopardize the system during recovery.

DEVELOPMENT ALTERNATIVES

Video Subsystem

No important changes in the video subsystem appear warranted at this point. A modest effort to isolate and shield the cameras and telemetry system should end noise problems or reduce them to a tolerable level. Setup and adjustment of the cameras and telemetry should then give acceptable picture quality. Other lens alternatives may be desirable but should await further field experience.

Judgments about the adequacy of the 300W lighting now used also should be postponed until more testing with a properly tuned video system can be performed. Hydro Products is offering an extended lamp envelope and improved lamp reflector for the RCV-225 color option which eliminates the lighting dead spot and may make more efficient use of lighting.

Each camera offers advantages and may be preferred in different situations. The pitching ability of a CCD camera is highly desirable in most operational scenarios. The added visibility can help to avoid cable entanglements especially in tight places. However, tube cameras will probably maintain a performance edge over color CCD's in the near term. They should be considered for best video quality, perhaps being used after first exploring an area with a pitching camera. A camera swap between dives poses no problems but would be facilitated with a

spare housing and electronics or a second vehicle assembly.

Vehicle Subsystem

Configured as a camera platform only, the vehicle needs only small refinements. With component locations now known, the junction block and external wiring can be simplified for easier servicing. Since the lamps are now being powered directly from the primary 120V supply, the connections can be made externally, freeing two penetrators for other uses. The motor controllers should be scaled to match the vehicle's propeller configuration.

The 3-blade propellers now being used do not take advantage of the full motor power but give a level of thrust comparable to that of the original system. This is adequate for observation and inspection missions but may prove inadequate for future applications needing a manipulator or other external package. Matched left- and right-handed props for motor pairs should reduce some torque imbalances and enhance vehicle stability. Consideration should be given to a separate testing program to select a standard prop which might be suitable for all DSL vehicles using the Inland motors.

Because of the vehicle's spherical shape and small reserve buoyancy, little improvement in pitch and roll stability can be achieved without significant modifications. The configuration is acceptable as a camera platform but would present problems in supporting a manipulator with vertical load at a distance from the center of gravity. A slightly larger body or lower density foam could show some improvement but a modified body shape may be preferred.

Microprocessor Control Subsystem

The microprocessor hardware needs no substantial changes but should be repackaged for rack-mounting. External wiring can be simplified to reduce the difficulty of working in ALVIN's sphere. With ROM-based software, the disk drives may be excluded from the control console and mounted in a separate chassis for development work.

Hydro Products has plans to shift its RCV-225 microprocessors to an Intel 80188-based architecture. First prototypes of the vehicle microprocessor motherboard are expected to be available this Fall. Functionally, the board will be identical with the 8751 controller now used in AMUVS. Though a move to such an

architecture is in line with DSL plans to use the iAPX86 processor family for its ROV systems, prudence suggests that the upgrade be delayed. With the time constraints on AMUVS modifications this year, dependence on a yet-to-be-released product, a first iteration prototype, is risky and the surface-mount design may be difficult to modify for AMUVS. Also, Hydro Products will use Pascal for all software development. This would call for a time-consuming effort to develop C code for an unfamiliar system from scratch.

A simple 8751 serial controller could be developed to offload communications overhead from the main processor. The 8751's 9-bit serial capability matching that of the vehicle microprocessor's can be used to simplify the communications protocol and allow faster update rates for sensors and motor commands. This calls for modification of the vehicle programming but leads to streamlining and reduction in code size.

Hydro Products also has plans to adopt a rate gyro now used in other systems for the RCV-225. Should this develop in a timely fashion, it could be considered for an upgrade this year. In the meantime, the AMUVS gas rate transducer is being repaired under warranty and is adequate for good servo control of AMUVS. A higher resolution depth transducer could show modest benefit if one is available to match the AMUVS power and depth sensor circuitry. Ultimately, AMUVS should be upgraded to a multi-axis attitude package and major attention to the vehicle's sensors could be delayed until that time.

A new hand controller is warranted to replace the modified Benthos unit. This could incorporate a small keypad and added controls for the enhanced AMUVS. Joystick control of vehicle depth commands, azimuth gain control, and other switch options should be incorporated. A higher resolution color monitor is desirable, preferably a flat-screen model. An adjustable mounting arm would reduce clutter inside the sphere and allow more convenient viewing.

Most AMUVS software already written can be used without modification but, in general, needs some cleanup and refinement. Some problems seem to be traceable to the Lattice C compiler, appearing also in code developed on the AT's. Other compilers are being considered which offer library source code and ROM support. Code development should focus first on the vehicle data link and the move to ROM-resident code. As the system becomes operational, later work can improve the operator interface.

Power Subsystem

As part of this winter's overhaul, ALVIN's batteries will be upgraded to 120V to support a brushless DC motor drive system. AMUVS can take advantage of this change to directly power its motors, lights, and vehicle electronics, already rated at a nominal 115V. This will eliminate the inverters and regulated power supplies, reducing system wiring complexity, eliminating more than 250 lb of in-hull weight, and freeing about 18 in of rack space. The console microprocessor system, telemetry, and video equipment can be powered at 115 Vac from ALVIN's new high-efficiency inverter.

By removing the lighting power source from the vehicle's inverter system, the internal power demands are reduced to about 20% of the original load. This much lower demand facilitates modifying the vehicle power system to use more modular, high-efficiency DC/DC converters. The inverter card and troublesome heat sink assembly can be eliminated to free space for sensor enhancement or other purposes. Separate voltage regulators for such distinct functions as telemetry and video would help reduce conducted noise problems.

Launch/Retrieval Subsystem

For missions entailing penetration or work in congested areas, a reliable cable handling system is essential. The added need to reduce external weight suggests major changes to the subsystem. The spooler should be modified so that the drum and level-winder are powered in both directions and pinch-roller changed to act only as a tensioning device. This considerably reduces the needed pinch-roller friction for spooling out and reduces the risk of cable damage.

By upgrading the spooler and clamp drives to use the Inland 120V motors, other important problems can be addressed: the contactor junction box can be eliminated for increased reliability and wiring simplicity, the heaviest components are replaced with lighter ones, and a common motor for all functions can reduce the inventory of spares. Along with this change, the heavy slipring assembly should be replaced with a lighter, more compact version with the potential for upgrade to an electro-optical unit. A drum bearing should be located on the slipring end of the unit, perhaps incorporated in the slipring assembly. These changes could lead to reduction in external air

weight of about 150 lb.

Tom Coughlin of Vector Cable has confirmed that they will honor the original agreement to build a cable to George Wilkins's original specifications for the quoted price. Delivery is estimated at 12 weeks. George concurs that the experience with Vector's interim cable design does not negatively effect his original proposal and would like to continue his involvement with the engineering and manufacturing processes.

The AMUVS mounting arrangement is patterned on the standard ALVIN basket and could be modified to reduce the load on ALVIN's release mechanism. An effort should be made to move the spooler and other heavy components closer to the sphere to reduce the cantilever moment. A lighter, more compact external assembly could end the need to remove ALVIN's electric arm for AMUVS operations.

OTHER OPTIONS

ARGO/SEA CLIFF Operation

None of these development alternatives compromise the potential for operating AMUVS from such platforms as ARGO, SEA CLIFF, NR1, or other of the Navy's manned submersibles. Reductions in size, weight, and power requirements can only help this kind of effort. A custom DC/DC converter for SEA CLIFF and a modified mounting arrangement for external components would be needed. Skip Gleason is making further inquiries at SubDev Group 1 relating to the interface.

The AMUVS Colmek telemetry system would simplify adaptation to the ARGO and an upgrade to Inland motors would facilitate remote operation of the L/R system. For this application, the second vehicle pressure housing and nearly identical electronics could be employed. This would provide a camera to monitor remote L/R operation, a compatible telemetry link for surface control, and a tested motor command architecture for its control.

Second Vehicle and L/R Unit

Consideration should be given to upgrading the second vehicle and developing a spare L/R unit and basket assembly. A spare vehicle enhances the prospects of a successful mission and offers an easily interchangeable camera option. For a second operational vehicle, a pressure housing and camera are already on hand. The upgrade would entail the acquisition of a spare set of vehicle electronics, motors, and optionally, an improved syntactic foam body.

A second external L/R system would require the construction of an all-new spooler, clamp, and basket assembly. Though this could be modeled after the upgraded AMUVS L/R components, a design study should be undertaken to evaluate newer approaches. Such an undertaking could produce a more practical, reliable design that could contribute to the JASON effort and other long-range programs.

Augmented Spares

As an alternative to a second vehicle and L/R assembly, a generous allotment of spares is recommended. Though the engineering test dives did not suffer any debilitating failures, the summer '86 operations should have better safety margins. Items which should be duplicated include vehicle and console PC boards, heading and depth sensors, cables and connectors, lamps, motors, and hand controller components.

Mini-manipulator

For the coming summer's operations, the development of a simple, one-degree-of-freedom manipulator is a practical goal. Such an arm could consist of a solenoid/spring actuated gripper or other simple tool mounted on a lightweight arm. Friction-clamped ball joints at wrist and elbow would allow the arm to be configured at the surface for different needs.

Though a more complex 3- or 4-degree-of-freedom arm could be developed for AMUVS, the constraints of AMUVS small size and payload call for a more sophisticated development effort. The

problem of providing enough stability to successfully use such an arm would further increase the required investment in resources. A preferred approach might first consider a new body style providing more stability and payload suitable to a range of external options.

Scanning Sonar

To compensate for the reduced visual range of a color camera system, a vehicle-mounted sonar system offers a way of providing the operator with piloting and position information. Hydro Products has provided a quote for the ASI scanning sonar developed for the RCV-225. The system consists of a set of electronics boards designed for the AMUVS vehicle, a pair of acoustic transducers, and a console display unit. Adaptation to AMUVS requires a separate Colmek telemetry channel, transducers rated to a greater depth, and a modest hardware/software effort to interface the console and display units.

High-resolution Positioning System

A modified version of the high-frequency responder system being tested on the RPV would aid in remote operation of AMUVS from such fixed platforms such as ALVIN or SEA CLIFF. Two receiving transducers fixed to ALVIN with a baseline of a few meters could provide positioning information over a limited area with good accuracy. Depth information from the vehicle would furnish the remaining parameter to fix a position in three dimensions. Development would call for some modifications to an RPV-type system, an added Colmek telemetry channel, console programming, and an appropriate display device.

Optical Video Link

Discussions about a student engineering project have been held with faculty of the University of New Hampshire regarding an optical video link over the AMUVS electro-optical cable. Depending on the quality of ideas generated, some funding of joint development costs might be considered. Such a pilot program could lay the foundation of a knowledge base for ARGO/JASON development.

A Computer Model for Prediction of Underwater Images

Jules S. Jaffe, Stewart E. Harris, Robert Squires

Woods Hole Oceanographic Institution
Woods Hole, Massachusetts 02543

ABSTRACT

As part of a continuing effort to develop effective tools for deep ocean exploration, the Deep Submergence Laboratory (DSL) at the Woods Hole Oceanographic Institution has developed a computer model to simulate underwater image formation. The predictions of the model are in good qualitative agreement with the data collected from the first ARGO field operation in the summer of 1984. Computer modeling of underwater images can be used as a computer aided design (CAD) tool in that the simulation of underwater imaging configurations will give the engineer valuable information about the performance of a given imaging system. This paper describes the model briefly.

INTRODUCTION

The development of underwater manned and unmanned platforms for the exploration of the ocean floor is the primary goal of the ARGO/JASON program of the DSL. To aid in the design of these underwater platforms we have developed a system of computer programs for Underwater Camera Light Experiment Simulation (UNCLES). The system of computer programs is interactive and menu driven. When used in the design mode, the system will facilitate the design of effective underwater lighting systems. This is accomplished by allowing the designer to simulate the appearance of underwater objects for different underwater viewing conditions and different geometries.

The UNCLES system will allow the design engineer to place any number of lighting sources at arbitrary positions in 3 dimensional space. A planar reflectance pattern is then positioned anywhere in 3 dimensional space at a given orientation. After reflection of the light from the reflectance map, the light is propagated to the camera where it forms an image of the given scene.

The UNCLES system will allow many different lighting geometries to be tested for a variety of water conditions. Our initial investigations with this system of computer programs have allowed us to simulate a great variety of imaging configurations. We anticipate that this system of computer programs will play a valuable role in our future design of underwater lighting systems.

HISTORICAL REVIEW

Comprehensive scientific studies of the propagation of light in water were carried out by Duntley and coworkers in the early 1960s [1,2]. Research at that time established the fundamental limitations for underwater viewing as being due to the attenuating and scattering properties of water. The limitations described in those studies are still relevant to our current generation of imaging systems although advances in electronics have allowed the collection of images to go from hours to milliseconds.

Additional contributions to the field of underwater imaging by the navy resulted in a handbook [3] of underwater imaging. This report consisted of a series of charts and nomograms that were used to predict the outcome of a given underwater imaging configuration. Additional work at the Scripps Institution of Oceanography by McGlamery [4] resulted in a system of computer programs which formed the basis for our work at DSL.

IMAGING FUNDAMENTALS

In designing the configuration of an underwater platform the system designer is initially confronted with the fact that water is both an attenuating and scattering medium. The

physical quantities that describe the importance of attenuation and scattering are the attenuation constant and the volume scattering function.

The attenuation constant describes the magnitude of the exponential decay of light as it propagates from one location to another. The volume scattering function describes the probability of a scattering event per unit distance at a given angle to the direction of light propagation. This function is radially symmetric. A sample of this function is graphed in Figure 1.

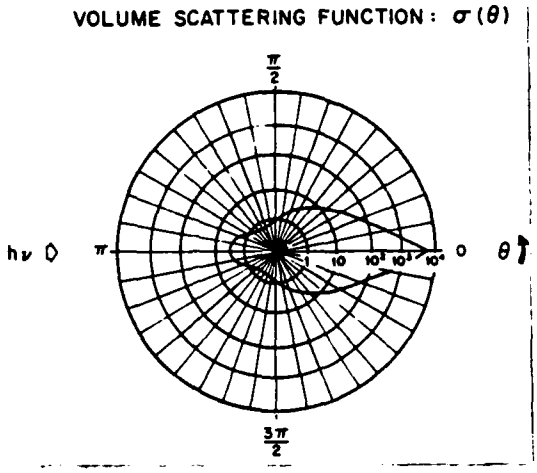

Figure 1: An Example of a Volume Scattering Function

Taken together, these two quantities are all that one needs in order to describe the propagation of light from lighting source to the target and then on to the camera. However, simplification of the problem and additional insight can be gained from dividing the light into three categories: 1)light that propagates without scattering and is merely attenuated, 2)light that has been scattered on its way to the camera after it is reflected from the object, and 3)light that has been scattered into the camera without being reflected from the target. These components are identified as the direct, the forward scatterred, and the backscattered components and are illustrated in Figure 2.

INPUT AND OUTPUT OF THE MODEL

The inputs to the model are the above mentioned quantities, the attenuation coefficent and the volume scattering function, along with the basic geometry of the system. The geometry consists of the X,Y, and Z position of the camera,light source, and reflectance plane. In addition, the beam pattern for the light, along with some empirical constants that describe the transfer characteristics of the system must be input. Other input parameters describe the camera component of the system and consist of features like the size of the aperture and the focal length of the camera.

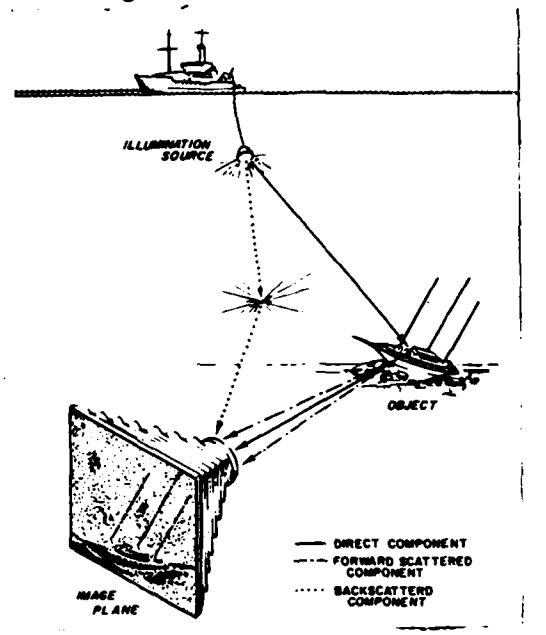

Figure 2: The 3 Components of an Underwater Image

We will illustrate the performance of the program with a test case. The geometry of the test case along with the reflectance map are illustrated in Figure 3. The output of the system is in the form of a matrix of values that are proportional to the incident irradiance onto the camera plane. The user then has the option of outputing the results at a video monitor as a grey level map, or as a graph at a graphics terminal. Here, we illustrate the output that one would obtain with a graphics device.

The set of curves in Figure 4 illustrates a cross section of the irradiance pattern that would be incident on the target. Note that the incident irradiance consists of two parts: 1) a forward scattered part labeled G, and 2) an unscattered or

direct part labeled D. The curve labeled T is the total irradiance that is incident on the bar pattern.

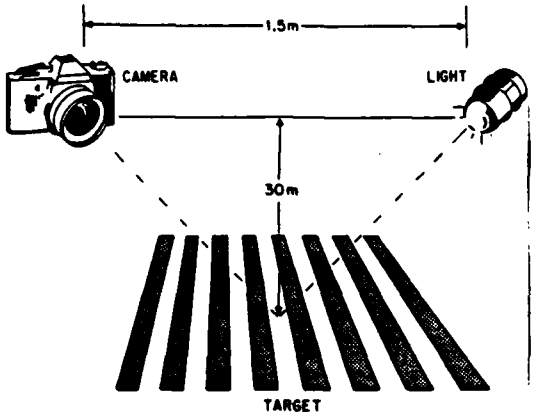

Figure 3: Geometry of the Test Case

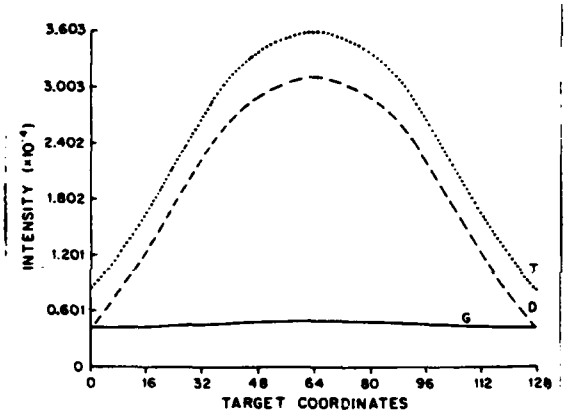

Figure 4: The Irradiance Pattern on the Target Plane

After the light is reflected by the bar pattern it propagates to the camera where it is recorded. The pattern that is incident on the camera plane consists again of several components. These components are illustrated in Figure 5. Here we have labeled the backscattered component B. It has not been reflected by the bar pattern but has been scattered to the camera. Another component is the reflected component which is blurred or scattered on its way to the camera. This is labeled G in the drawing. Note also the component labeled D which has been been reflected by the object but has not been scattered on its way to the camera. This component is our signal. The total irradiance that is incident on the camera is labeled T in Figure 5.

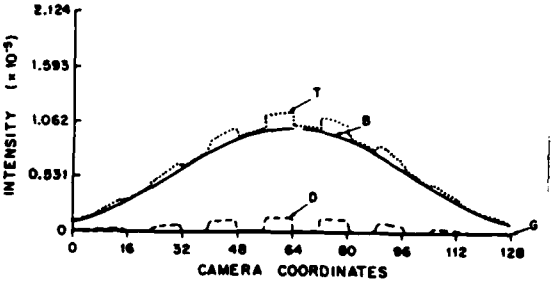

Figure 5: The Irradiance Pattern on the Camera Plane

A very interesting parameter to examine in predicting the performance of an underwater imaging system is the contrast transmittance. In our case, we define the contrast transmittance to be the ratio of the magnitude of the direct component D divided by the magnitude of the sum of all of the other components. This quantity is illustrated in Figure 6.

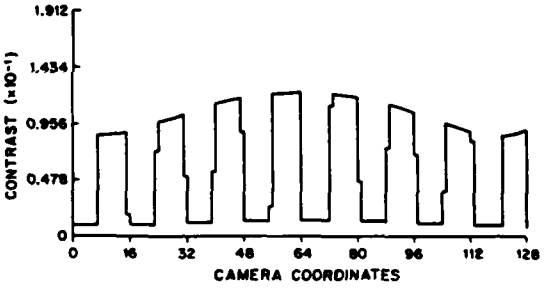

Figure 6: The Contrast Transmittance Values for the Test Case

CONVERSION OF THE IRRADIANCE PATTERN TO A VIDEO SIGNAL

The next step that must be taken in relating the performance of the model to the real world must be the prediction of the output image that will be generated by the imaging device. We illustrate the system perfomance in this case with a computation for a video signal. In order to predict the quality of the resultant video image, we must first determine the absolute output of the

lighting source. The UNCLES system assumes that the output pattern from the source has been normalized to unity. All of the irradiance values at the camera plane are expressed as a fraction of this value.

An additional complication arises in that various imaging systems employ both continuous lighting and strobe lighting. In the case of continuous lighting we can take the number of lumens/watt produced by the lighting source and multiply by the number of watts to get the output of the lighting source in lumens. Next, we must compute the effective transfer of radiant energy through the water. For example, for a typical Xenon tube only 10% of the light will get through the passband of 450-500 nanometers. After correction for the reflector efficency, we have the output of the light in lumens.

Next, in order to calculate camera response to this light source, the designer needs to multiply the values obtained from the computer model by the light output. This will yield the incident irradiance (lumens/sq. meter) on the camera faceplate. Standard graphs of the camera transfer function can be used to convert this illuminance into nanoamps or a percentage of the full video output.

The situation for strobe lights is somewhat different because their output is a quantity of luminous energy, not a continuous luminous flux with which cameras are normally calibrated. Since a television camera integrates light for 1/60'th of a second and a strobe pulse is much shorter than that, the equivalent luminous flux to produce the same camera response continuously is 60 times the strobe output in lumen-seconds. This calculation yields an equivalent value of light output in lumens. This can then be applied to the calculation in a manner equivalent to the above example for the continuous case.

CONCLUSION

This paper has described the implementation of a system of computer programs to simulate the process of underwater image formation. The goal of the system of programs is to allow a system designer to optimize the performance of an underwater imaging system. The inputs to the model are the system geometry along with environmental parameters that describe the water. We plan to use the UNCLES system as a CAD adjunct in order to help design better lighting systems for the future.

ACKNOWLEDGMENTS

The authors would like to thank the Pew Memorial Trust Foundation for support of this work.

REFERENCES

[1] Duntley,S.Q.,(1963) Light in the Sea, J. Opt. Soc. Am.,53,214.

[2] Duntley,S.Q.,(1973) Underwater Lighting With Submerged Lasers and Incandescent Sources, SIO Ref. 71-1

[3] Funk,C.J., Bryant,S.B., and P.J. Heckman Jr.,(1972) Handbook of Underwater Imaging System Design, Ocean Technology Dept., NUSC

[4] McGlamery, B.J.,(1979) A Computer Model for Underwater Camera Systems, SPIE, V28,Ocean Optics VI,S.Q. Duntley, ed.,221.

THE APPLICATION OF DIFFERENTIAL GPS TO MARINE VESSEL DYNAMIC POSITIONING

ROBERT P. DENARO
DR. PETER V.W. LOOMIS
TAU CORPORATION
LOS GATOS, CA

DR. DANA YOERGER
WOODS HOLE OCEANOGRAPHIC INSTITUTION
MASSACHUSETTS

BIOGRAPHIES

Mr. Robert Denaro is a founder and Vice President of TAU Corporation and manages the Navigation Systems Division. The primary thrusts of his work are GPS-based integrated navigation systems, differential GPS systems, and advanced processing techniques. Prior to his work at TAU, Mr. Denaro was with Systems Control, Inc., and he spent eight years in the Air Force conducting navigation and flight control research, including three years at the GPS Joint Program Office in Los Angeles. Mr. Denaro holds a B.S. in Engineering Sciences from the Air Force Academy, and M.S. degree in Electrical Engineering and Systems Management from the Air Force Institute of Technology and USC, respectively.

Dr. Peter Loomis is a Senior Engineer with TAU Corporation. He is responsible for GPS positioning and navigation advanced concept development, including the development of estimation algorithms for real-time and post-mission navigation processing. Before joining TAU, Dr. Loomis worked in accuracy analysis and evaluation of advanced reentry navigation systems at Lockheed Missiles and Space Corporation at Sunnyvale, California. Dr. Loomis holds a Ph.D in Mathematics from the University of California at Davis.

Dr. Dana Yoerger is an Assistant Scientist with the Woods Hole Oceanographic Institution in Woods Hole, MA. Dr. Yoerger works in the Deep Submergence Laboratory of the Department of Ocean Engineering where his interests include modeling, design and control of dynamic systems, particularly as applied to remotely operated underwater vehicles and manipulators. Dr. Yoerger received his Ph.D from the Massachusetts Institute of Technology in 1982.

ABSTRACT

Dynamic Positioning of marine vessels is conducted to support at-sea drilling operations, survey, diver and submersible vehicle support. Current sensors used for position reference experience a variety of error characteristics and reliability problems, and often require extensive installation effort. As an alternative, differential GPS, used in conjunction with other low-cost sensors, may eliminate many of these problems. This paper discusses the dynamic positioning application of differential GPS in terms of error sources and design concepts.

INTRODUCTION

Dynamic Positioning (DP) of marine vessels is the task of maintaining position over a particular ocean bottom feature or operation, with such typical applications as oil well drilling, static survey, and diver support. Ocean current drifts, wind, and sea state activity perturb the vessel from its desired position, and fore/aft hull thrusters are used to regain position. Various types of positioning systems and motion sensors are currently used to sense deviations from nominal.

Current sensors used or in study for DP include hydrophonic transponders, taut-wire systems, local shore-based radiolocation sensors, and even inertial measurement units. All systems suffer from various deficiencies comprising reliability, accuracy, depth-sensitive error growth, and shore proximity range or accuracy restrictions.

Differential GPS offers potential relief from many of these problems. As a relative velocity sensor, GPS is very precise, provided antenna placement does not amplify vessel rotational motion severely. In the differential mode, the geodetic positioning stability of the position solution is similarly dependable. Moreover, differential GPS allows vessel flexibility for operations further offshore and in deeper water.

In this paper, DP requirements and the use of existing systems are first described. Differential GPS error sources, as distinguished from stand-alone GPS error sources, are analyzed. Differential GPS implementation, as tailored for the DP application, is discussed. Particular emphasis is placed on design drivers from the DP environment. Finally, a high level candidate system design is presented to summarized the analysis of differential GPS in the Dynamic Positioning application.

DYNAMIC POSITIONING TASKS AND MEASUREMENT REQUIREMENTS

This discussion will focus on representative applications of dynamic positioning where local navigation techniques (such as shore or platform based radar navigation) are not practical. These include drilling and coring operations, drill hole reentry, and remotely operated vehicle (ROV) support.

DRILLING AND CORING

For drilling and coring, the positioning requirement is determined by the maximum amount of angular deflection of the drill string [1]. Therefore, allowable position excursions can be expressed as a percentage of the water depth, typically about 3% [2]. Drilling has been accomplished in water depths of over 2000 meters, and coring operations have been done in over 8000 meters of water.

Performance of the position measurements and state estimation process must be better than the required performance of the DP system as a whole. Many factors will greatly influence the relationship between the magnitude of random sensor noise and the size of expected vessel motions including sensor update rates and time delays, vessel dynamics and the certainty to which they are modelled, disturbances (primarily wind and current), and the structure of the controller and state estimators. Results from recent deep water drilling operations with high disturbance levels show vessel "watch circles" of 5 to 10 times the random sensor noise magnitude [2].

Reliability requirements are stringent for drilling and coring. Depending on wind and current, loss of position sensor information for as little as one minute may require disconnect, a costly and time consuming procedure. Drilling operations may last for many months, so highly redundant systems with substantial subsea infrastructure may be justified. Coring operations are usually of shorter duration, however, reducing the amount of effort that can be justified to deploy and recover a navigation beacons.

DRILL HOLE REENTRY AND REMOTELY OPERATED VEHICLE SUPPORT

Drill hole reentry and ROV support differ from drilling and coring in several respects. Performance requirements do not decrease directly with water depth. In addition, precise subsea position measurements are required.

For reentry operations, positional performance will be determined largely by the size of the reentry cone (typically 5 meters). The location of the end of the drill string must be known to a fraction of the cone size. Likewise, the movement of the ship must be controllable enough to move the string across the cone so it can be inserted.

For ROV support, the platform from which the ROV is deployed must be kept within a prescribed watch circle, rather than the ship. In the ARGO-JASON system shown in Figure 1, the ARGO vehicle will act as a "garage" for JASON, and also will aid the operators by allowing them to view both JASON and the surrounding terrain. Keeping JASON within ARGO's optical footprint will require that ARGO be kept within a radius of about 20 meters. An absolute limit is imposed by the length of JASON's tether, which will be about 100 meters long.

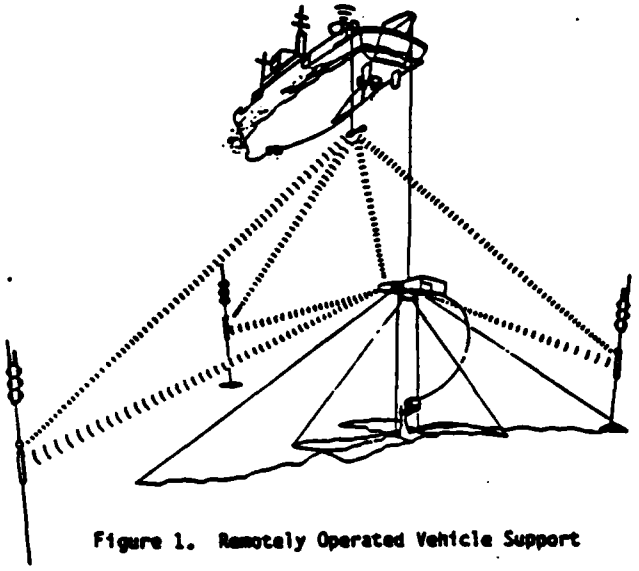

Figure 1. Remotely Operated Vehicle Support

EXISTING POSITION MEASURING SYSTEMS FOR DYNAMIC POSITIONING

A large number of sensors are used for dynamic positioning. Systems in shallow water or near structures may use taut wires. Optical tracking systems may be used near structures as well. Radar navigation may be used near short or structures. However, in deep water, hydroacoustic navigation systems are the mainstays.

Acoustic systems have several disadvantages. They may be prone to acoustic interference from the vessel thrusters. Often, combinations of several types of acoustic navigation must be employed to obtain sufficient reliability [3]. Given the magnitude of sensor noise and the dynamic uncertainty of the vessel and the disturbances, the quality of estimates of vessel velocity can impose significant limits on overall positioning performance.

PULSE SYSTEMS

A long baseline acoustic navigation system uses multiple transponders on the seafloor and a single transmitting and receiving hydrophone on the vessel, as illustrated in Figure 2. Given round trip travel times of acoustic pulses for each of the transponders and the sound velocity profile (which varies significantly with depth), the range to each of the transponders can be determined. From knowledge of the geometry of the net and the range estimates, vessel position can be determined. Net geometry is usually determined through a survey. Better accuracy can be obtained and the need for a survey eliminated by using "self calibrating" transponders. These units sense depth and transmit the results to the surface acoustically, and also permit the travel-times between transponders to be determined.

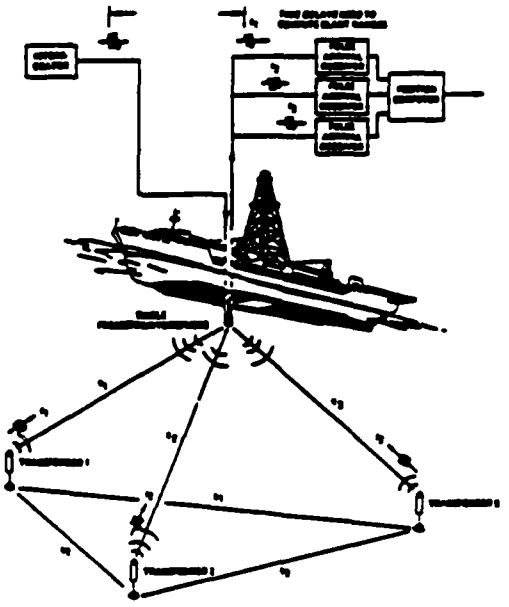

Figure 2. Acoustic Navigation System

The accuracy and precision of such a system is influenced by a variety of constraints. The extent to which the net geometry is known is often the most significant limit to accuracy, although it does not effect repeatability. Determination of the range estimates may be limited by the accuracy to which the travel time can be determined, or by knowledge of the sound speed as a function of depth.

The performance of long baseline systems is influenced by depth, but not as strongly as some other methods. Travel time measurement accuracy decreases slightly as operating depth increases, since lower frequencies must be used for longer ranges. The delays incurred due to the length of the round-trip travel time increase directly with depth, and may be quite significant. In deep water, this delay will limit the dynamics of the state estimates. Random sensor noise magnitudes of about 0.5 meter are reported in deep water applications [2].

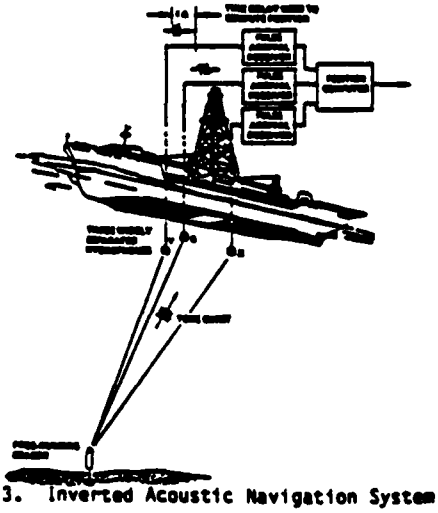

Figure 3. Inverted Acoustic Navigation System

Such a system may be inverted, with the baseline on the vessel and a single transponder on the seafloor as shown in Figure 3. Since the baseline is smaller than in the long baseline system described earlier, the position estimate is less certain for given errors in the slant ranges. However, the relative positions of each element of the acoustic net are very well known, reducing survey error. Vessel pitch and roll must be well instrumented. Errors in the position estimates obtained from such a system tend to increase linearly with range to the subsea transponder. Random sensor noise magnitudes of about 0.2% of water depth are reported [2].

PHASE SYSTEMS

The direction to a single subsea pinger or transponder may be determined by measuring the phase relationship of the acoustic signal received at a cluster of hydrophones as shown in Figure 4. If all hydrophones are within a single acoustic wavelength, phase represents an unambiguous indicator of direction. Like the pulse system with multiple receivers mounted on the vessel, only a single transponder is required subsea. The attitude of the hydrophone array must be well instrumented.

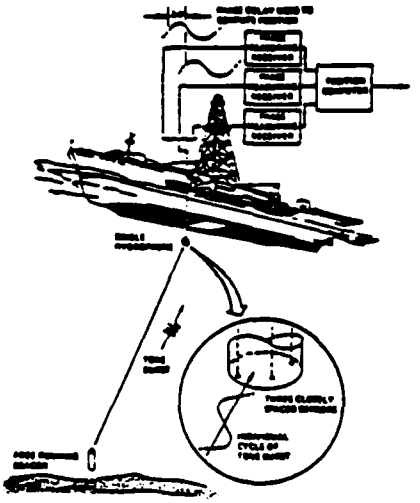

Figure 4. Phase-Based Acoustic Navigation System

In such a system, positional performance is linearly dependent on distance to the subsea transponder, as the phase measurement yields a direction. Typical performance is between 1% and 0.1% of range to the transponder. Phase systems tend to be more susceptable to noise than pulse systems.

PULSE DOPPLER SYSTEMS

Performance of a pulse system can be significantly improved by combining it with a Doppler system [4]. In such a system, the transponders on the seafloor are augmented by continuous beacons operating on different frequencies. The Doppler system provides very high accuracy relative motion information, while the pulse system allows the system to be initialized and prevents cumulative errors. The relative motion information provided by the Doppler system would allow very high quality velocity estimates to be obtained, improving dynamic positioning performance substantially. Such systems have been used for oceanographic work, but no applications to dynamic positioning are known.

INERTIAL REFERENCE SYSTEMS

Inertial reference systems could be used to supplement other forms of position measurement. Units used for commercial aircraft are of moderate cost and have well documented reliability [5]. The performance of such units (approximately 2 km./hr.) precludes their use as a primary sensor, however they can greatly improve the quality of the position and velocity estimates obtained from other sources. An inertial reference would also greatly improve the performance of the state estimator during loss of primary navigation information.

DIFFERENTIAL GPS FUNDAMENTALS

DIFFERENTIAL GPS CONCEPT

Differential GPS is a concept that eliminates some of the common, bias errors experienced by conventional GPS. Differential GPS derives its potential from the fact that the measurement errors are highly correlated between different users (as well as highly autocorrelated). By employing a second GPS receiver with comparison to truth, slowly varying, correlated errors can be isolated and eliminated. In addition, depending on the relative rates, intentional degradation of the C/A signal may be eliminated by differential GPS as well. Measurement errors are also highly correlated between satellites for any particular user, but such common errors are removed by the conventional GPS solution as they are indistinguishable from user clock bias, hence corrupt only that estimate.

In differential GPS, a receiver reference station is located on the shore in the area where greater accuracy is desired, as illustrated in Figure 5. The correlated errors that a receiver experiences (such as satellite ephemeris errors) should be common to all users in a relatively close geographical area. If the reference station can obtain a reliable estimate of its actual error and transmit that to dynamic users, the dynamic users may be able to compensate for a large portion of their errors.

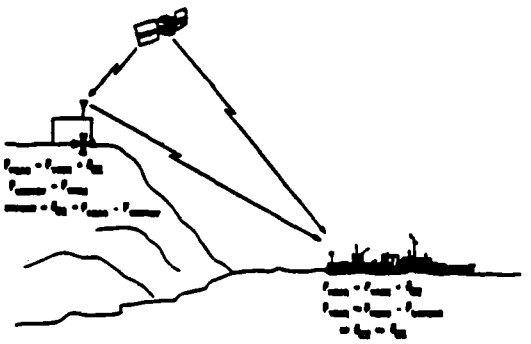

Figure 5. Differential GPS Concept

DIFFERENTIAL GPS DESIGN ISSUES FOR DYNAMIC POSITIONING APPLICATION

The subject of differential GPS has been discussed in numerous publications in the generic sense [6, 7, 8] and occasionally for specific applications [9, 10, 11]. In most cases, when considering a specific application, one of the various differential GPS implementation methods emerges as a preferred candidate. Furthermore, specific characteristics of the application amplify certain issues of significance to the implementation. This is the case for the dynamic positioning application; several design and implementation issues need to be resolved for a successful application. These issues are listed in Table 1.

- DIFFERENTIAL ERROR SOURCES/ACCURACY
- DIFFERENTIAL UPDATE RATE/DATA LATENCY
- DATA TRANSIENT COMPENSATION
- DATA LINK SELECTION
- DATA INTEGRITY MANAGEMENT/RELIABILITY
- SYSTEM INTEGRATION
- SYSTEM OPERATION

Table 1. DP Differential GPS Design/Performance Issues

Differential GPS Error Sources, Update Rates, and System Accuracy

The factors affecting differential GPS accuracy in the DP application are:

- Spatial decorrelation of "common" errors
- Temporal decorrelation/correction update rate
- Uncompensated vessel motion-induced errors
- Reference station or vessel position computational (filtering) errors

GPS error sources have varying sensitivities to ship-to-reference station separation distance. The generally accepted set of GPS error sources is listed in Table 2. Their relative error contributions under differential operation conditions are also indicated.

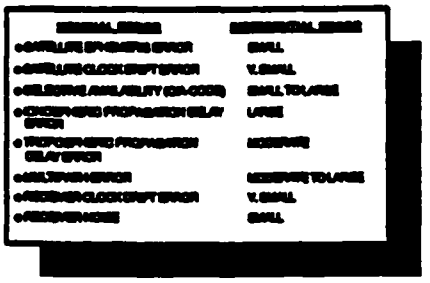

Table 2. GPS Error Sources

Satellite ephemeris and clock errors have small error effects on the differential user caused by slightly different look angles to each satellite by the ship and reference station. The effect is small due to the high altitude of the GPS satellite orbits which dwarfs any reasonable ship-to-reference station separation distance, as illustrated in Figure 6. The decorrelation in this case is caused by the different line-of-sight component of the satellites' three-dimensional orbital error on the two different lines-of-sight. As illustrated in Figure 6, for a separation distance of 200 nm, the angular separation of the two lines-of-sight is less than 18 milliradians (1 degree). In fact, as shown by Beser [11], for certain components of ephemeris error, the ship and reference station may observe their respective line-of-sight errors with opposite sign, although this applies to the least sensitive ephemeris error axis. In total, the differential error due to ephemeris can be expected to cause a magnitude of about .001% of the baseline distance for typical ephemeris errors (e.g., 100 m in-track, 15 m cross-track, and 2 m radial).

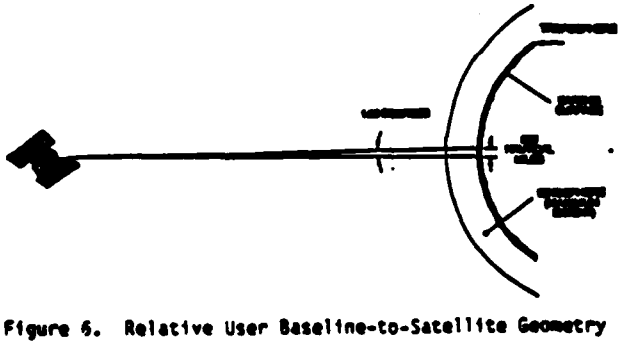

Figure 6. Relative User Baseline-to-Satellite Geometry

Satellite clock drift error is completely observed in the line-of-sight range. However, if differential updates (including range correction and rate of change of range correction) are accomplished infrequently, the residual drift between the clocks actual drift and the linear assumption inherent in the correction rate of change will introduce an error. This, too, should be negligible for updates even as seldom as every few minutes, unless some sort of clock anomaly transient occurs.

Selective availability is a potentially large source of differential error. In analysis of typical S/A data, Kalafus [8] has shown that the expected range error and first two derivatives of range error due to S/A should be

$$E(\tilde{r}) = E(\dot{\tilde{r}}) = E(\ddot{\tilde{r}}) = 0 \qquad \sigma_r = 100 \text{ m}$$
$$\sigma_{\dot{r}} = .14 \text{ m/s}$$
$$\sigma_{\ddot{r}} = .004 \text{ m/s}^2$$

As with other errors, a constant $\dot{r}$ due to S/A will not introduce any residual differential error, but $\ddot{r}$ or higher derivatives will cause the actual error to deviate from the predicted linear estimate in correction rate of change. Once again, this is a correction update rate issue. For the above data, an error due to S/A of .2 m can be expected for an update interval of 10 sec.

The ionosphere is a major source of error in standalone C/A-Code GPS. For differential GPS, the well-behaved temporal and spatial variability of ionospheric delay in mid-latitude regions make it generally well-compensated by differential GPS. However, the ionosphere does have a peculiar personality. Studies by the Air Force Geophysics Laboratory [12] have shown somewhat ill-behaved results at high latitudes and at the equator (the former due in part to the Aurora Borealis, the latter due to the electrojet). Ionospheric delay is caused by an electron layer at about 100 to 1700 km altitude above the earth. Figure 6a illustrates the general shape of the ionosphere, indicating its diurnal variation and its latitudinal variation. Moving satellite lines of sight that intersect high gradients in this ionospheric shell may experience much higher dynamic errors than experienced in more benign regions.

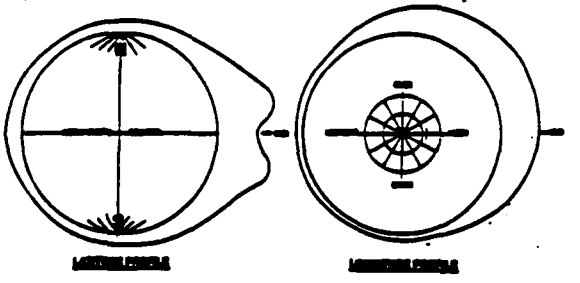

Figure 6a. Diurnal and Polar Variation of Ionosphere

Figure 7 compares a month's worth of daily ionospheric total electron content densities for two sites, one at 42 degrees north latitude and one at 0 degrees latitude [12]. Note the unpredictability of the dusk ionospheric delay reduction, and more importantly for differential GPS considerations, the high rates during these periods in the equatorial example. Even so, it is difficult to imagine ionospheric rates of change in excess of 5-10 mm/sec, with appropriate second derivatives. Residual errors for updates of 10 seconds should be submeter. It is important to note that these data may be quite different during an active part of the solar sunspot cycle (11 years), the height of which will occur again in about 1989.

The above considerations refer to the temporal correlation of ionospheric errors. The spatial decorrelation of the ionosphere is perhaps a more significant problem for differential GPS, and probably as poorly understood as yet. Figure 8 illustrates worldwide isoclines for

smoothed only outside of the bandwidth of the ship dynamics which must be tracked, unless other aiding sensors are used to allow increased isolation and smoothing of measurement noise. Reference receiver noise is smoothable outside of the expected bandwidth of the GPS signal error dynamics, which is a much more satisfying result. However, while the error dynamics can be highly filtered, care must be taken to allow for tracking of anomalous ionospheric transients and, in the case of C/A-code operation, selective availability signal dynamics. The DP application requires highly reliable positioning stability under all conditions.

DATA TRANSIENT COMPENSATION

Because the differential-GPS dynamic positioning system would be used in a reasonably high authority feedback system using the hull thrusters, it is important that any transients be "filtered out." However, sea motions and other effects may cause bona fide transient motions, so simple editing or averaging is not the entire answer. Figure 12 illustrates the GPS transient problem for DP.

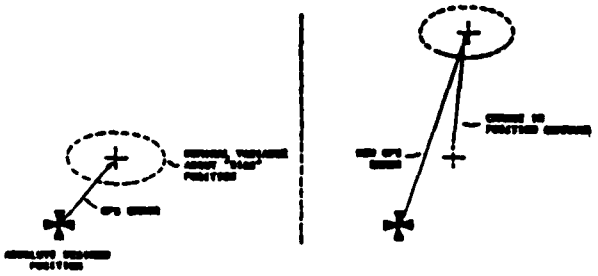

Figure 12. GPS Transient Effects on Dynamic Positioning

Possible natural sources of transients in GPS operation come from satellite switches to accommodate setting satellites or optimum geometry constellation selection. Of course, if less than 4 satellites must be tracked, serious changes in performance will occur. In this case, last altitude can be held fixed, and stable horizontal solutions should continue for some time.

In general, a change in satellites tracked can introduce transient errors in two ways, a change in uncorrelated range error and a change in geometric dilution of precision. Both of these are somewhat mitigated in differential operation because the differential corrections should eliminate nearly all of the satellite ephemeris or clock error. Of course, path changes could introduce new atmospheric or multipath errors as well. In general, it is a good idea to provide a software "switch" to compensate for the measured delta before incorporating the new satellite; this function would be accomplished at the reference station. A "constellation bias" would be computed and carried in software, and possibly slowly washed out over the next several minutes.

DATA LINK SELECTION

Data link selection is a straightforward tradeoff of bandwidth, update rate, and range. Furthermore, for DP applications, there may well be existing links that provide the best solution.

Of more interest for this application is the possibility of a "pseudolite" data link. This data link is named for its similarly to a standard GPS satellite transmitter. The pseudolite transmits differential corrections in place of the standard navigation message on a GPS L-Band signal, therefore requires no separate datalink receiver. The GPS receiver must be modified to decode the differential message.

The particular attractiveness of the pseudolite technique for DP applications is that the vessel receiver can also range to it. This provides a highly precise relative velocity reference along the axis (or axes) of reference. The application of this technique is discussed later.

DATA INTEGRITY MANAGEMENT AND RELIABILITY

As discussed previously, DP applications are sensitive to anomalous transients due to high authority feedback loops and control thrusters. Since some of these transients could originate from erroneous differential corrections as well as anomalous vessel receiver operation, it is important to incorporate some sort of integrity management in both subsystems.

Included in the types of data problems are loss of data, transient or outline measurements, decorrelated biases in the residual errors, computational errors, and various types of interference. Data integrity management features designed to combat these problems include data editing, filtering and smoothing, automatic fault detection and isolation algorithms, redundant data comparison, and software bias adjustment. Typical tests include satellite signal monitoring, receiver clock modeling, filter residuals tests and adaptation, and dynamics reasonableness tests.

DIFFERENTIAL GPS IMPLEMENTATION FOR DYNAMIC POSITIONING

The DGPS dynamic positioning system emcompasses the shipborne station; a reference station; and a data link between the two.

SHIPBORNE STATION

The shipborne station is a normal GPS receiver equipped for conventional standalone navigation, with an additional input for differential corrections broadcast from the reference station. The differential interface does not substantially alter its design as a standalone navigation aid, except that certain error sources that would be negligible in the face of ionospheric and satellite vehicle ephemeris errors grow to prominence when those errors are removed.

One error source that becomes significant is the displacement between antenna and the reference center (e.g., vessel center of gravity) for the dynamic positioning system. The GPS receiver tracks the position of the antenna, which is typically mounted high above the platform on a mast to provide maximum visibility of the satellites. Any pitch, roll, or heading error will cause an error in translating from the measured antenna location to the desired reference coordinates. The accuracy of the pitch/roll/ heading information necessary to locate the reference point depends strongly on its position relative to the antenna; if directly below the antenna, for instance, the displacement is insensitive to heading error. Inclinometers and/or heading sensors will provide enough pitch/ roll/heading information to solve the displacement problems in most dynamic positioning applications.

In its navigation role, the receiver is tied to the guidance and control system of the dynamic positioning system with a navigation update rate and accuracy sufficient to drive the thrust system. Current receiver designs can easily maintain update rates of one Hz or faster, well within the sensor bandwidth required for the dynamic positioning thrusters.

The accuracy of the navigation inputs to the dynamic positioning system vary considerably with the implementation, as will become evident below. As a general rule, the differential system increases the accuracy over the standalone system by replacing the several locally common system biases (ionosphere, satellite ephemeris error, etc.) with a smaller residual differential error. This differential error is roughly submeter for very closely spaced antennas and ranges

upward with distance at a general rate of roughly one part in 100,000 in the absence of Selective Availability.

The GPS receiver requires four near-simultaneous ranges from four GPS satellites to establish position and time. These ranges come from measuring the code phase of coded signals sent from each of the one millisecond frequency (300 km wavelength). The noise in measuring the L1 code phase at a 1 Hz rate is in the 3-10 meter range, depending on the quality of equipment and environmental conditions. For a single shot four-dimensional position-time fix using four ranges, this variability due to noise translates to position error on the order of 10-20 meters or worse, depending on the geometry of the satellites relative to the user. This 10-20 meter variability must be smoothed in order to track vessel motion in high seas sufficiently accurately for the dynamic positioning system. There are three methods of smoothing being considered for DP systems to reduce the effective noise: dead-reckoning, aiding instruments, and GPS carrier measurements.

Dead-reckoning is the process of using a priori knowledge of the dynamics of the vessel, which implies that the motion of the vessel is fairly regular and predictable. The reliability of this method decreases as the sea state increases, but if the vessel motion can be modeled for the sea state conditions, this can produce a smoothing effect. Note that pitch/roll/heading motion must be included in the model to account for mast motion effects on the antenna.

Aiding instruments relate to some inertial measurement package (gyro/accelerometer) or other sensor that can provide improved short-term motion tracking. If the motion history of the vessel can be accurately tracked over a period of seconds then the position measurements of the GPS receiver can be averaged over that same period, using the measured motion history to tie the measurements together. This is most often done through a Kalman filter that automatically weights the accuracy of the measurements and the decay of their importance with age. The traditional problem of long-term drift is not relevant when the inertial instruments are used in this context, because position error is bounded by the GPS range measurements. This allows the use of less expensive inertial instruments.

The L1 frequency carrier provides an extremely accurate secondary measurement mode for the GPS receiver [14, 15]. Although carrier tracking cannot practically measure range to the satellite, it does measure the change in position or average velocity range over time to a very high level of precision. Thus, carrier tracking is most important in situations where tracking the motion is as important as fixing the position.

For dynamic positioning applications, carrier tracking can replace other methods of smoothing the noisy code measurements. There are two drawbacks to relying only on carrier tracking to provide smoothing for the code, and the effect of these drawbacks vary widely with the application. The first is that increasing or decreasing ionospheric delay has the opposite (and equal) effect on carrier; i.e., an increase in ionosphere will produce an apparent increase in range-rate from backwards-differenced pseudoranges and a decrease in range-rate from the carrier measurements. In the majority of cases this effect is extremely minor; ionospheric delay rates in the waters off the continental United States are always quite low, on the order of .5 mm/sec or less. The inconsistent ionospheric effect on code smoothing becomes neglibible in such conditions with a properly tuned filter. In some areas of the world, such as on the geomagnetic equator or the poles, ionospheric rates can be much higher. Smoothing can still be used, but tuning the filter to accommodate the possible ionospheric effects makes the output substantially noisier.

A second problem with carrier smoothing concerns the probability of carrier loop loss-of-lock and the resulting loss of range-rate data. The carrier tracking loop is often much more sensitive than the code tracking loop and will lose lock in cases of severe ionospheric disturbances, severe multipath conditions, or extreme dynamics. A typical case of severe dynamics has been reported in USCG tests in small craft, in which receivers lose lock under heavy jerk conditions experienced when the bow slams into a wave. This can cause a data dropout for a short period of time, during which the navigation system must rely on some alternative means to smooth the noisy code data. A second aspect to this problem, more difficult to detect, is cycle slippage; this causes abrupt 19 cm. errors in the range history. Such an error is not detectable by comparing against the code readings; neither is this error detectable by dead-reckoning unless the measurement rate is high compared to the dynamics. For all-in-view receivers, a cycle slip can be detected if at least five satellites were being tracked and can be corrected if at least six were being tracked. If either cycle-slip or loss-of-lock is a potential problem in the particular DP application, an inertial measurement unit or multichannel receiver may be required to provide complete reliability.

There are a few other instruments that bear mentioning as part of the shipborne DGPS implementation. Tropospheric conditions can induce large errors, especially on low elevation satellites. For precision systems, even differential GPS may not be sufficient to bring this error source down to an appropriate level. An alternative method is to actually measure the surface refractivity using temperature-pressure-humidity instruments and modeling the troposphere locally. Secondly, in the absence of the two-frequency ionospheric correction used by authorized military GPS sets, ionospheric monitoring services may be able to model the ionosphere over large areas and predict its differential effect between the shipborne and reference station. Thirdly, a highly accurate frequency standard (rebidium or cesium) can increase the accuracy of the receiver and aid in coasting through poor satellite geometry and short loss-of-lock episodes. Any of these instruments, if available, could easily be incorporated into the shipborne system.

A last concern is the short-term effect that occurs when the GPS receiver switches satellites in or out of the current constellation. Most current receivers are designed to track only four satellites at a time; when the constellation geometry changes to favor a different choice of four satellites, the receiver will switch satellites out of and into its tracking set. Each change incurs a sudden quantum jump in the position solution which must be smoothed out over time using dead reckoning or external aiding sensors. This also happens as satellites rise and set. These transients can be removed by filtering, which damps the response to the transients, but some integrity of the solution is lost in the process. To alleviate this problem, the GPS receiver should be able to track more than four satellites at once to achieve enough redundancy so that the transition in adding or dropping satellites is minimized. All-in-view tracking with a precise clock (which acts as an extra channel) is preferred. All-in-view would provide sufficient redundancy to detect and isolate most failures in the receiver or GPS satellite system, protect against degradation due to carrier loss-of-lock or lack of visibile satellites, and allow graceful transitions during satellite switches.

REFERENCE STATION AND DATA LINK

The reference station is a reference receiver mounted on shore or in shoal waters. It should be surveyed and tied to the WGS 72 coordinate system within a few meters. The receiver should track and broadcast corrections for all satellites in view continuously so that the user(s) can choose any or all satellites in common view. The pseudorange errors can be filtered from the code and carrier measurements to a high degree of accuracy because both the unknown dynamics of both the receiver and GPS signal are very low, on the sub-cm/sec level. This allows bandwidths on the receiver to be narrowed considerably. Other benefits of the ground station are that the daily multipath problems can be identified and compensated and that loss-of-lock due to dynamics or shadowing are much less frequent.

A second concept for the reference station is as a pseudolite, an earth-bound L1 code broadcaster. Just as the satellites broadcast a data stream superimposed on the L1 code, the pseudolite broadcasts not only its own location and time information but the differential corrections for all satellites in view. The drawback to this concept is that the signal from the pseudolite would be difficult to attenuate so that it does not overwhelm GPS receivers operating in its vicinity, and yet still be received by receivers hundreds of kilometers away. Time division multiple access (TDMA) pseudolite schemes have been suggested [16], but these carry the drawback that carrier loop will be overwhelmed during the pseudolite burst transmissions and loss of lock will occur. The pseudolite can also broadcast on a frequency other than L1. This will not interfere with reception of the satellite transmissions, and is equivalent to a radiolocation beacon with a differential GPS data stream.

The minimum requirement for the data link is that it broadcast the pseudorange corrections quickly enough to prevent degraded accuracy from aging. Typically the correction is linear with time, the reference station broadcasting the predicted correction and correction rate for each satellite over the next interval; with lively signal dynamics such as can happen under severe Selective Availability conditions, the accuracy of this linear correction may exceed the system accuracy requirements within a few seconds. The data link requirements must balance available bandwidth against the dynamic range of the corrections, the degradation of a linear correction over short intervals of time, and the accuracy requirements of the navigation system.

CANDIDATE GPS-BASED DYNAMIC POSITIONING SYSTEM DESIGN

To illustrate the application of these concepts to DP vessel operations, a candidate system design has been devised. Figure 13 shows the major components of the system. On the shore is a Differential GPS Reference Station, consisting of a GPS 8 to 10-channel receiver, a local meteorological sensor suite, a rubidium frequency standard, a differential correction processor, and an RF datalink transmitter.

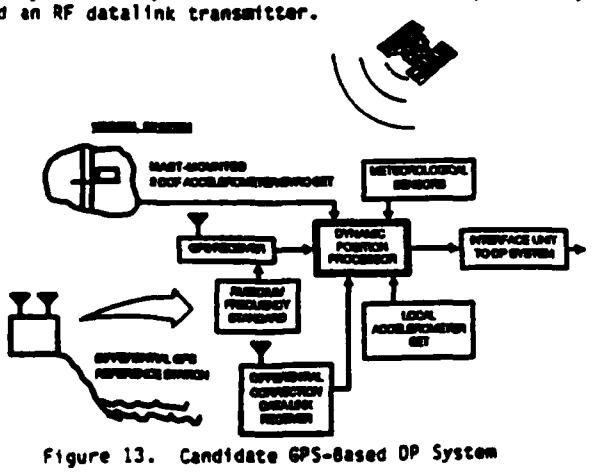

Figure 13. Candidate GPS-Based DP System

The vessel system is based on a 4 or 5-channel, or preferably an 8-10 channel, GPS receiver, with a differential correction RF data link receiver for receiving the corrections broadcast by the Shore Reference Station. The GPS receiver is also slaved to a rubidium frequency standard for further smoothing and carrier loop stability as discussed in the previous section. A separate computer is used for processing the GPS data, decoding the differential correction data, as well as processing the other aiding data.

The aiding data include meteorological sensors and inertial (gyro/accelerometer) components. The role of the inertial components is twofold to address the issues presented earlier. First, separate sensors are mounted in the antenna base as well as at the processor site, the comparison of the outputs of these sensors, along with known level arms, allows resolution of most motion (roll, pitch, yaw). Second, the local suite provides short-term precise measurements of vessel motion to smooth (via improved process modeling) GPS position estimates. These sensors are sufficient to compute vessel center-of-gravity motion which is input to the DP system, via an acceptable interface, as position and velocity feedback to the control algorithm.

The inertial sensors can be low grade with relatively imprecise mounting. If, due to antenna mounting constraints, mast flexure is also a significant factor, then an addition sensor elsewhere on the mast may be required. The dynamic position processor uses an extended Kalman filter to compute vessel position and velocity from the desired holding position. State vector formulation depends on the update rate of the GPS receiver and the relative quality, and contribution, of the inertial sensors. Filter tuning is very critical if anomalous transients are to be eliminated while correlated error source dynamics are still tracked.

In summary, the GPS-based DP system can be a robust, precise relative positioning sensor for most applications of vessel dynamic positioning. Several options exist for sensor tradeoff, processing algorithms, and data link method which will impact performance, cost, and reliability. Field test and data collection relative to these issues is in progress, and evaluation of the results will define the optimal configuration for an operational system.

ACKNOWLEDGMENTS

The authors would like to express their appreciation to the staff of Honeywell Marine Systems in Seattle, Washington, for their informative inputs concerning dynamic positioning systems.

REFERENCES

1. Morgan, Max, "Dynamic Positioning of Offshore Vessels," PPC Books Division, Tulsa, OK, 1978.

2. Shatto, H. L.and H. Van Calcar, "Improving Dynamic Positioning Performance in the Deepwater, High-Current, Rough Water Environment," Proceedings 1984 Offshore Tech. Conf., Houston, TX, 1984.

3. Roberts, J. L., "A Multimode Acoustic Position Indicator for Greater Accuracy and Reliability," Proceedings 1985 Offshore Tech. Conf., Houston, TX, 1985.

4. Spindel, R. C., R. P. Porter, W. M. Marquet, and J. L. Durham, "A High-Resolution Pulse-Doppler Underwater Acoustic Navigation System," IEEE J. Oceanic Eng., Vol. OE-1 No. 1, Sept. 1976.

5. Stensland, R. A., "Principles of Strapdown Inertial Navigation," Proceedings Avionics Maintenance Conf., Seattle, WA, 1984.

6. Denaro, R. and A. Cabak, "Simulation and Analysis of Differential GPS," National Technical Meeting of the Institute of Navigation, January 1984.

7. Parkinson, B. W., "GPS Accuracy and Reliability Improved with Pseudolites," Microwave Systems News, November 1984.

8. Kalafus, R. M., J. Vilcans, and N. Knable, "Differential Operation of NAVSTAR GPS," Journal of the Institute of Navigation, Volume 30, No. 3, 1983.

9. Denaro, R., "Application of Differential GPS to Civil Helicopter Terminal Guidance," Proceedings of Digital Avionics System Conference, December 1984.

10. Edwards, F. and Loomis, P. V. W., "Civil Helicopter Flight Operations Using Differential GPS," Proceedings of Institute of Navigation Technical Meeting, Annapolis, MD, June 1985.

11. Beser, J. and B. W. Parkinson, "The Application of NAVSTAR Differential GPS in the Civilian Community," Journal of the Institute of Navigation, Volume 29, No. 2, 1982

12. Klobuchar, J. A., "Ionospheric Effects on Earth-Space Propagation," AFGL-TR-84-0004, December 1983.

13. Bishop, G. J. and Klobuchar, J. A., "Multipath Effects on the Determination of Absolute Ionospheric Time Delay from GPS Signals," Radio Science, 20:3, pages 388-396, May 1985.

14. Hatch, R., "Synergism of GPS Code and Carrier Measurements," Proceedings of 3rd International Geodetic Symposium on Satellite Doppler Positioning, Las Cruces, NM, 1982.

15. Ashjaee, J., "GPS Doppler Processing for Precise Positioning in Dynamic Applications," Institute of Navigation Proceedings, San Diego, CA, January 1986.

16. VanDierendonck, A. J., "Time Division Multiple Access Differential GPS," IEEE 1983 National Telesystems Conference.

END

11-86

DTIC